Super-resolution imaging reveals differential organization and regulation of NMDA receptor subtypes

Blanka Kellermayer

université de BORDEAUX

THÈSE PRÉSENTÉE

POUR OBTENIR LE GRADE DE

DOCTEUR DE

L'UNIVERSITÉ DE BORDEAUX

ÉCOLE DOCTORALE "SCIENCES DE LA VIE ET DE LA SANTÉ"

SPÉCIALITÉ NEUROSCIENCES

Par Blanka KELLERMAYER

Organisation et régulation différentielles des sous-types de Récepteurs NMDA révélées par imagerie de super résolution

Sous la direction de: Laurent GROC
(co-directeur: Ana Luísa CARVALHO)

Soutenue le 25 Janvier, 2018

Membres du jury:

Mme CAVADAS, Claudia, Professeur, Faculty of Pharmacy, University of Coimbra, Président
M. ESTEBAN, Jose, Directeur de Recherche, Centre for Molecular Biology, Espagne, Rapporteur
Mme SEBASTIAO, Ana, Professeur, Instituto de Medicina Molecular Joao Lobo Antunes, Portugal, Rapporteur
Mme SOUSA, Monica, Directeur de Recherche, Institute for Molecular and Cell Biology, Portugal, Rapporteur
M.RELVAS, Joao, Directeur de Recherche, Institute for Molecular and Cell Biology, Portugal Examinateur
M. OLIET, Stephane, Directeur de Recherche, Neurocentre Magendie INSERM U862, Examinateur
M.DUARTE, Carlos, Professeur, Department of Zoology, University of Coimbra, Portugal, Invité
M.GROC, Laurent, Chargé de Recherche, Institut Interdisciplinaire de Neurosciences, Directeur

Super-resolution imaging reveals differential organization and regulation of NMDA receptor subtypes

Blanka Kellermayer

August, 2017

PhD Degree in Experimental Biology and Biomedicine

Specialization: Neuroscience and Disease

Supervised by Ana Luísa Carvalho, PhD and Laurent Groc, PhD

Presented to the Institute for Interdisciplinary Research of the University of Coimbra in cotutelle with the Doctoral School of Health and Life Sciences of the University of Bordeaux

“Látni, amit már mindenki látott –
és azt gondolni róla,
amire még senki sem gondolt.”

Szent-Györgyi Albert

“Discovery consists of seeing
what everybody has seen, and
thinking what nobody has
thought.”

Albert Szent-Györgyi

Acknowledgements

First, I want to thank the European Neuroscience Campus (ENC) Network and the Erasmus Mundus Joint Doctorate (EMJD) program for giving me the opportunity to perform my doctoral studies in such prestigious institutes, with special thank you to Arjen Brussaard and Maaike Leusden for their constant support.

Next, I would like to thank all members of my thesis committee for accepting to judge my work: Cláudia Cavadas, Carlos Duarte, José Esteban, Stephane Oliet, João Relvas, Ana Sebastião and Mónica Sousa.

Most importantly, I would like to express my sincere gratitude to my two thesis supervisors, Ana Luísa Carvalho and Laurent Groc. I am extremely thankful for the both of you for your positive attitudes, the warm welcome I received in your labs, for training and mentoring me and always supporting me to aim higher. Ana Luísa, even though I spent less time physically in Coimbra, your knowledge and wisdom helped me mature immensely. Thank you for setting me an admiring example in how to be a successful scientist as a woman and a mother. Laurent, your enthusiasm is always infectious. I want to thank you for consistently finding the best way to motivate me and for giving me the freedom and trust to follow through with my ideas.

I am extremely grateful for the help of my colleagues, especially Joana Ferreira, not only for the long hours spent at the microscope or discussing my project but also for continuously helping me find my way in the labyrinth of Portuguese bureaucracy. I want to thank Delphine Bouchet and Pauline Durand and all other members of the culture team for their never-ending work to make our lives easier. I also want to thank Pauline Durand for the help in molecular biology. I will always be thankful for Silvia Ciappelloni for our many lunch dates and long discussions about science and life. I am grateful for the warm welcome and friendship of Juan Varela and, of course, all our surf sessions. I was happy to share the office with Alexandra Fernandes and Pauline Letard in the old building; our coffee breaks definitely helped during the long hours of analysis. I am thankful for Ezequiel Saraceno for the advice in writing this doctoral thesis. I am extremely grateful for all other, former and present members of the ‘Groc team’: Elena Avignone, Hélène Grea, Julien Dupuis, François Maingret, Marilyn Lepleux, Emily Johansson, Julie Jezequel, Laetitia Etchepare, Charlotte Bertot, Tingting Huang and Sebastien Habé for all the scientific discussions and help in my life in France as a foreigner.

I wish to thank all members of Ana Luísa's group: Sandra D Santos and Tatiana Catarino for helping with the cell cultures, Jeannette Schmidt for giving away the secrets of the GluN2B knockout cultures, and Dominique Fernandes, Gladys Caldeira, Mariline Silva, as well as other members of the Center for Neuroscience and Cell Biology: Carlos Duarte, João Peça, Joana Fernandes, Joana Pedro and Mohamed Edfawy Hussein, for welcoming me and making my transition to Coimbra easier. I appreciate the never-ending efforts of Sílvia Sousa in taking care of all my paperwork in Coimbra.

I would like to express my gratitude to Christel Pujol and Patrice Mascalchi from the Bordeaux Imaging Center for their help with the microscopes. Patrice, you were always available for discussing and helping me with my analysis. I also want to thank Sebastian Malkusch and Mike Heilemann for the Lama Software and assistance in setting up the correct parameters to analyze my data.

Szeretnék köszönetet mondani az egész családomnak a rengeteg támogatásért. Rendkívül hálás vagyok a szüleimnek, hogy egész életemben biztosították számomra a kiegyensúlyozott, nyugodt családi és tanulmányi hátteret, hogy el tudjam érni a céljaimat, még ha ez azzal is jár, hogy távol vagyok otthontól. Édesanyámnak, aki számomra egy igazi hős, ahogy a család összetartása mellett orvosként dolgozik, köszönöm, hogy mindig egy biztos támaszt nyújt számomra. Édesapámnak köszönöm, hogy a tudomány iránti elhivatottságával és az igazságot kutató szemléletével mindig példát állít elém. Testvéreimnek, Zoltánnak, Bernátnak, Dalmának és Annának köszönöm a sok bíztatást doktori éveim alatt és a disszertáció írása közben. Nagyszüleimnek, Erzsébetnek, Ildikónak, Miklósnak és Sándornak köszönöm a sok szeretetet, amivel elhalmoztak egész életemben. Marcsinak és Bélának köszönöm, hogy a távolból is sok energiát adtak a doktori munkámhoz és a dolgozat megírásához. Köszönöm Priskin Katának és Aladics Ágnesnek a barátságát és a folyamatos bátorításukat tanulmányaim során,.

És a legfontosabbat hagyva a végére, szeretnék köszönetet mondani a férjemnek és a kisfiamnak. Péter, köszönöm, hogy mindvégig hittél bennem és kitartottál mellettem, bíztattál, hogy ne adjam fel, amikor még saját magamban sem hittem. Nélküled nem tartanék ma itt, sem kutatóként, sem emberként. Ábel, az angyali mosolyod és huncut tekinteted annyi energiát ad nap mint nap, hogy nagy részed volt abban, hogy minél hamarabb elkészüljek az írással. Ez a dolgozat legalább annyira a Ti érdemetek, mint az enyém, ezért a disszertációmat és a doktori fokozatomat Nektek ajánlom.

Table of Contents

Organisation et régulation différentielles des sous-types de Récepteurs NMDA révélées par imagerie de super résolution

Résumé

Introduction

Les NMDA récepteurs (NMDAR) sont un sous-type de canaux ioniques induits par le glutamate (iGluR), perméables au sodium et au calcium (influx) et au potassium (efflux), qui jouent un rôle essentiel dans la neurotransmission excitatoire dans le système nerveux central. L'augmentation des taux de calcium postsynaptique à la suite de l'activation de NMDAR entraîne des modifications de l'efficacité synaptique et de la morphologie neuronale. Les NMDAR sont impliqués dans plusieurs processus physiologiques et pathologiques tels que la plasticité synaptique, l'excotoxicité et de multiples troubles du système nerveux central, par exemple la schizophrénie, l'encéphalite anti-NMDAR, les troubles du spectre autistique, la maladie d'Alzheimer, la maladie de Huntington et la maladie de Parkinson.

Les NMDAR forment des tétramères à la membrane plasmique, constitués de deux sous-unités obligatoires GluN1 et deux sous-unités variables GluN2 (GluN2A-D) ou GluN3. Dans le prosencéphale, les récepteurs comportant les sous-unités GluN2A (GluN2A-NMDAR) et GluN2B (GluN2B-NMDAR) sont les plus abondants. Au cours du développement ils présentent des profils d'expression différents, les GluN2B-NMDAR étant fortement exprimés aux stades précoces tandis que l'expression des GluN2A-NMDAR augmente progressivement au cours du développement postnatal. Cette expression, ainsi que leur localisation précise dans la synapse, est contrôlée par diverses interactions protéine-protéine, par exemple, des protéines d'échafaudage contenant un domaine PDZ (protéine de densité postsynaptique 95, PSD95) et la protéine kinase II dépendante de Ca2 + / calmoduline

(CaMKII). Des contributions relatives de GluN2A-NMDAR and GluN2B-NMDAR aux propriétés de signalisation distinctes dépendent directement les phénomènes de plasticité neuronale, tels que l'adaptation des synapses glutamatergiques et des circuits neuronaux excitateurs.

Bien que la régulation moléculaire des NMDAR ait fait l'objet d'intenses recherches ces dernières décennies, la localisation précise de ces deux sous-types de récepteurs dans la membrane postsynaptique demeurait méconnue. Pour répondre à cette question, nous avons étudié la distribution des NMDAR à la surface de neurones d'hippocampe de rats en combinant deux techniques de microscopie de super-résolution - la microscopie de reconstruction optique stochastique directe *(dSTORM)* et la déplétion d'émission stimulée *(STED)* - permettant de dépasser la limite de résolution inhérente à la diffraction de la lumière. Ces techniques nous ont permis de mettre en évidence que les sous-types de récepteurs GluN2A- et GluN2B-NMDAR présentent une nano-organisation différente à la surface neuronale.

Les méthodes

Le concept principal de la microscopie STED consiste à améliorer la résolution spatiale en désactivant l'émission de fluorescence à la périphérie de la fonction d'étalement de points (PSF), de sorte que l'émission ne puisse se produire qu'à partir d'un point limité par diffraction à l'intérieur de la PSF. Ceci est réalisé par un laser spécial appelé laser STED qui, grâce à sa forme unique en forme de beignet, désexcite les molécules fluorescentes externes à l'état fondamental (S0) par une émission stimulée à une longueur d'onde plus longue que celle utilisée pour l'excitation de fluorescence. Par conséquent, l'émission de fluorescence ne se produit qu'à partir du centre de la PSF qui est détecté par un photodétecteur. En revanche, dSTORM est fondamentalement différent de STED en ce sens qu'il présente des molécules uniques. Le principe de base de dSTORM est que la position d'une seule molécule peut être

identifiée avec une précision d'environ 1 nm si suffisamment de photons sont collectés et qu'il n'existe aucun autre émetteur similaire à moins de 200 nm. Le dSTORM (ou l'appauvrissement de l'état fondamental suivi du retour d'une molécule individuelle, GSDIM) utilise la commutation réversible des fluorophores classiques pour obtenir une émission aussi rare. Les fluorophores passent en état triplet (T1) ou en un autre état sombre métastable en utilisant une puissance laser à forte excitation, tandis que les fluorophores restant ou revenant à l'état fondamental (S0) peuvent être excités et détectés. La commutation des fluorophores est contrôlée par un 'tampon de commutation' contenant des désoxygénants et des agents réducteurs. L'image super résolue est reconstruite à partir d'un grand nombre d'images conventionnelles à grand champ, chacune contenant les informations de position haute précision d'un sous-ensemble de molécules fluorescentes dispersées.

Objectifs

Le but de ce projet est de répondre à plusieurs questions fondamentales sur la localisation précise et l'organisation à l'échelle nanométrique de deux sous-types importants de NMDAR, en tirant parti des techniques de super-résolution telles que la microscopie dSTORM et STED. Le projet est divisé en sections suivantes:

1. Visualisation de la distribution nanoscopique de GluN2A- et de GluN2B-NMDAR de surface à l'aide de dSTORM dans des cultures d'hippocampe primaires matures (17 jours in vitro).

2. Détermination du nanocluster de GluN2A- et de GluN2B-NMDAR.

3. Caractérisation de l'organisation nanométrique à l'échelle nanométrique de GluN2A- et de GluN2B-NMDAR dans des structures synaptiques utilisant le PSD-95 comme marqueur postsynaptique.

4. Examen des modifications de la nano-organisation de GluN2A- et de GluN2B-NMDAR au cours du développement.

5. Étude de la régulation de l'organisation nanométrique du NMDAR avec un accent particulier sur les interactions avec les échafaudages PDZ et l'activité CaMKII.

Résultats

En effet, GluN2A- et GluN2B-NMDAR sont organisés en structures nanoscopiques (nanodomaines) qui diffèrent en nombre, en surface et en morphologie, notamment au niveau des synapses. Au cours du développement, l'organisation membranaire des deux sous-types de NMDAR évolue, avec en particulier de profonds changements de distribution des GluN2A-NMDAR. De plus, cette organisation nanoscopique est impactée différemment par des modulations de l'interaction avec les protéines d'échafaudage à domaine PDZ ou de l'activité de la kinase CaMKII suivant le sous-type de NMDAR considéré. En effet, la réorganisation des GluN2A-NMDAR implique principalement des changements de nombre de récepteurs dans les nanodomaines sans modification de leur localisation, tandis que la réorganisation des GluN2B-NMDAR passe essentiellement par des modifications de localisation des nanodomaines sans changements du nombre de récepteurs qu'ils contiennent. Ainsi, les GluN2A- et GluN2B-NMDAR présentent des nano-organisations différentes dans la membrane postsynaptique, reposant vraisemblablement sur des voies de régulation et des complexes de signalisation distincts.

Super-resolution imaging reveals differential organization and regulation of NMDA receptor subtypes

Summary

NMDA-type glutamate receptors (NMDARs) are a type of ion permeable channels playing critical roles in excitatory neurotransmission in the central nervous system by mediating different forms of synaptic plasticity, a mechanism thought to be the molecular basis of neuronal development, learning and memory formation. NMDARs form tetramers in the postsynaptic membrane, most generally associating two obligatory GluN1 subunits and two modulatory GluN2 (GluN2A-D) or GluN3 (GluN3A-B) subunits. In the hippocampus, the dominant GluN2 subunits are GluN2A and GluN2B, displaying different expression patterns, with GluN2B being highly expressed in early development while GluN2A levels increase gradually during postnatal development. In the forebrain, the plastic processes mediated by NMDARs, such as the adaptation of glutamate synapses and excitatory neuronal networks, mostly rely on the relative implication of GluN2A- and GluN2B-containing NMDARs that have different signaling properties. Although the molecular regulation of synaptic NMDARs has been under intense investigation over the last decades, the exact topology of these two subtypes within the postsynaptic membrane has remained elusive. Here we used a combination of super-resolution microscopy techniques such as direct stochastic optical reconstruction microscopy (dSTORM) and stimulated emission depletion (STED) microscopy to characterize the surface distribution of GluN2A- or GluN2B-containing NMDARs. Both dSTORM and STED microscopy, based on different principles, enable to overcome the resolution barrier due to the diffraction limit of light. Using these techniques, we here unveil a differential nanoscale organization of native GluN2A- and GluN2B-NMDARs in rat hippocampal neurons. Both NMDAR subtypes are organized in nanoscale structures (termed nanodomains) that differ in their number, area, and shape. These observed differences are also maintained in synaptic structures. During development of hippocampal cultures, the membrane organization of both NMDAR subtypes evolves, with marked changes for the topology of GluN2A-NMDARs. Furthermore, GluN2A- and GluN2B-NMDAR nanoscale organizations are differentially affected by alterations of either interactions with PDZ scaffold proteins or CaMKII activity. The regulation of GluN2A-NMDARs mostly implicates changes in the number of receptors in fixed nanodomains, whereas the regulation of GluN2B-NMDARs mostly implicates changes in

the nanodomain topography with fixed numbers of receptors. Thus, GluN2A- and GluN2B-NMDARs have distinct organizations in the postsynaptic membrane, likely implicating different regulatory pathways and signaling complexes.

Organisation et régulation différentielles des sous-types de Récepteurs NMDA révélées par imagerie de super résolution

Résumé court

Les récepteurs du glutamate de type NMDA (NMDAR) sont des canaux ioniques impliqués dans les phénomènes de plasticité de la transmission synaptique dans le système nerveux central, des mécanismes supposés être à la base du développement neuronal, de l'apprentissage et de la formation de la mémoire. Les NMDAR forment des tétramères à la membrane plasmique, constitués de deux sous-unités obligatoires GluN1 et deux sous-unités variables GluN2 (GluN2A-D) ou GluN3. Dans le prosencéphale, les récepteurs comportant les sous-unités GluN2A (GluN2A-NMDAR) et GluN2B (GluN2B-NMDAR) sont les plus abondants et présentent des profils d'expression différents au cours du développement, les GluN2B-NMDAR étant fortement exprimés aux stades précoces tandis que l'expression des GluN2A-NMDAR augmente progressivement au cours du développement postnatal. Des contributions relatives de ces deux sous-types majoritaires de NMDAR aux propriétés de signalisation distinctes dépendent directement les phénomènes de plasticité neuronale, tels que l'adaptation des synapses glutamatergiques et des circuits neuronaux excitateurs. Bien que la régulation moléculaire des NMDAR ait fait l'objet d'intenses recherches ces dernières décennies, la localisation précise de ces deux sous-types de récepteurs dans la membrane postsynaptique demeurait méconnue. Pour répondre à cette question, nous avons étudié la distribution des NMDAR à la surface de neurones d'hippocampe de rats en combinant deux techniques de microscopie de super-résolution - la microscopie de reconstruction optique stochastique directe *(dSTORM)* et la déplétion d'émission stimulée *(STED)* - permettant de dépasser la limite de résolution inhérente à la diffraction de la lumière. Ces techniques nous ont permis de mettre en évidence que les sous-types de récepteurs GluN2A- et GluN2B-NMDAR présentent une nano-organisation différente à la surface neuronale. En effet, ils sont organisés en structures nanoscopiques (nanodomaines) qui diffèrent en nombre, en surface et en morphologie, notamment au niveau des synapses. Au cours du développement, l'organisation membranaire des deux sous-types de NMDAR évolue, avec en particulier de profonds changements de distribution des GluN2A-NMDAR. De plus, cette organisation nanoscopique est impactée différemment par des modulations de l'interaction avec les protéines d'échafaudage à domaine PDZ ou de l'activité de la kinase CaMKII suivant le sous-

type de NMDAR considéré. En effet, la réorganisation des GluN2A-NMDAR implique principalement des changements de nombre de récepteurs dans les nanodomaines sans modification de leur localisation, tandis que la réorganisation des GluN2B-NMDAR passe essentiellement par des modifications de localisation des nanodomaines sans changements du nombre de récepteurs qu'ils contiennent. Ainsi, les GluN2A- et GluN2B-NMDAR présentent des nano-organisations différentes dans la membrane postsynaptique, reposant vraisemblablement sur des voies de régulation et des complexes de signalisation distincts.

Microscopia de alta-resolução revela diferente organização e regulação de subtipos de receptores NMDA

Resumo

Os recetores do glutamato do tipo NMDA são canais iónicos que desempenham um papel de especial relevância na neurotransmissão excitatória no sistema nervoso central, e são responsáveis por mediar diferentes formas de plasticidade sináptica, o mecanismo considerado na base do desenvolvimento neuronal, aprendizagem e formação da memória. Os recetores NMDA dispõem-se em tetrâmeros na membrana pós-sináptica e são normalmente constituídos por duas subunidades obrigatórias GluN1 e duas subunidades modeladoras GluN2 (GluN2A-D) ou GluN3 (GluN3A-B). No hipocampo as duas subunidades GluN2 mais expressas são as subunidades GluN2A e GluN2B, que se caracterizam por padrões de expressão diferentes; enquanto a subunidade GluN2B é expressa cedo no desenvolvimento em níveis elevados, os níveis de expressão da subunidade GluN2A vão aumentando gradualmente durante o desenvolvimento pós-natal. Na região do prosencéfalo, os mecanismos de plasticidade mediados pelos recetores NMDA, tais como a adaptação de sinapses glutamatérgicas e das redes neuronais excitatórias, são altamente dependentes da diferente contribuição dos recetores que contêm a subunidade GluN2A (recetores GluN2A-NMDA) ou a subunidade GluN2B (recetores GluN2B-NMDA), os quais apresentam diferentes propriedades de sinalização. Embora a regulação molecular sináptica dos recetores NMDA tenha sido intensamente estudada durante as últimas décadas, a topografia exacta destes dois tipos de recetores, GluN2A-NMDA e GluN2B-NMDA, na membrana pós-sináptica continua a ser largamente desconhecida. Neste trabalho, foi utilizado uma combinação de duas técnicas de microspocia de alta-resolução, dSTORM (*direct stochastic optical reconstruction microscopy*) e STED (*stimulated emission depletion microscopy),* para caracterizar a distribuição dos recetores GluN2A-NMDA e GluN2B-NMDA à superfície da membrana pós-sináptica. As duas técnicas de microscopia, dSTORM e STED, baseiam-se em diferentes princípios físicos, mas ambas permitem ultrapassar o limite de resolução devido à difração da luz. A utilização destas técnicas permitiu definir a diferente organização à escala nanométrica dos recetores nativos GluN2A-NMDA e GluN2B-NMDA, em neurónios de hipocampo de rato. Os dois subtipos de recetores organizam-se em estruturas com o tamanho de alguns nanómetros (definidas como "nanodomínio") mas que diferem em número, área ou forma.

Estas diferenças são mantidas se avaliadas especificamente dentro das estruturas sinápticas. Durante o desenvolvimento das culturas de hipocampo, a organização membranar de ambos os subtipos de recetores NMDA vai-se modificando, particularmente a topologia dos recetores GluN2A-NMDA. A organização à escala nanométrica dos recetores GluN2A-NMDA ou GluN2B-NMDA é afetada de forma diferente pela alteração da interação dos recetores com as proteínas âncora que contêm o domínio PDZ, ou pela modificação da atividade da proteína CaMKII. A regulação dos recetores GluN2A-NMDA baseia-se sobretudo na alteração do número de recetores dentro de determinados nanodomínios, enquanto a regulação dos recetores GluN2B-NMDA se baseia principalmente nas alterações da topografia dos nanodomínios, sem alterar o número de recetores. Em conclusão, os recetores GluN2A-NMDA ou GluN2B-NMDA apresentam uma organização distinta na membrana pós-sináptica, o que sugere que poderá estar associada a diferentes vias de regulação e complexos de sinalização.

Abbreviations

ABD	Agonist-Binding Domain
AMPA	α-amino-3-hydroxy-5-methyl-4-isoxazolepropionic acid
AMPAR(s)	α-amino-3-hydroxy-5-methyl-4-isoxazolepropionic acid receptor(s)
CaMKII	Ca^{2+}/calmodulin-dependent protein Kinase II
Cdk5	Cyclin dependent kinase 5
CK2	Casein Kinase 2
CNS	Central Nervous System
CREB	Cyclic-AMP Response Element Binding protein
CRMP2	Collapsin Receptor Mediator Protein 2
CTD	Carboxyl (C-)-terminal Domain
D-APV	D(−)-2-Amino-5-phosphonopentanoic acid
DBSCAN	Density-Based Spatial Clustering of Applications with Noise
DIV	Days *In Vitro*
DLG	Discs Large Homologue
dSTORM	direct Stochastic Optical Reconstruction Microscopy
EM	Electron Microscopy
EMCCD	Electron Multiplying Charged Coupled Device
EPSC	Excitatory Postsynaptic Current
EPSP	Excitatory Postsynaptic Potential
ER	Endoplasmic Reticulum
GIPC	GAIP Interacting Protein C-terminus
GK	Guanylate Kinase
GKAP	Guanylate Kinase-Associated Protein
Grin2a	Glutamate ionotropic receptor NMDA type subunit 2A gene
Grin2b	Glutamate ionotropic receptor NMDA type subunit 2B gene
HBSS	Hank's Balanced Salt Solution
iGluRs	ionotropic Glutamate Receptors
IPSP	Inhibitory Postsynaptic Potential
KO	Knockout
LAMA	Localization Microscopy Analyzer
LSE	Least Squares Estimation
LTD	Long-Term Depression

LTP	Long-Term Potentiation
MAGUK	Membrane-Associated Guanylate Kinase
MEM	Minimum Essential Medium
mGluRs	metabotropic Glutamate Receptors
MIA	Multidimensional Image Analysis
mRNA	messenger Ribonucleic Acid
NMDA	N-methyl-D-aspartic Acid
NMDAR(s)	N-methyl-D-aspartic Acid Receptor(s)
nNOS	neuronal Nitric Oxide Synthase
NTD	Amino (N-)-terminal Domain
PALM	Photoactivated Localization Microscopy
PDZ	PSD95/Discs-large/ZO-1
PKA	Protein Kinase A
PKC	Protein Kinase C
PLL	Poly-L-Lisine
P_{min}	Minimal cluster size
PML	Promyelocytic Leukemia
preNMDAR	presynaptic NMDAR
PS	Penicillin-Streptomycin
PSD	Postsynaptic Density
PSD93	Postsynaptic Density protein 93
PSD95	Postsynaptic Density protein 95
PSF	Point Spread Function
REST	RE1-Silencing Transcription factor
Rho GEF	Rho Guanine Exchange Factor
SAP102	Synapse-Associated Protein 102
SAP97	Synapse-Associated Protein 97
SFK	Src Family Kinase
SH3	Src-Homology 3
SIM	Structured Illumination Microscopy
SMLM	Single-Molecule Localization Microscopy
STED	Stimulated Emission Depletion
$STEP_{61}$	Striatal-Enriched Protein Tyrosine Phosphatase 61
STORM	Stochastic Optical Reconstruction Microscopy

SynGAP	Synaptic Ras GTPase-Activating Protein
TGN	Trans-Golgi Network
TIRF	Total Internal Reflection Fluorescence
TMD	Transmembrane Domain
UPS	Ubiquitin-Proteasome System
VGLUT	Vesicular Glutamate Transporter
WIV	Weeks *In Vitro*
ε	Observation Radius

Index of figures and tables

Figures:

Tables:

Chapter 1: Introduction

1. The chemical synapse

Chemical synapses are specialized junctions that make up the main form of contact and communication between neuronal cells of the brain (Sheng & Hoogenraad, 2007). They are composed of a highly specialized pre- and postsynaptic compartment with a 20 to 30 nm gap between the two called the synaptic cleft (Gray, 1959a; Palay, 1956; reviewed in: Klemann & Roubos, 2011 and McAllister, 2007), and the communication between the two cells is mediated by neurotransmitters (O'Rourke et al., 2012). Depending on the effect of the neurotransmitter on the postsynaptic cell, synapses can be classified into two major groups: excitatory and inhibitory synapses (O'Rourke et al., 2012). Excitatory neurotransmitters cause the depolarization of the postsynaptic cell – an event termed as excitatory postsynaptic potential (EPSP) – due to the influx of positive ions. In contrast, inhibitory synapses hyperpolarize the postsynaptic membrane (inhibitory postsynaptic potential, IPSP) due to the influx of negative or the efflux of positive ions. The concerted and balanced operation of these synapses allows our brains to function properly and respond to environmental changes. Based on differences in their morphology and size, the excitatory and inhibitory synapses were first identified by E. G. Gray (Gray, 1959a) as asymmetric or symmetric synapses, respectively. The term "asymmetric" originates from the characteristic specialization and thickening of the postsynaptic membrane called the postsynaptic density (PSD) (Sheng and Kim, 2011). Excitatory synapses are mainly found along the dendrites in small, mushroom-like membrane protrusions called dendritic spines (**Figure 1A**) (Bosch & Hayashi, 2012; Gray, 1959b; Harris et al., 2012), whereas inhibitory synapses are present at the cell soma and the axonal initial segment as well as the proximal and distal dendrites (Moss and Smart, 2001; Sheng and Kim, 2011). Dendritic spines are 0.5-2 µm in length (Hering and Sheng, 2001) and contain specialized subdomains like the PSD, the machinery for endo- and exocytosis (Newpher and Ehlers, 2009) and intracellular membranous structures (spine apparatus, polyribosomes, mitochondria) (Bosch and Hayashi, 2012). Neuronal maturation and changes in synaptic plasticity affect the size and morphology of the spine (Hlushchenko et al., 2016). Typically, a single excitatory synapse is located in a mature spine head (Hering and Sheng, 2001; Bosch and Hayashi, 2012).

1.1. The glutamatergic synapse

Excitatory neurotransmission is predominantly mediated by the neurotransmitter glutamate which is released into the synaptic cleft from the ~40-50 nm diameter synaptic vesicles of the presynaptic terminal (active zone) (McAllister, 2007; Sheng & Hoogenraad, 2007). Glutamate diffuses from the release site across the synaptic cleft and acts on glutamate receptors present in the postsynaptic membrane. Two classes of glutamate receptors are distinguished: ion channel forming – ionotropic – (iGluRs) and G-protein coupled – metabotropic – glutamate receptors (mGluRs) which modulate synaptic transmission and neural excitability throughout the central nervous system (CNS) (reviewed in Niswender & Conn, 2010). iGluRs are highly expressed in the PSD (Petralia et al., 2005).

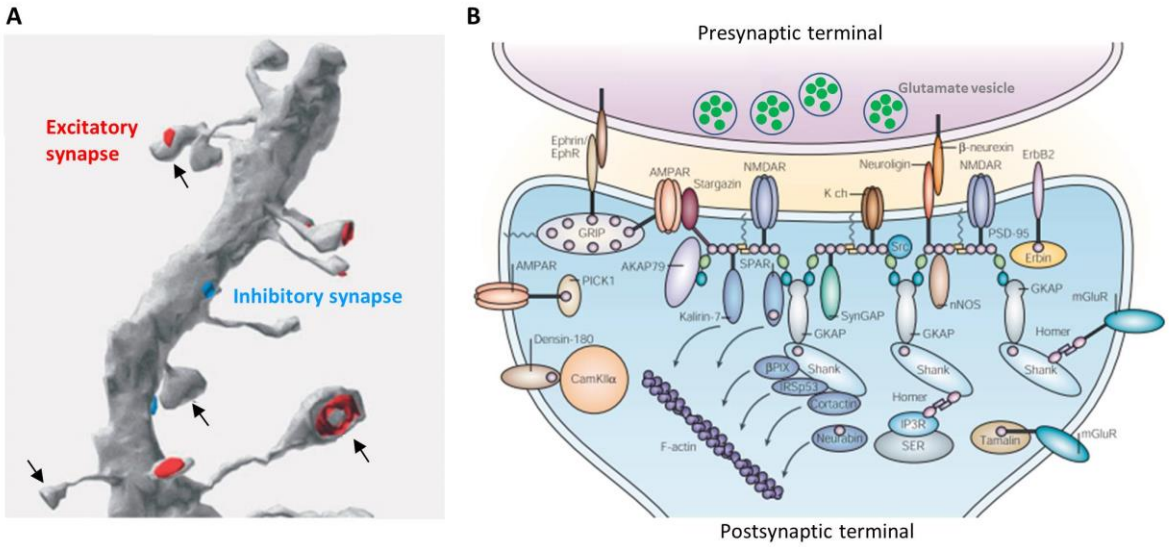

Figure 1. The chemical synapse
A. Three-dimensional EM reconstruction of a dendritic segment from the hippocampus. Red color indicates PSDs of excitatory synapses. Blue color indicates inhibitory synapses. Arrows point to examples of dendritic spines. Adapted from (Sheng and Hoogenraad, 2007). **B.** Schematic representation of the PSD of excitatory neurons. Adapted from (Kim and Sheng, 2004).

The PSD (**Figure 1B**), localized at the distal tip of the spine head opposing the presynaptic active zone, is an electron-dense structure of ~100-500 nm diameter, ~30-60 nm thickness and an average mass of 1 GDa (Carlin et al., 1980; Cotman et al., 1974; Palay & Palade, 1955). The PSD is considered to be the organizer of postsynaptic functions by coordinating and supporting neurotransmitter receptors of the synaptic membrane and by coupling receptor activation to cytoplasmic signaling proteins crucial for synaptic

transmission (Sheng & Kim, 2011). Proteomic analyses have identified ~1000 highly conserved proteins within the PSD including neurotransmitter receptors, cell-adhesion proteins, signaling molecules (kinases and phosphatases), cytoskeletal proteins and scaffolding and adaptor proteins (Baucum, 2017; Bayés et al., 2011, 2012; Collins et al., 2005; Collins et al., 2006; Dosemeci et al., 2006; Peng et al., 2004; Yoshimura et al., 2003). Electron microscopy (EM) (Chen et al., 2008) and super-resolution light microscopy (Dani et al., 2010; MacGillavry & Hoogenraad, 2015; Maglione & Sigrist, 2013; O'Rourke et al., 2012; Sigrist & Sabatini, 2012) studies demonstrate that proteins within the PSD form distinct layers along the axo-dendritic axis of synapses with a sequential order of membrane-spanning glutamate receptors and cell adhesion molecules, PSD scaffolds, and the actin cytoskeleton contacting the interior face of PSDs (**Figure 1B**). Among the most abundant proteins of the PSD are Ca^{2+}/calmodulin-dependent protein kinase II (CaMKII), membrane-associated guanylate kinases (MAGUKs) and subunits of two major iGluR families, the α-amino-3-hydroxy-5-methyl-4-isoxazolepropionic acid receptors (AMPARs) and the N-methyl-D-aspartic acid receptors (NMDARs). The activation of iGluRs results in the influx of sodium ions leading to the depolarization of the postsynaptic cell and, ultimately, an increase in intracellular calcium levels, triggering a cascade of signaling events that induce changes in synaptic plasticity (Sheng & Kim, 2002).

2. AMPA-type glutamate receptors

AMPARs are a type of iGluRs permeable to sodium (influx) and potassium (efflux), but impermeable for calcium (however, a group of calcium-permeable AMPARs have been identified [Wenthold et al., 1996]), mediating the majority of fast excitatory neurotransmission in the CNS (reviewed in Gereau and Swanson, 2008; Chater and Goda, 2014; Henley and Wilkinson, 2016). AMPARs are tetrameric receptors composed of different combinations of four AMPAR subunits (GluA1-4) (Hollmann and Heinemann, 1994). They are enriched in the PSD, moreover, they are highly dynamic, moving in and out of the synaptic area in an activity-dependent manner (Choquet and Triller, 2013). AMPARs are required for adaptive changes in the brain by mediating different forms of synaptic plasticity. Synaptic plasticity is the strengthening or weakening of synaptic transmission in response to specific patterns of activity. The two main forms of synaptic plasticity are long-term potentiation (LTP) and long-term depression (LTD). In LTP, the long-lasting strengthening of

synaptic transmission depends on an increase in the number of synaptic AMPARs (Kennedy, 2013). This process is related to memory formation and learning (Keifer and Zheng, 2010). In contrast, the persistent reduction in synaptic strength observed in LTD is mainly due to a decrease in the number of synaptic AMPARs. Changes in AMPAR subunit composition, phosphorylation state and different accessory proteins regulate AMPARs and therefore impact synaptic strength (Chater and Goda, 2014).

3. NMDA-type glutamate receptors

NMDARs are a subtype of glutamate-gated ion channels (iGluRs), permeable to sodium and calcium (influx) and potassium (efflux), which play critical roles in excitatory neurotransmission in the CNS. The increase in postsynaptic calcium levels following NMDAR activation leads to changes in synaptic efficacy and neuronal morphology (Malenka and Bear, 2004). NMDARs are implicated in several physiological and pathological processes such as synaptic plasticity, excitotoxicity and several CNS disorders, e.g. schizophrenia (Law and Deakin, 2001), anti-NMDAR encephalitis (Dalmau et al., 2008; Hughes et al., 2010; Mikasova et al., 2012), autism spectrum disorders (Won et al., 2012), Alzheimer's disease (Snyder et al., 2005; Hoover et al., 2010), Huntington's disease (Heng et al., 2009; Milnerwood et al., 2010) and Parkinson's disease (Sgambato-Faure and Cenci, 2012). NMDARs form tetramers in the postsynaptic membrane, most generally, associating two obligatory GluN1 subunits and two modulatory GluN2 subunits (Al-Hallaq et al., 2001). The versatility of NMDAR functions may be attributed to its subunit content and organization at the synapse.

3.1. NMDAR structure and expression

3.1.1. NMDAR genes and spatial expression pattern

To date, seven different NMDAR subunits have been identified (**Figure 2**). Based on their sequence homology, the subunits are grouped into 3 subfamilies: the GluN1 (Moriyoshi et al., 1991), the GluN2 (GluN2A, GluN2B, GluN2C, GluN2D) (Monyer et al., 1992) and the GluN3 (GluN3A and GluN3B) (Ciabarra et al., 1995; Sucher et al., 1995) NMDAR subunits. The length of the subunits ranges between ~900 and ~1480 amino acids (Gereau & Swanson,

2008; Paoletti et al., 2013) which is mainly due to differences in the length of the carboxyl (C-)-terminal domain (CTD) (Ryan et al., 2008).

The obligatory GluN1 subunit is encoded by a single gene but has eight distinct isoforms (GluN1-1a to 4a and GluN1-1b to 4b) due to alternative splicing (Moriyoshi et al., 1991) that can take place at exon 5 encoding the N1 cassette of the amino (N-)-terminal domain, or exons 21 or 22 encoding the C1 or C2 cassette of the CTD, respectively. The GluN1 subunit is ubiquitously expressed in the CNS throughout embryonic development and adulthood (**Figure 2**) (Watanabe et al., 1992; Akazawa et al., 1994; Monyer et al., 1994), although there are specific differences in isoform expression. Overall, GluN1-2 isoforms are the most extensively distributed throughout the CNS whereas GluN1-1 (mostly concentrated in the hippocampus and cortex) and GluN1-4 (predominantly found in the thalamus and cerebellum) share complementary distribution patterns and, finally, GluN1-3 is the least abundant (Laurie and Seeburg, 1994; Ferreira et al., 2011).

The four GluN2 subunits, encoded by four different genes, have distinct spatiotemporal expression patterns (**Figure 2**) with GluN2A and GluN2B being the most abundant in the adult forebrain (Watanabe et al., 1992; Akazawa et al., 1994; Monyer et al., 1994). During embryonic and early postnatal development, only GluN2B and GluN2D are expressed, the latter is mainly found in the diencephalon and the brainstem. During the first two postnatal weeks in rodents the expression level of GluN2A gradually increases and becomes abundantly expressed in the entire adult CNS. Meanwhile, the expression of GluN2B peaks between postnatal days (P) 7-10 followed by a restriction to the cortex, hippocampus, striatum and olfactory bulb. The GluN2C subunit is abundant in adult cerebellar granule cells and the olfactory bulb.

The two GluN3 subunits arise from two separate genes and have unique expression patterns (reviewed in Henson et al., 2010) with widespread GluN3A expression during early postnatal life (~P8) followed by a decline and low expression in adulthood (**Figure 2**). GluN3B demonstrates the opposite expression profile compared to that of GluN3A, meaning a low expression in early stages of postnatal development and a progressive increase later on, reaching a full maximum in adulthood (**Figure 2**). GluN3B is ubiquitously expressed in the adult CNS, such as GluN1, suggesting a role for GluN3B in adult NMDAR function (Wee et al., 2008).

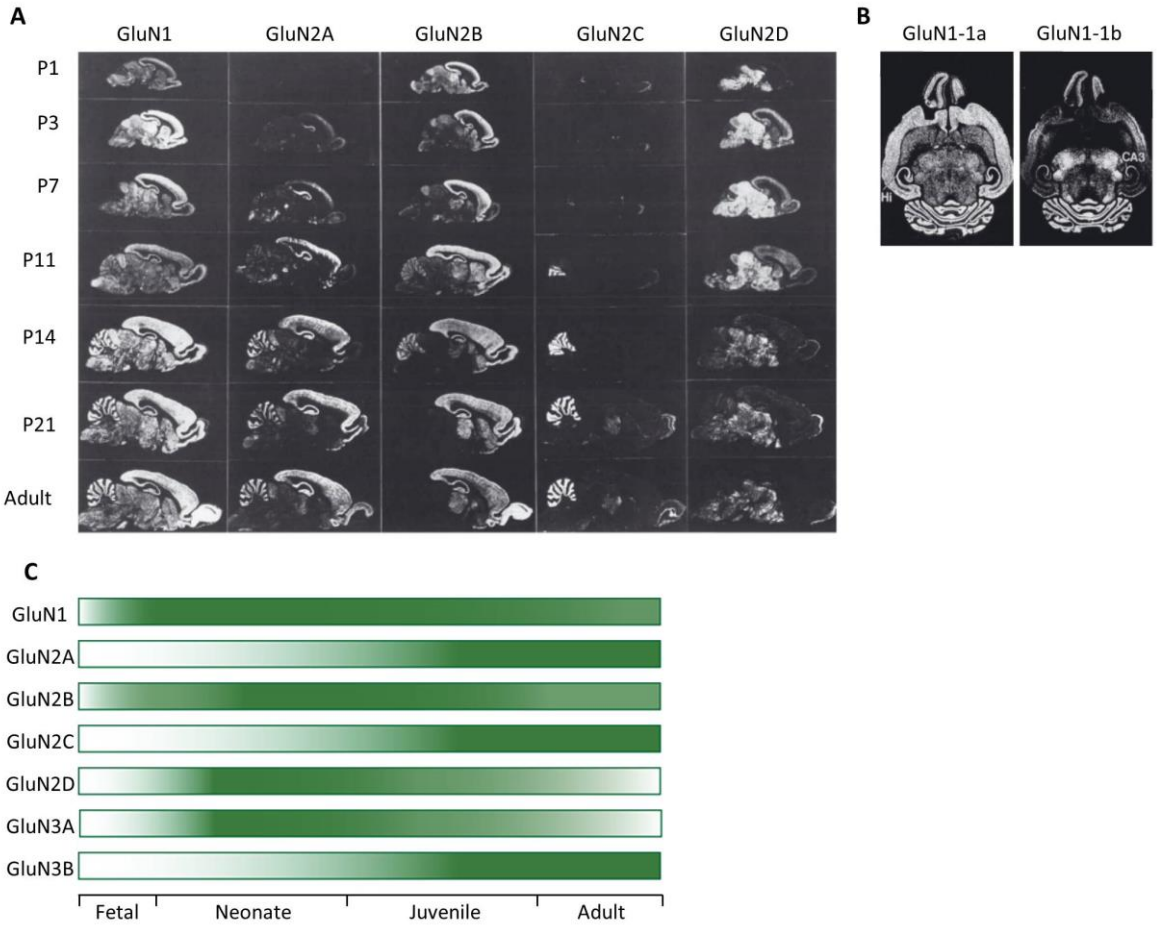

Figure 2. Spatiotemporal expression of NMDAR subunits in the developing rat brain
A. Changes in NMDAR subtype mRNA expression in sagittal brain sections. In situ hybridization data from (Akazawa et al., 1994). **B.** Expression of the GluN1-1a and GluN1-1b splice variants (containing the extracellular N1 cassette) in horizontal sections at P12. In situ hybridization data from (Laurie and Seeburg, 1994). **C.** Schematic representation of the differential expression of NMDAR subunits. The green scale gradient shows the level of expression relative to maximum, with the darkest regions reflecting the highest expression. Adapted from (Henson et al., 2010). P: postnatal day.

3.1.2. NMDAR subunit membrane topology and organization

Similarly to other iGluRs, all NMDAR subunits share a common membrane topology consisting of four distinct modules, further confirmed by its crystal structure (Lee et al., 2014) (**Figure 3**):

1) The first ~380 amino acids comprise the extracellular amino (N-)-terminal domain (NTD) folding into a clamshell-like domain (Karakas et al., 2009) which is responsible for subunit assembly and allosteric regulation (Meddows et al., 2001). This domain has a regulatory role in modulating receptor open probability, deactivation and desensitization (Yuan et al., 2009). The NTD may also contain binding domains for extracellular proteins (Dalva et al., 2000; Wang et al., 2006).

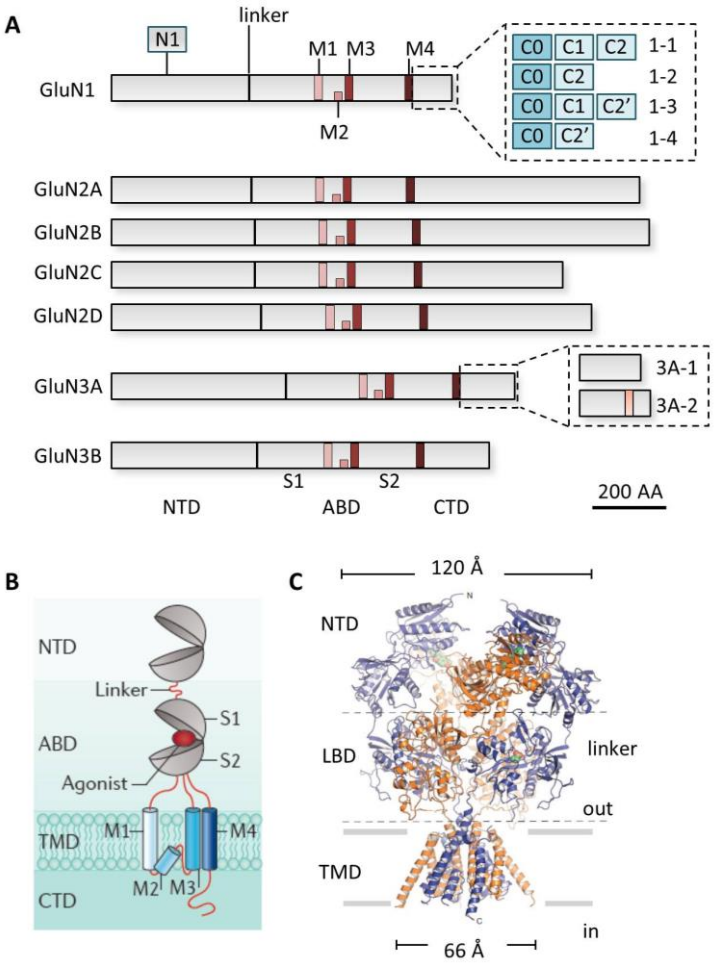

Figure 3. Structure of NMDAR subunits

A. Structural domains of NMDAR subtypes. Subunit heterogeneity is further increased by alternative splicing of the GluN1 and GluN3A subunits. The most divergent regions are the NTD and CTD. Adapted from (Paoletti et al., 2013). **B.** NMDAR subunit organization in the membrane: extracellular N-terminal domain (NTD), agonist-binding domain (ABD), transmembrane domain (TMD), intracellular C-terminal domain (CTD). Adapted from (Paoletti et al., 2013). **C.** X-ray crystal structure of GluN1-GluN2B NMDAR reveals a mushroom-like shape with a height of 120Å and width of 150Å. Data from (Lee et al., 2014).

2) The extracellular agonist-binding domain (ABD, ~300 amino acids) is formed by two discontinuous segments S1 and S2 adopting a clamshell-like conformation (Stern-Bach et al., 1994). The ABD is responsible for binding glycine or D-serine in case of the GluN1 and GluN3 subunits and glutamate in GluN2 subunits (Furukawa et al., 2005; Yao & Mayer, 2006).

3) The transmembrane domain (TMD) is composed of three transmembrane helices (M1, M3 and M4) and the M2 pore loop that together form the ion channel pore and define receptor conductance, ion selectivity and affinity for the Mg^{2+} block (reviewed in Paoletti, 2011).

4) The intracellular CTD, which is highly variable in length depending on the subunit, provides multiple sites of posttranslational modifications and interaction with intracellular proteins implicated in receptor trafficking, anchoring and signaling (Sheng, 2001).

3.2. NMDAR assembly and trafficking

3.2.1. Processing of NMDARs in the endoplasmic reticulum

Similarly to other membrane proteins, NMDAR subunits go through a quality check in the endoplasmic reticulum (ER) that ensures proper protein folding. In the case of multimeric NMDARs the monomeric subunits are retained in the ER, due to different ER retention signals/mechanisms, until assembly of the complete and functionally active NMDAR (reviewed in Gereau & Swanson, 2008; Horak et al., 2014; Prybylowski & Wenthold, 2004a; Traynelis et al., 2010). These retention signals can be suppressed by conformational changes or overridden by export signals once the subunits form a proper combination ready to exit the ER (reviewed in Horak et al., 2014; Prybylowski & Wenthold, 2004; Wenthold et al., 2003).

In neurons, the GluN1 subunit is produced in excess in the ER compared to the GluN2 subunits, allowing for sufficient amounts of GluN1 subunits available for newly synthesized GluN2 and GluN3 subunits (Chazot & Stephenson, 1997; Huh & Wenthold, 1999). The pool of GluN1 monomers is rapidly degraded (half-life: ~2 hours) if no assembly occurs (Huh and Wenthold, 1999), suggesting a rate limiting role of the availability of GluN2 subunits in the generation of new functional receptors.

Several models exist for the assembly of NMDARs (reviewed in Horak et al., 2014 and Traynelis et al., 2010). The first model proposes that a GluN1-GluN1 homodimer forms a functional heterotetramer with a pre-formed GluN2-GluN2 homodimer (Hansen et al., 2010; Meddows et al., 2001; Papadakis et al., 2004; Qiu et al., 2005; Schorge & Colquhoun, 2003). The second model suggests that two GluN1-GluN2 heterodimers form the heterotetrameric receptor (Schüler et al., 2008) while the third model proposes the sequential addition of two GluN2 monomers to an already existing GluN1-GluN1 homodimer (Atlason et al., 2007).

3.2.2. NMDAR trafficking to the synapse

Once a heterotetrameric NMDAR is released from the ER, it is transported to the Golgi apparatus for further modifications and then sorted in the trans-Golgi network (TGN) into mobile packets or endosomes that reach the plasma membrane *via* kinesin and myosin motor proteins (**Figure 4**) (Guillaud et al., 2003; Setou et al., 2000; Washbourne et al., 2002; Washbourne et al., 2004). In young cortical neurons, prior to synapse formation, NMDARs are continuously recycled from the cell surface to intracellular organelles (Washbourne et al., 2004).

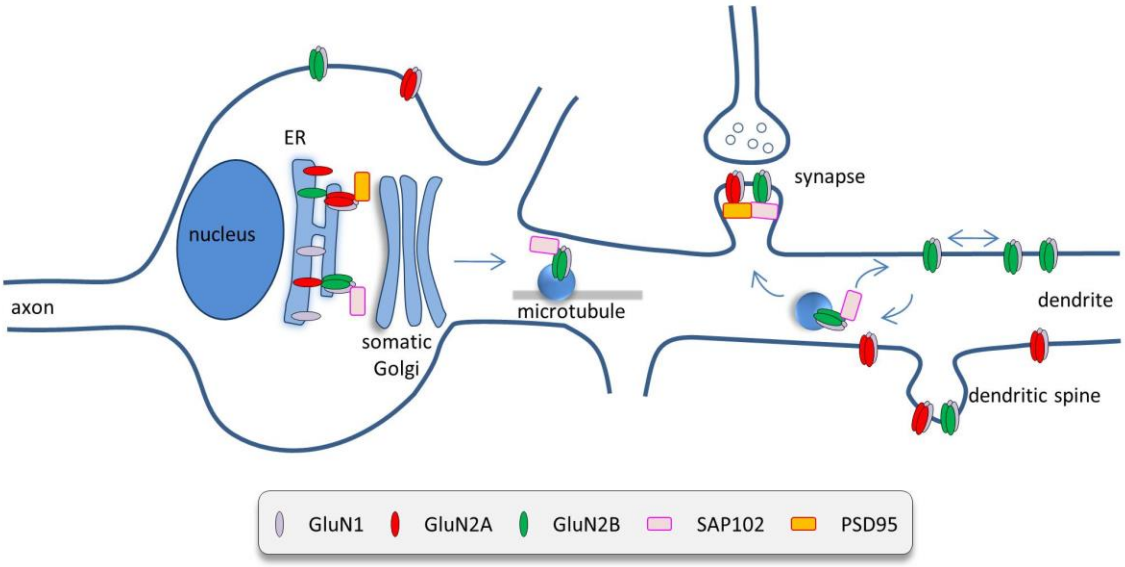

Figure 4. NMDAR assembly and trafficking from the ER to the membrane
Schematic representation of NMDAR tetrameric assembly and intracellular trafficking: after being processed in the endoplasmic reticulum (ER), functional NMDARs associated to their protein partners such as PSD95 or SAP102 are sorted into vesicles in the somatic Golgi network and transported along microtubules to the dendritic shaft. NMDARs are expressed at the cell surface by exocytosis. The number of surface NMDARs relies on a dynamic equilibrium between exo- and endocytosis as well as lateral diffusion. Adapted from (Bard and Groc, 2011).

Cycling of NMDARs to and from the synapse depends highly on synaptic activity and is regulated by different factors (reviewed in Nong et al., 2004; Pérez-Otaño & Ehlers, 2004). The site for exocytosis of NMDARs is not clear but it may occur at extrasynaptic sites (Rao et al., 1998) followed by receptor diffusion to the synaptic site (Groc et al., 2004; Tovar & Westbrook, 2002; Triller & Choquet, 2005), or NMDARs may be directly inserted into the synapses *via* actin/myosin transport (Guillaud et al., 2003).

It has been proposed that PDZ (PSD95/Discs-large/ZO-1) domain containing proteins, such as the membrane-associated guanylate kinase (MAGUK) family (e.g. PSD95, PSD93, SAP102 and SAP97) – apart from their anchoring role (discussed in detail in chapter 4.3.1.) – are important for NMDAR trafficking to and from the synapse (reviewed in Elias & Nicoll, 2007; Kneussel, 2005; Wenthold et al., 2003). NMDARs associate with PSD95 and SAP102 along the secretory pathway which promotes their insertion into the postsynaptic membrane (Lin et al., 2004; Sans et al., 2003; Standley et al., 2012; Standley et al., 2000).

The rate of NMDAR exocytosis may also be regulated by posttranslational modifications such as phosphorylation by protein kinase C (PKC) (Lan et al., 2001; Scott et al., 2001) or palmitoylation (Mattison et al., 2012). The activation of dopamine receptors

(Dunah & Standaert, 2001; Hu et al., 2010) and TNFα (Wheeler et al., 2009) also promotes the insertion of NMDARs into the cell membrane.

While most NMDARs are processed and assembled in the cell body and then transported to the synapse (termed canonical trafficking), NMDAR subunit mRNAs have been found in dendrites (Benson, 1997; Steward and Schuman, 2003), suggesting a role of synaptic NMDAR synthesis. In this case, the proteins are thought to be assembled and transported within the ER to dendritic Golgi outposts (termed non-canonical trafficking) (Mauceri et al., 2007; Pierce et al., 2001; Ramírez & Couve, 2011). Interestingly, dendritic GluN2A synthesis is followed by insertion of this subunit into the membrane (Swanger et al., 2013).

3.2.3. NMDAR recycling

NMDARs undergo rapid and constitutive endocytosis as observed in young cortical neurons (Roche et al., 2001). This process is mediated by clathrin-coated vesicles with a rate of internalization that depends on the association of the receptors with the AP-2 adaptor protein that links cargo proteins to clathrin-coated pits (Roche et al., 2001). NMDAR internalization may also occur *via* clathrin-independent endocytosis (Kato et al., 2005; Swanwick et al., 2009).

The rate of NMDAR internalization depends also on synaptic activity (agonist binding), the type of NMDAR subunit expressed (Lavezzari et al., 2004) as well as binding to scaffold proteins (reviewed in Gereau & Swanson, 2008; Nong et al., 2004). NMDAR autoantibodies present in various diseases also induce the internalization of the receptors (reviewed in Masdeu et al., 2016). The presence of specialized endocytic zones at the edge of the synaptic active zone (Blanpied et al., 2002; Petralia et al., 2003) suggests that NMDAR might be required to move laterally away from the PSD for internalization.

3.2.4. NMDAR lateral mobility

Similarly to other neurotransmitter receptors (reviewed in Choquet & Triller, 2013), NMDARs are highly mobile and may be exchanged between synaptic and extrasynaptic sites (Groc et al., 2004) as observed primarily by rapid recovery in the synaptic NMDAR current following selective blocking of synaptic NMDAR channels (Tovar and Westbrook, 2002). NMDAR surface mobility depends mainly on the subunit composition, with GluN2A-NMDARs being less mobile and spending more time in the PSD area compared to GluN2B-NMDARs (Groc et al., 2006). However, other regulators of NMDAR mobility have also been

described. A decrease in the synaptic residency time of GluN2B-NMDARs is observed during development, accompanied by stronger synaptic stabilization of GluN2A-NMDARs in later stages of development (Groc et al., 2006). Extracellular regulators, such as NMDAR co-agonists and extracellular matrix proteins, also affect receptor mobility (Groc et al., 2007; Papouin et al., 2012; Ferreira et al., 2017). D-serine and glycine have been shown to differentially modulate the surface behavior of GluN2 subunits with a preferential negative effect of glycine on GluN2A-NMDARs while D-serine decreases GluN2B-NMDAR surface diffusion (Papouin et al., 2012; Ferreira et al., 2017). The extracellular matrix protein reelin specifically reduces GluN2B-NMDAR mobility while increasing its time spent within the synaptic area (Groc et al., 2007). Additionally, protein kinase activity (Groc et al., 2004; Dupuis et al., 2014) and interactions with other membrane receptors (Ladepeche et al., 2013; Dupuis et al., 2014) or intracellular scaffolds (Bard et al., 2010) also control the surface dynamics of NMDARs.

3.3. NMDAR localization

NMDARs are primarily localized at postsynaptic sites; however, they can also be found in perisynaptic (Zhang and Diamond, 2009), extrasynaptic (Brickley et al., 2003; Thomas et al., 2006; Harris and Pettit, 2007; Petralia et al., 2010) and presynaptic locations (Bidoret et al., 2009) – regulating neurotransmitter release – and peripheral (non CNS) NMDARs have also been found (Moroni et al.,1986; Nishikawa et al., 1982).

3.3.1. NMDAR expression throughout the body

NMDARs have been identified in a number of different non-neuronal cell types and tissues throughout the body such as keratinocytes, lymphocytes, arteries, bone cells, heart, lung, thymus, stomach, ovaries, spleen, skeletal muscle, pancreas, lower urogenital tract, renal pelvis and kidney (reviewed in Bozic & Valdivielso, 2015; Genever & Skerry, 2000 and Hogan-Cann & Anderson, 2016). Emerging data suggest that peripheral NMDARs maybe involved in a wide range of physiological and pathophysiological processes including but not limited to bone deposition, wound healing, insulin secretion, blood–brain barrier integrity, inflammation, pain sensitivity, and myelination. NMDARs expressed in bone, kidney, pancreas, and other tissues are promising therapeutic targets for disorders such as osteoporosis, acute renal injury, diabetes, and cancer (Hogan-Cann and Anderson, 2016).

3.3.2. Presynaptic NMDARs

In the CNS, NMDARs are predominantly postsynaptic, but there is increasing anatomical and physiological evidence that they are also present in the pre-synapse (reviewed in Banerjee et al., 2016; and Bouvier et al., 2015). Presynaptic NMDARs (preNMDARs) are thought to modulate neurotransmitter release (Berretta and Jones, 1996; Sjöström et al., 2003; Brasier and Feldman, 2008). Subunit composition of preNMDARs varies similarly to postsynaptic NMDARs (reviewed in Bouvier et al., 2015) and they are expressed at both excitatory and inhibitory (Duguid and Smart, 2004; Xu and Smith, 2015) synapses. Their expression is most abundant during early developmental stages suggesting a role in maturation of synapses and the neural network (reviewed in Bouvier et al., 2015). PreNMDARs have also been linked to CNS disorders, such as epilepsy (Yang et al., 2006).

3.3.3. Extrasynaptic NMDARs

The subcellular localization of NMDARs was first assessed using classical immunohistochemical techniques, revealing a wide distribution of NMDARs throughout the dendritic arborization, both at synaptic and extrasynaptic sites (Aoki et al., 1994; Siegel et al., 1994). The extrasynaptic zone refers to all parts of the neuron outside the synaptic active zone, therefore these receptors can be found in the dendritic spine neck, the dendritic shaft or even the soma (reviewed in Newpher & Ehlers, 2008 and Petralia, 2012).

Young developing neurons show a high expression of extrasynaptic NMDARs which are thought to have a role in synaptogenesis and neuronal development (Georgiev et al., 2008; Sin et al., 2002; Wang et al., 2011). In developing hippocampal neurons *in vivo*, extrasynaptic NMDARs can be found in distinctive densities (Sans et al., 2000; Petralia et al., 2003, 2005, 2010) proposed to be either sites of new synapse formation or remnants of former synapses containing NMDAR partners such as PSD95 or SAP102 (Petralia, 2012). Based on physiological studies performed on neuronal cultures at early developmental stages (~1 week in vitro, WIV), approximately 75% of NMDARs are extrasynaptic (Tovar and Westbrook, 1999) with a decrease observed at 2 WIV to 20-50% (Ivanov et al., 2006). Based on work by Groc and colleagues, the levels of extrasynaptic GluN2B-containing NMDARs remain high throughout this developmental window while GluN2A-containing NMDARs preferentially move to synaptic areas (Groc et al., 2004; Groc et al., 2006; Groc et al., 2009). Therefore, the best-characterized extrasynaptic NMDARs are mainly composed of GluN1 and GluN2B or

GluN2D subunits, however, GluN2D may be exclusively extrasynaptic (Brickley et al., 2003; Harney et al., 2008).

Extrasynaptic NMDARs may be activated by glutamate spillover (Chen & Diamond, 2002; Higgs & Lukasiewicz, 1999) or by ectopic glutamate released from glial cells (Jourdain et al., 2007; Le Meur et al., 2007; Matsui, 2005). Their activation is generally related to pathological conditions leading to cell damage and cell death or even diseases (reviewed in Hardingham & Bading, 2010), however, extrasynaptic NMDARs may also be activated under physiological conditions (Harris & Pettit, 2007).

3.4. NMDAR activation

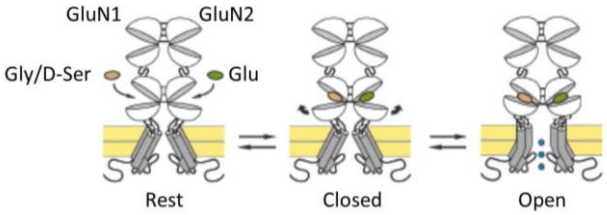

Figure 5. Mechanism of NMDAR activation
NMDAR channel opening requires the simultaneous binding of glycine/D-serine (GluN1) and glutamate (GluN2). Adapted from (Paoletti, 2011).

Uniquely among iGluRs, NMDARs require the simultaneous binding of two co-agonists, glycine (or D-serine, Mothet et al., 2000; Schell et al., 1995) and glutamate (Johnson & Ascher, 1987; Kleckner & Dingledine, 1988) (**Figure 5**). Glycine (or D-serine) binds to the GluN1 (Furukawa and Gouaux, 2003) and GluN3 (Yao et al., 2008) subunits while glutamate binds to GluN2 subunits (Furukawa et al., 2005). At resting membrane potential, the NMDAR channel pore is blocked by extracellular Mg^{2+} in a voltage-dependent manner (Mayer et al., 1984). This defines the unique role of NMDARs as molecular coincidence detectors since ion influx only occurs when both postsynaptic depolarization (to relieve the Mg^{2+} block) and presynaptic release of glutamate occur simultaneously. In other words, the simultaneous stimulation of both the pre- and postsynaptic neuron is required for NMDAR activation, as well as a third element, which is the binding of the co-agonist glycine or D-serine (Sanz-Clemente et al., 2013b). Following binding of the agonists, the cleft formed by the ABD dimer closes, triggering rearrangement of the channel pore-forming TMDs, thus promoting channel pore opening (Mayer, 2006). This activation sequence seems to be conserved in NMDARs even though differences exist between receptor subclasses (Furukawa et al., 2005; Mayer, 2006; Paoletti & Neyton, 2007). NMDAR activity can also be modulated by extracellular compounds such as ions (H^+ or Zn^{2+}) or polyamines (e.g. spermine) (reviewed in Traynelis et al., 2010).

3.4.1. NMDARs in synaptic plasticity

Long-lasting experience-dependent changes in the efficacy of synaptic transmission are believed to represent the cellular basis of learning and memory. These adaptive processes often require the activation of postsynaptic NMDARs and NMDAR-dependent Ca^{2+} influx. As detailed above, the activation of NMDARs not only requires the binding of glutamate and co-agonists, but also depends upon membrane depolarization to remove the voltage-dependent Mg^{2+} block. This combined requirement for agonists and postsynaptic depolarization enables NMDARs to function as molecular coincidence detectors of pre- and postsynaptic activity, a prerequisite for the induction of synaptic plasticity such as LTP or LTD (reviewed in Lau and Zukin, 2007; Collingridge et al., 2010; Volianskis et al., 2015). Most generally, LTP is induced by high frequency tetanic stimulation, leading to Na^{+}-influx *via* AMPARs which depolarizes the postsynaptic compartment, and induces NMDAR activation. The NMDAR-mediated rise in postsynaptic Ca^{2+} levels results in the activation of CaMKII – among other kinases and phosphatases – which phosphorylates AMPARs and thus promotes an increase in the number of synaptic AMPARs (Lau and Zukin, 2007; Chater and Goda, 2014). In contrast, LTD involves the de-phosphorylation of AMPARs and a decrease in synaptic AMPAR number (Lau and Zukin, 2007).

3.5. NMDAR subtypes and functional properties

Functional NMDARs are tetramers composed of different subunits. Generally, NMDARs are diheteromers containing two GluN1 subunits and two identical GluN2 or GluN3 subunits, assembling as a dimer of dimers. One neuron can simultaneously express different GluN1 isoforms and GluN2 subunits (Cull-Candy and Leszkiewicz, 2004) giving rise to various NMDAR subtypes. Examples of receptors with two different GluN1 isoforms have been reported (Sheng et al., 1994). Besides the diheteromeric NMDARs, receptors containing two different types of GluN2 subunits – termed triheteromeric – have been described (Sheng et al., 1994). Triheteromeric GluN1/GluN2A/GluN2B receptors are abundant in the hippocampus and the cortex (Chazot & Stephenson, 1997) while GluN1/GluN2B/GluN2D receptors are expressed in the diencephalon (Brickley et al., 2003; Dunah et al., 1998) and GluN1/GluN2A/GluN2C receptors in the cerebellum (Cathala et al., 2000). The subunit composition defines the expression, biophysical, pharmacological and signaling properties of NMDARs.

Table 1. Comparing permeation and gating properties of different GluN2B subunits. Adapted from (Paoletti, 2011).

GluN2-subunit specific characteristics				
	GluN2A	**GluN2B**	**GluN2C**	**GluN2D**
Conductance (pS)	50	50	37	37
Mean open time (ms)	3-5	3-5	0.5-1	0.5-1
EC_{50} (glycine), µM	1.7	0.4	0.3	0.1
EC_{50} (glutamate), µM	4	2	1	0.4
τ_{off} (glycine), ms	140		680	
τ_{off} (glutamate), ms	40	300	300	2000
IC_{50} (Mg^{2+}), µM (Vm=-100mV)	2	2	12	12
P_f (Ca^{2+}), %	18	18	8	n.d.

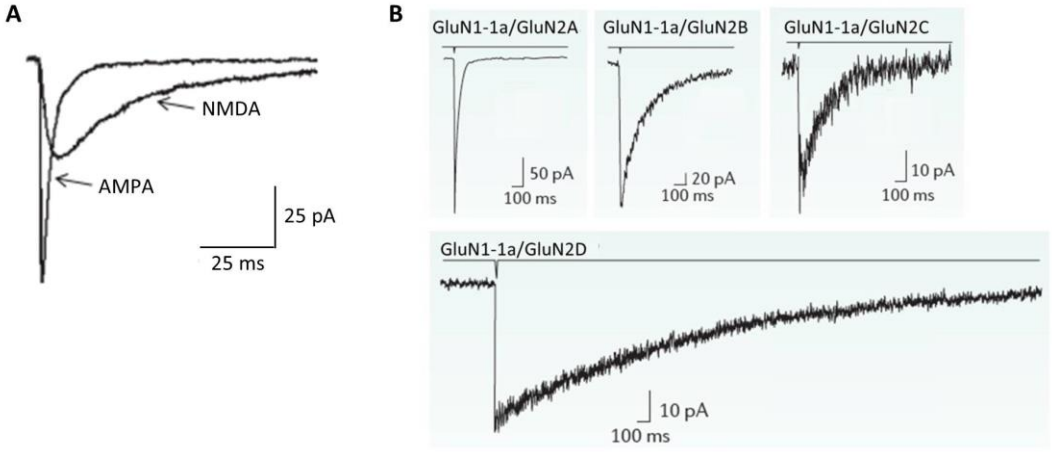

Figure 6. NMDAR channel characteristics
A. Comparison of NMDAR and AMPAR current kinetics at: glutamate binding to synaptic AMPARs triggers a brief, rapidly rising conductance decaying in 1-2 ms compared to the slower activation (rise time) and longer-lasting (long deactivation) current of NMDARs. Data from (Traynelis et al., 2010). **B.** Differential deactivation kinetics of NMDARs based on subunit composition: human embryonic kidney cells (HEK) were transfected with GluN1-1a isoform and one GluN2 subunit. NMDAR-mediated currents were induced by a brief (<5 ms) application of saturating glutamate (1 mM). GluN2A-containing receptors deactivate the fastest compared to all other receptor subtypes. Adapted from (Paoletti et al., 2013)**.**

Compared to other iGluRs, NMDARs exhibit unique activation characteristics, as described above (chapter 3.4.) (voltage-dependent Mg^{2+} block and binding of two agonists). Moreover, NMDARs are highly permeable to Ca^{2+} and they possess unusually slow activation and deactivation kinetics due to the slow release of glutamate (**Figure 6A**). These unique features are influenced by the subunit composition (**Table 1, Figure 6B**). Diheteromeric GluN1/GluN2A or GluN1/GluN2B receptors generally display large conductance (Stern et al., 1992), high sensitivity to the Mg^{2+} block (Kuner and Schoepfer, 1996) and high Ca^{2+} permeability (Burnashev et al., 1995; Schneggenburger, 1996) compared to GluN2C- or

GluN2D-containing receptors (reviewed in Dingledine et al., 1999 and Farrant et al., 1994). Incorporation of a GluN3 subunit results in an even more dramatic decrease in the Mg^{2+} blockade (Matsuda et al., 2002). GluN3 subunits bind glycine and not glutamate, thus NMDARs containing exclusively GluN1/GluN3 subunits can act as excitatory glycine receptors, which are impermeable to Ca^{2+} (Pérez-Otaño et al., 2016). The subunit composition also determines NMDAR agonist sensitivity, activation and deactivation kinetics, as well as open channel probability and duration (reviewed in Paoletti, 2011; Traynelis et al., 2010). GluN1/GluN2A receptors have the shortest deactivation constant (Vicini et al., 1998) and a higher open probability compared to GluN2B-, GluN2C- or GluN2D-containing receptors (Chen et al., 1999); however, they have the lowest sensitivity to both glutamate and glycine (Yuan et al., 2009). Many pharmacological compounds can also discriminate between NMDAR subtypes. Ifenprodil, a potent non-competitive NMDAR antagonist, and its derivatives (e.g. Ro 25-6981) selectively inhibit GluN1/GluN2B receptors by stabilizing the GluN2B NTD in a closed conformation (Karakas et al., 2011).

3.6. Implication of NMDARs in CNS disorders

NMDARs are indispensable for proper neuronal development and synaptic plasticity. Therefore, NMDAR dysfunction, expressed as altered subunit expression, trafficking, localization or activity, has been reported in several brain disorders (**Table 2**) (reviewed in Paoletti et al., 2013; Sanz-Clemente et al., 2013; Sun et al., 2017). Both NMDAR hyperactivity and hypofunction can be extremely harmful; increased NMDAR signaling (leading to neuronal cell death) has been implicated in various neurodegenerative diseases, such as Alzheimer's (Snyder et al., 2005; Hoover et al., 2010), Parkinson's (Sgambato-Faure and Cenci, 2012) or Huntington's (Heng et al., 2009; Milnerwood et al., 2010) diseases, whereas reduced NMDAR signaling has been shown in patients with schizophrenia (Law and Deakin, 2001). NMDAR antagonists or NMDAR potentiators have been successfully used – or are currently being tested – in therapy; however, as not all NMDAR subtypes contribute equally to CNS diseases (**Table 2**), subunit-selective modulators can be effective in targeting certain diseases (reviewed in Paoletti et al., 2013).

Table 2. Implications of NMDARs in CNS disorders. Adapted from (Paoletti et al., 2013; Sanz-Clemente et al., 2013b).

Disorder	NMDAR subunit related alterations	Therapy
Alzheimer's disease	Reduced GluN2B surface expression; GluN2B-NMDAR activation mediates amyloid-β (Aβ)-induced alterations in synaptic plasticity and synapse loss, enhanced excitotoxicity	NMDAR antagonist (memantine), GluN2B-selective antagonist
Parkinson's disease	Increased synaptic GluN2A expression; GluN2B redistribution from synaptic to extrasynaptic locations	GluN2B-selective antagonists; interventions targeting GluN2A subunits (possibly)
Huntington's disease	Increased extrasynaptic GluN2B-NMDAR activation, enhanced excitotoxicity	NMDAR antagonist, GluN2B-selective antagonist
Ischemia and stroke	Enhanced levels of extracellular glutamate leading to increased extrasynaptic GluN2B-NMDAR activation	GluN2B-selective antagonists, peptides disrupting GluN2B-interacting partners
Schizophrenia	Reduced NMDAR function; altered NMDAR trafficking	NMDAR potentiators; D-serine, glycine and glycine transporter 1 inhibitors
Chronic pain	Alterations in GluN2B-NMDAR synaptic expression and phosphorylation state; potential involvement of GluN2A-NMDARs	GluN2B-selective antagonists
Depression	NMDAR inhibitors induce reduction in depressive symptoms	NMDAR antagonists (ketamine) or GluN2B-selective antagonists
Autism spectrum disorders	Unclear; either reduced or enhanced NMDAR function is implicated	Potentially NMDAR antagonists or potentiators
Anti-NMDAR encephalitis	Presence of anti-NMDAR antibodies; reduced NMDAR density, impairments in synaptic plasticity; dispersion of GluN2A from the synapse	Potentially NMDAR potentiators

4. GluN2A- and GluN2B-NMDARs

In the past few decades, the GluN2A and GluN2B subunits have been most extensively studied and are the best characterized NMDAR subunits. Both are highly expressed in the cortex and hippocampus playing central roles in synaptic plasticity and they are also involved in learning and memory. Additionally, both GluN2A and GluN2B have been implicated in several neurological disorders. Nonetheless, despite their intense investigation, many open questions remain about their precise subcellular localization and contribution to NMDAR-mediated signaling.

4.1. Comparison of GluN2A- and GluN2B-NMDARs

The GluN2A and GluN2B NMDAR subunits are encoded by two separate genes, *Grin2a* and *Grin2b*, respectively. They are closely related in amino acid sequence (68%); however, the sequence homology is differentially distributed according to the structural domains: homology is especially high in the TMD (92.3%), yet modest in the NTD (80.3%) and very low in the large intracellular CTD (48.6%) (**Figure 7**) (Ishii et al., 1993) important for subunit-specific interactions and posttranslational modifications (Salter & Kalia, 2004; Sheng, 2001).

Mice lacking the GluN2A subunit are viable; however, they show impairment in synaptic plasticity mechanisms translating into deficiency in spatial learning (Sakimura et al., 1995). In contrast, mice lacking the GluN2B subunit die shortly after birth due to the absence of the suckling response, indicating an essential role for GluN2B in neuronal development (Kutsuwada et al., 1996). Interestingly, overexpression of GluN2B enhances memory and learning abilities (Tang et al., 1999).

Depending on the GluN2 subunit expressed, NMDARs have different characteristics (**Table 3**). Briefly, GluN2A-NMDARs have higher open probability and peak current, faster deactivation, rise and decay times compared to GluN2B-NMDARs; however, they have a lower permeability to Ca^{2+} than GluN2B-NMDARs.

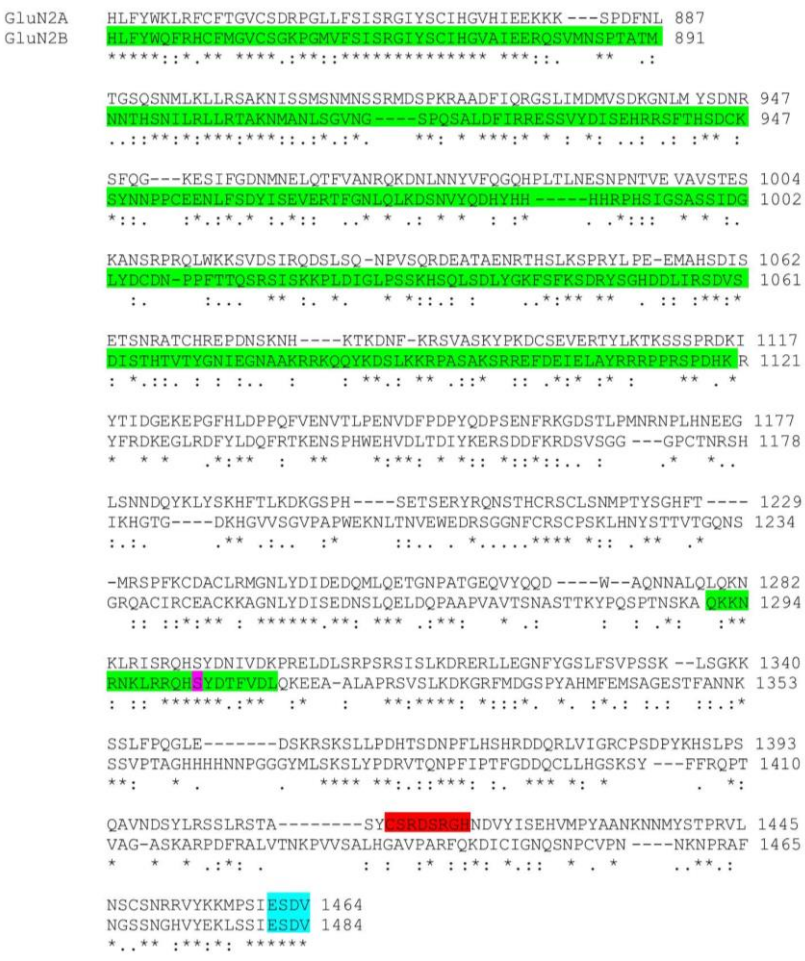

Figure 7. Comparison of the CTDs of GluN2A and GluN2B
Alignment of the CTD sequences of human GluN2A (amino acids 838-1464) and GluN2B (amino acids 839-1484) was done in UniProt using Clustal Omega. Alignment shows a 32.8% sequence identity and 48.6% sequence homology.
(*****) indicates positions which have a single, fully conserved residue.
(**:**) indicates conservation between groups of strongly similar properties.
(.) indicates conservation between groups of weakly similar properties.
Color code: turquoise: PDZ-binding motif, red: CaMKII-binding site in GluN2A, bright green: CaMKII-binding sites in GluN2B, pink: CaMKII phosphorylation site in GluN2B.

The GluN2B subunit is important in maintaining normal spine density and regular numbers of NMDARs at the synapse (Abe, 2004; Akashi et al., 2009; Brigman et al., 2010; Kim et al., 2005). Interestingly, overexpression of GluN2B does not affect synapse number and growth; however, it does increase spine motility, adding and retracting spines at a higher rate (Gambrill and Barria, 2011). In contrast, early expression of GluN2A reduces the number of synapses, as well as the spine volume and dynamics (Gambrill and Barria, 2011). GluN2B-NMDARs have also been shown to restrict the synaptic insertion of AMPARs (Hall et al., 2007; Gray et al., 2011; Ferreira et al., 2015).

The GluN2A and GluN2B subunits are also thought to regulate the synaptic localization of NMDARs *via* different interaction partners which define their coupling to independent signaling cascades and, thus, differentially impact synaptic plasticity (detailed in chapter 4.4.) (reviewed in Shipton & Paulsen, 2014).

Table 3. Comparison of GluN2A- and GluN2B-containing NMDARs. Adapted from (Sanz-Clemente et al., 2013; Yashiro & Philpot, 2008).

GluN2A- *versus* GluN2B-NMDARs		
Developmental Expression	**GluN2A**	**GluN2B**
Expression start	postnatal	prenatal
Expression peak	adulthood	rodent: P7-P10; human: early childhood
Regional expression	Ubiquitous in CNS	Forebrain
Channel properties		
Glutamate affinity	low	high
Open probability	high	low
Deactivation kinetics	fast	slow
Rise and decay time	fast	slow
Peak current	high	low
Charge transfer	low	high
Ca^{2+} influx	low	high
Transport		
Preferential binding	SAP97	KIF 17
Surface diffusion	low	high
Endocytosis		
Preferential association	late endosomes	recycling endosomes
Localization in mature neurons	mainly synaptic	synaptic and extrasynaptic
Posttranslational modifications		
Phosphorylation		
CaMKII binding	weak	strong
Unique phosphosites	Ser-1232 by Cdk5	Ser-1480 by Ck2
Synaptic delivery	activity and glutamate binding dependent	activity-dependent
Knockout mice	viable	non-viable

4.2. The GluN2B-to-GluN2A developmental switch

The expression of GluN2A and GluN2B is relatively broad throughout the CNS and both are developmentally regulated with a concurrent decrease in GluN2B and increase in GluN2A subunits (Monyer et al., 1994; Sans et al., 2000; Sheng et al., 1994).

In early developmental stages, GluN1/GluN2B diheteromers represent the majority of synaptic NMDARs, indicated by the high sensitivity of excitatory post-synaptic currents (EPSCs) to selective GluN2B inhibitor ifenprodil (Bellone and Nicoll, 2007). The expression of GluN2A increases during development and in mature synapses this subunit forms the primary type of NMDARs expressed at the synapse, as suggested from the reduced sensitivity to ifenprodil (Bellone and Nicoll, 2007). These changes occur both at the mRNA (Liu et al., 2004; Nase et al., 1999) and protein level (Chen et al., 2000; Quinlan et al., 1999; Roberts & Ramoa, 1999; Siu et al., 2017) and are evolutionarily conserved, from amphibians to mammals (Sanz-Clemente et al., 2013b). Surprisingly, Frank and colleagues recently demonstrated a four-fold molar excess of GluN2B compared to GluN2A in the adult mouse forebrain (Frank et al., 2016).

An extensive study using human postmortem visual cortex samples demonstrated high expression of GluN2B in childhood (peak at 1.2±0.7 years) with a relatively constant expression through teens, young adults, and older adults (Siu et al., 2017). Interestingly, they observed an increase in GluN2A expression until ~40 years followed by a dramatic decrease during aging (**Figure 8**) (Siu et al., 2017).

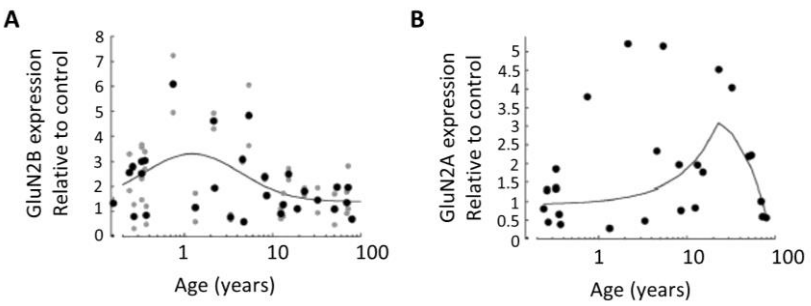

Figure 8. Developmental changes of GluN2A and GluN2B expression in the human visual cortex
Scatterplots of GluN2B (**A**) or GluN2A (**B**) protein expression across the lifespan fit with a Gaussian function (**A**) or weighted curve (**B**). Data from (Siu et al., 2017).

The shift from GluN2B to GluN2A has been observed in several brain areas, such as cortex (Flint et al., 1997; Sheng et al., 1994; Williams et al., 1993), hippocampus (Monyer et al., 1994), and cerebellum (Akazawa et al., 1994; reviewed in Dumas, 2005). In the neocortex, it occurs during the critical period of visual development, and the switch is

influenced by sensory experience (Philpot et al., 2001). The developmental switch is important in many aspects since GluN2B expression can inhibit the synaptic incorporation of AMPARs (Gray et al., 2011; Hall et al., 2007) and reduce the threshold for LTP and increase its magnitude (Lee, 2010; Xu et al., 2009; Yashiro & Philpot, 2008). Moreover, GluN2B-NMDARs promote plasticity-induced spine growth (Lee et al., 2010), dendritic patterning critical for information processing (Espinosa et al., 2009) and hippocampus-dependent learning (von Engelhardt et al., 2008). The change in subunit composition affects the kinetics of EPSCs (Monyer et al., 1992, 1994; Flint et al., 1997) and the Ca^{2+} current per unit charge (Sobczyk et al., 2005). Interestingly, experimental elimination of GluN2B in adult animals or adult neuronal cultures increased the number of functional synapses and the absence of GluN2A increased the strength of unitary connections (Gray et al., 2011; Hall et al., 2007).

Groc and colleagues demonstrated that the developmental change in the synaptic content of GluN2A and GluN2B subunits is correlated with changes in the time spent within the synapse (Groc et al., 2006). The synaptic residency time of GluN2B-NMDARs decreased by three-fold from 8 to 15 days *in vitro* (DIV), indicating an increased surface stabilization of the GluN2B subunit in young synapses. Consistently, GluN2A-NMDARs displayed a symmetric evolution with stronger stabilization in mature synapses (Groc et al., 2006).

Although the expression of GluN2A and GluN2B are crucial in many developmental and pathological processes, the regulation of their expression is poorly understood. Thus far, two regulatory mechanisms have been identified: 1) the transcriptional repressor REST has been shown to repress *Grin2b* signaling *via* epigenetic remodeling (Rodenas-Ruano et al., 2012), 2) two miRNAs miR-19a and miR-539 – in collaboration with REST – can influence the levels of GluN2A and GluN2B, respectively (Corbel et al., 2015).

4.3. Regulation of GluN2A- and GluN2B-NMDARs

The cytoplasmic CTDs are the least conserved regions among GluN2A and GluN2B (48.6% sequence homology), and thus they provide sites of subunit-specific regulations with implications in receptor trafficking, localization and signaling (discussed in detail below).

4.3.1. MAGUKs

The regulation of NMDARs by the MAGUK family has been extensively studied over the past 20 years. MAGUKs are a family of scaffold proteins highly enriched in the PSD

which are the best characterized interaction partners of NMDARs (reviewed in Elias & Nicoll, 2007; Gardoni et al., 2009; Won et al., 2017; Zhu et al., 2016). They have a central role in organizing the numerous protein complexes required for synaptic development and plasticity. One subfamily of MAGUKs is the Discs large homologue- (DLG-) or PSD-MAGUK subfamily, consisting of PSD95 (the most abundant protein in the PSD with its ~100µM concentration [Cheng et al., 2006]), PSD93, SAP97 and SAP102, all of which interact with the GluN2 NMDAR subunits (Brenman et al., 1996; Kim et al., 1996; Kornau et al., 1995; Lau et al., 1996; Müller et al., 1996; Niethammer et al., 1996). All PSD-MAGUKs contain three PSD95/Discs large/Zona occludens 1 (PDZ) domains, an src-homology 3 (SH3) domain and a C-terminal guanylate kinase (GK) domain (**Figure 9**).

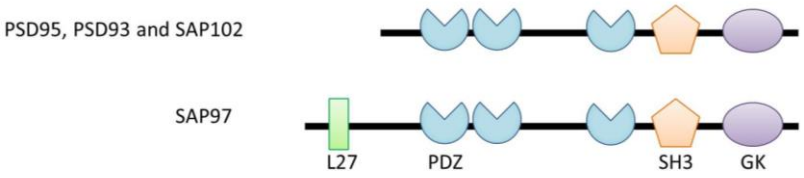

Figure 9. Structural domains of the PSD-MAGUK family
All PSD-MAGUKs have three PDZ domains, an SH3 domain and a GK domain. In the N-terminal region, SAP97 has a L27 domain involved in multimerization.

Members of the PSD-MAGUK family show differential subcellular localization, influenced by their posttranslational modifications (Colledge et al., 2003; El-Husseini et al., 2000a; Kim et al., 2007), with PSD95 and PSD93 predominantly expressed at the PSD, while SAP97 and SAP102 are found both in dendrites and axons and are also abundant in the cytoplasm (El-Husseini et al., 2000b; Gardoni et al., 2009; van Zundert et al., 2004). Additionally, PSD-MAGUKs have different temporal expression patterns (Kim & Sheng, 2004; Sans et al., 2000) with high SAP102 expression in early postnatal development – which has a dominant role in trafficking and anchoring NMDARs at immature synapses (Sans et al., 2003; Washbourne et al., 2004) – and predominant PSD95 and PSD93 expression in later stages – involved in maturation and stabilization of excitatory synapses (El-Husseini et al., 2000).

Both GluN2A and GluN2B interact with all members of the PSD-MAGUK subfamily (Al-Hallaq et al., 2007; Howard et al., 2010; Lau et al., 1996; Müller et al., 1996; Sans et al., 2000). This direct interaction mainly occurs between the first and second PDZ domains of the PSD-MAGUK and the ES(E/D)V PDZ-binding motif (PBM) in the CTD of the GluN2 subunit (Chung et al., 2004; Kornau et al., 1995). However, other non-ESDV regions have

been identified in both GluN2A and GluN2B: GluN2A subunits directly interact with PSD95 *via* an SH3 domain-binding motif that associates with the SH3 domain of PSD95, while the additional PSD95-binding site in the GluN2B subunit mapped to the region 1149-1157 (Cousins et al., 2009; Cousins & Stephenson, 2012). A non-PDZ interaction has also been reported between GluN2B and SAP102 involving two critical residues in the GluN2B CTD and the unique NTD of SAP102 (Chen et al., 2011; Chen et al., 2012).

Several studies suggest a preferential binding of GluN2A to PSD95 and GluN2B to SAP102 which is related to the developmental regulation of PSD-MAGUK expression as well as the differential localization of GluN2A and GluN2B at synaptic or extrasynaptic sites (Sans et al., 2000; Petralia et al., 2005; Zhang and Diamond, 2009).

The interaction of GluN2A- or GluN2B-NMDARs with PSD-MAGUKs is important in many aspects:

1) Promoting NMDAR clustering and anchoring at the synapse

Binding of GluN2A or GluN2B to PSD95 promotes NMDAR clustering (El-Husseini et al., 2000) and surface expression while decreases their internalization (Cousins et al., 2008; Lin et al., 2004, 2006; Losi et al., 2003). Disruption of the GluN2/PSD-MAGUK interaction has been shown to decrease the expression of GluN2 subunits at the synaptic membrane (Gardoni et al., 2006a, 2012). SAP102-PDZ mutants show decreased synaptic clustering of both GluN2A and GluN2B without effecting their trafficking (Minatohara et al., 2013). The interaction *via* the CTD of GluN2 subunits and the PDZ domain of PSD-MAGUKs seems to have a vital role in the clustering of surface NMDARs. Disruption of the GluN2A/PDZ interactions, in the presence of a GluN2A CTD-specific competing peptide, leads to a ~50% decrease in the synaptic content of GluN2A-NMDARs (Bard et al., 2010). Interestingly, swapping the CTD of GluN2A and GluN2B in 7 DIV cultured rat hippocampal neurons completely blocked the surface clustering of GluN2A-NMDARs; however, GluN2B clustering was significantly increased (Yan et al., 2014). An interesting indirect GluN2B-NMDAR stabilization role of PSD95 has been observed by promoting synaptic exclusion and degradation of the negative regulator $STEP_{61}$ (Won et al., 2016). Although PSD-MAGUKs are generally thought to stabilize synaptic NMDARs, Chen and colleagues demonstrate a surprising role of SAP102 in clearing GluN2B-NMDARs from synaptic sites (Chen et al., 2012).

2) Coupling of NMDARs to other proteins

PSD-MAGUKs also have a role in coupling NMDAR subunits to adhesion molecules such as neuroligin-1 (Irie et al., 1997; Levinson et al., 2005; Song et al., 1999) and other

signaling proteins, such as neuronal nitric oxide synthase (nNOS) (Sattler et al., 1999), SynGAP (Chen et al., 1998; Kim et al., 1998) and GKAP (Hirao et al., 1998; Kim et al., 1997).

3) Regulating functional properties of NMDARs

PSD95 promotes NMDAR channel opening (Lin et al., 2004) while inhibiting desensitization (Li et al., 2003; Sornarajah et al., 2008), potentiating NMDAR currents (Iwamoto et al., 2004; Yamada et al., 1999). Interestingly, PSD95 and PSD93 seem to exert compensatory mechanisms in the synaptic stabilization of NMDARs, since only the PSD95/PSD93 double knockout (KO) showed reduction in NMDAR transmission (Elias et al., 2006), whereas single KO of PSD95 or PSD93 have no effect on NMDAR currents (Béïque et al., 2006; Elias et al., 2006). However, when knocking down or overexpressing PSD95, the decay time of NMDAR currents is increased or decreased, respectively (Elias et al., 2008).

4) Modulating posttranslational modifications of NMDARs

PSD95 and PSD93 can couple both GluN2A and GluN2B to members (Src, Fyn) of the Src Family Kinases (SFKs) and promote SFK-mediated tyrosine phosphorylation of both subunits (Liao et al., 2000; Sun et al., 2015; Tezuka et al., 1999). PSD93 also mediates the synaptic localization of Fyn (Sato et al., 2008). In contrast to these findings, PSD95 has also been reported to negatively regulate Src and, subsequently, Src-induced GluN2A-NMDAR potentiation (Kalia et al., 2006; Yamada et al., 2002). Posttranslational modifications (discussed in chapter 4.3.3.) can alter the binding characteristics of GluN2A and GluN2B to their PSD-MAGUK partners which can, in turn, influence the synaptic localization of GluN2A- and GluN2B-NMDARs (Shipton and Paulsen, 2014).

PSD-MAGUKs themselves may undergo posttranslational modifications which affects their function (reviewed in Vallejo et al., 2017); PSD95 can be phosphorylated by the cyclin-dependent kinase 5 (CDK5), disrupting its ability to oligomerize (Morabito et al., 2004), or by CaMKII, which regulates the signal transduction pathways downstream of NMDARs and disrupts the PSD95/GluN2A interaction (Gardoni et al., 2006; Tsui & Malenka, 2006). CK2-dependent phosphorylation regulates PSD95/NMDAR interaction and modulates synaptic function and plasticity (Chung et al., 2004). Palmitoylation of PSD95 promotes its oligomerization, synaptic targeting, clustering of associated receptors and stabilization of spines (Christopherson, 2003; El-Husseini et al., 2000, 2002) but does not affect NMDAR levels (Jeyifous et al., 2016). In addition, PSD95 may also be ubiquitinated by Mdm2 and subsequently degraded following NMDAR activation (Colledge et al., 2003). Neddylation of

PSD95 by Nedd8 promotes its synaptic clustering (Vogl et al., 2015). Phosphorylation of other PSD-MAGUKs has been described, for instance, PSD93 can be phosphorylated by Fyn (Nada et al., 2003) and CaMKII-dependent phosphorylation of SAP97 promotes the release of SAP97/GluN2A complexes from the ER (Mauceri et al., 2007).

4.3.2. Other NMDAR regulators

Besides the PSD-MAGUKs, many other NMDAR regulators – either *via* direct or indirect interactions – have been identified, including *signaling molecules* (nNOS [Cao et al., 2005; Tang et al., 2012], SynGAP [Kim et al., 1998], Rho GEFs [Kiraly et al., 2011; Krapivinsky et al., 2003], Collapsin Receptor Mediator Protein 2 (CRMP2) [Al-Hallaq et al., 2007]), *membrane receptors* (dopamine D1 receptor [Lee et al., 2002; Lee & Liu, 2004]; Ephrin B2 receptor [Dalva et al., 2000], serotonin receptors [Vasefi et al., 2013], GABA receptors [Melamed et al., 2014; Zhang et al., 2007] and mGluRs [Perroy et al., 2008]), *cell adhesion molecules* (NCAM180 [Fux et al., 2003], SALM1 [Ko et al., 2006; Wang et al., 2006], integrins [Chavis & Westbrook, 2001; Xiao et al., 2016]), *cytoskeletal proteins* (α-actinin [Robison et al., 2005; Wyszynski et al., 1997], tubulin [van Rossum, Kuhse, & Betz, 1999], spectrin [Wechsler & Teichberg, 1998]) and the *auxiliary protein* Neto-1 (Ng et al., 2009).

4.3.3. Posttranslational modifications

The synaptic content of GluN2A- and GluN2B-NMDARs is also regulated by their various posttranslational modifications like phosphorylation (**Figure 10**), palmitoylation, glycosylation and ubiquitination. Phosphorylation of GluN2B at Ser1480 by CK2 disrupts its interaction with PSD95 and SAP102 and leads to a decrease in synaptic expression of GluN2B-NMDARs (Chung et al., 2004; Sanz-Clemente et al., 2010). Fyn and Src also phosphorylate GluN2B (at Tyr1472) which prevents its binding AP-2, thus inhibiting GluN2B endocytosis (Zhang et al., 2008). The GluN2A subunit can also be phosphorylated by Src and Fyn, positively regulating synaptic efficacy (Knox et al., 2013; Zhao et al., 2015). Protein kinase C (PKC) is a positive regulator of both GluN2A and GluN2B *via* tyrosine phosphorylation (Grant et al., 1998; Grosshans & Browning, 2001). PKC-dependent phosphorylation of GluN2A (at Ser1416) inhibits CaMKII/GluN2A interaction (Gardoni et al., 2001a). Phosphorylation of GluN2A at Ser1232 by CDK5 is important in synaptic transmission and plasticity (Li et al., 2001). Palmitoylation of both GluN2A and GluN2B

occurs at two cysteine residues in their CTDs regulating their retention in the Golgi apparatus and, therefore, their surface expression (Hayashi et al., 2012; Mattison et al., 2012). Two putative N-glycosylation sites were identified in GluN2B, although whether these are important in GluN2B surface trafficking is yet unknown (Lichnerova et al., 2015; Storey et al., 2011). NMDAR ubiquitination has also been described (Na et al., 2012; Wagner et al., 2012); members of the ubiquitin-proteasome system (UPS) have been shown to directly interact with GluN2B in a Fyn phosphorylation-dependent manner (Jurd et al., 2008). GluN2B has been shown to have a role in maintaining the proteasome at synapses as PSDs from GluN2B KO animals show decreased levels of proteasome subunits (Ferreira et al., 2015).

In addition to different regulatory pathways in controlling the levels of synaptic GluN2A- and GluN2B-NMDARs, the unique association between CaMKII and GluN2B also contributes to the subcellular localization of NMDARs and has a role in synaptic plasticity (Strack and Colbran, 1998).

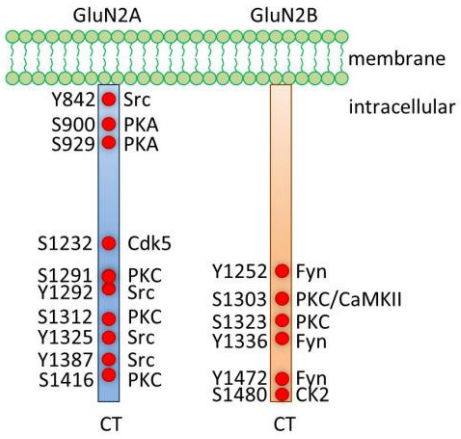

Figure 10. Phosphorylation sites of GluN2A and GluN2B CTDs
The particularly large CTDs of both GluN2A (627 amino acids) and GluN2B (644 amino acids) contain many phosphorylation sites, particularly in the distal segments. Adapted from (Wang et al., 2014).

CaMKII

CaMKII plays a crucial role in the regulation of synaptic strength during synaptic plasticity. It is an abundant protein of the PSD, estimated to represent 2-6% of the total mass of the PSD (Chen et al., 2005; Kennedy et al., 1983). CaMKII is a holoenzyme composed of 12 catalytically active subunits forming two stacked rings of 6 subunits each (Gaertner et al., 2004; Kolodziej et al., 2000). CaMKIIα and CaMKIIβ, encoded by two separate genes, are the two main isoforms present in the brain (Chen et al., 2005). CaMKII is essential in structurally organizing the PSD (Lin & Redmond, 2009) and in NMDAR-mediated LTP (Fink & Meyer, 2002; Lisman et al., 2002; Malenka et al., 1989). There is a basal level of CaMKII bound to NMDARs in the PSD (Gardoni et al., 1998; Leonard et al., 1999); however, in

response to NMDAR activation, CaMKII is activated by the Ca^{2+} influx, autophosphorylates at Thr286 and translocates to the synapse (Shen & Meyer, 1999; Strack et al., 1997). Once autophosphorylated, CaMKII remains active even in the absence of Ca^{2+} (Yang & Schulman, 1999). CaMKII directly interacts with GluN2B which anchors CaMKII at the synapse in an active conformation (Bayer et al., 2001). Targeting CaMKII to the PSD *via* its interaction with GluN2B is critical for the phosphorylation of GluA1 subunits of the AMPA receptor among many other PSD proteins (Lisman et al., 2002; Barria and Malinow, 2005; Zhou et al., 2007).

CaMKII directly binds both GluN2A and GluN2B subunits *via* binding sites located in the CTDs of the subunits (Bayer et al., 2001, 2006; Gardoni et al., 1999; Leonard et al., 1999; Strack et al., 2000); however, it has a greater affinity for GluN2B (Strack and Colbran, 1998). CaMKII binds GluN2A at residues 1412-1419 (Gardoni et al., 2001a, 2001b) and this interaction is enhanced by enzyme activation (Gardoni et al., 1999). CaMKII has been shown to phosphorylate GluN2A *in vitro* (Gardoni et al., 1999), competes with PSD95 for the binding of GluN2A (Gardoni et al., 2001b) and regulates binding of the SAP97 *via* Ser232phosphorylation of SAP97 (Gardoni et al., 2003). Two CaMKII-binding sites have been identified in the GluN2B subunit at residues 839–1120 and 1290–1310 (Strack and Colbran, 1998; Leonard et al., 1999; Strack et al., 2000; Bayer et al., 2001). Transient CaMKII activity evokes an initial reversible, Ca^{2+}/calmodulin-dependent binding of GluN2B to the substrate-binding site within the catalytic domain of CaMKII, whereas prolonged enzymatic activity leads to a persistent interaction between GluN2B and the Thr286-binding site of CaMKII, locking CaMKII in an active conformation, as mentioned above (Strack et al., 2000; Bayer et al., 2001, 2006). Not only does CaMKII bind to GluN2B, it also phosphorylates the subunit at site S1303 (Omkumar et al., 1996) which destabilizes CaMKII binding (Raveendran et al., 2009). CaMKII controls the binding of SAP102 and PSD95 to GluN2B (Chung et al., 2004). In addition, CaMKII regulates CK2-dependent GluN2B phosphorylation by coupling GluN2B and CK2 to form a tri-molecular complex and increase CK2-mediated phosphorylation of GluN2B at S1480 *via* physical interaction (Chung et al., 2004; Sanz-Clemente et al., 2013a).

Interestingly, CaMKII also has a role in regulating NMDAR surface expression and dynamics (Sanz-Clemente et al., 2013a; Dupuis et al., 2014). Disrupting the interaction between CaMKII and GluN2B reduces the number of synaptic connections, but increases the synaptic content of GluN2B (Sanz-Clemente et al., 2013a), while inhibiting CaMKII activity greatly decreases synaptic GluN2B dynamics with no effect on GluN2A (Dupuis et al., 2014).

4.4. *Subcellular localization of GluN2A- and GluN2B-NMDARs and its regulation*

Based on electrophysiological findings, in mature neurons, synaptic sites are thought to be predominantly occupied by GluN2A-NMDARs while GluN2B-NMDARs are enriched at extrasynaptic locations. The GluN2B-selective inhibitor ifenprodil blocks only 30% of NMDAR currents (Tovar and Westbrook, 1999), while the NMDAR open channel blocker MK-801 revealed a pool of ifenprodil-sensitive extrasynaptic NMDARs that can still be activated (Kew et al., 1998). Additionally, excessive glutamate, originating from astrocytes or neighboring neurons, activates primarily ifenprodil-sensitive NMDARs (Scimemi et al., 2004). Nonetheless, GluN2A has also been found at extrasynaptic locations, while GluN2B is present in the PSD (Thomas et al., 2006; Harris and Pettit, 2007; Petralia et al., 2010).

Interestingly, an asymmetry in the synaptic content of GluN2A- and GluN2B-NMDARs has been found between the left and right hemisphere CA3 inputs onto CA1 pyramidal cells of the adult hippocampus (Shinohara et al., 2008). Using freeze-fracture EM the authors demonstrate that different synaptic spine shapes have distinct receptor signatures with a relatively homogenous distribution of GluN2A, increasing with the spine size, whereas GluN2B is predominantly expressed in the synapse periphery at similar levels, independent of the spine size (Shinohara et al., 2008).

NMDAR clusters vary in size with extrasynaptic clusters generally thought to be smaller than synaptic clusters (Petralia, 2012). Extrasynaptic NMDARs as small as 30-50 nm clusters have been observed using EM and super-resolution microscopy (**Figure 11**) (Petralia et al., 2010). The authors suggest that these clusters potentially correspond to a single NMDAR molecule, although this cannot be conclusively determined due to technical limitations.

The subcellular localization of GluN2A- and GluN2B-NMDARs is most likely regulated by protein-protein interactions such as their binding to different PSD-MAGUKs. As mentioned earlier, PSD-MAGUKs present a controlled subcellular and temporal expression with SAP102 being evenly distributed throughout the neuronal membrane in early development, while PSD95 is predominantly located at the PSD in mature neurons (Sans et al., 2000). This expression pattern mirrors the changes observed in GluN2A/GluN2B expression, thus a preferential binding of GluN2A/PSD95 and GluN2B/SAP102 has been suggested (Sans et al., 2000); however, biochemical studies have not confirmed this (Al-Hallaq et al., 2007). In support of this idea, mice lacking the C-terminus of GluN2A display

reduced synaptic GluN2A expression and slower NMDAR kinetics (Steigerwald et al., 2000). In addition, disrupting the interaction between GluN2A or GluN2B and their PDZ partners results in a decrease in their synaptic content (Chung et al., 2004; Prybylowski et al., 2005; Bard et al., 2010). It has been shown that extrasynaptic NMDARs may form associations with various adhesion proteins (Petralia et al., 2010) and PDZ scaffolding proteins such as GIPC (Yi et al., 2007), PSD95 (Petralia et al., 2010) and SAP102 (Sans et al., 2003).

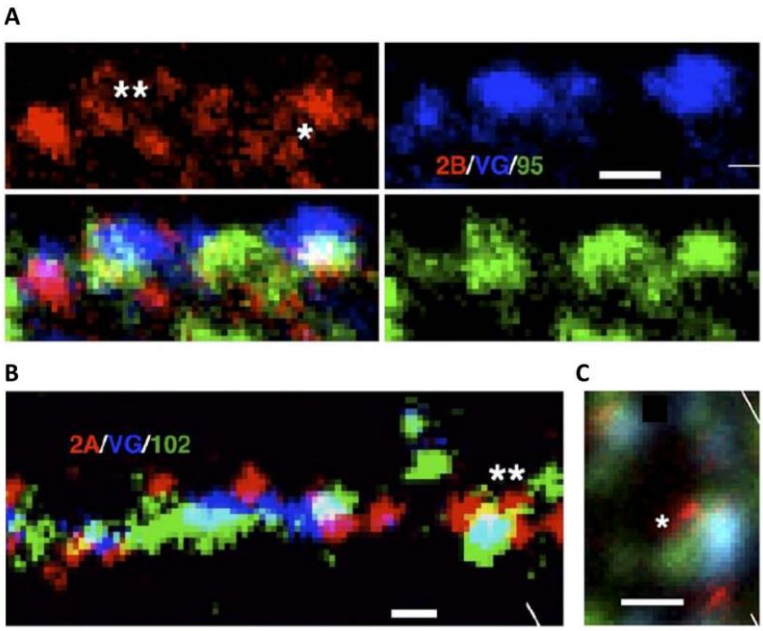

Figure 11. Subcellular distribution of GluN2A- and GluN2B-NMDARs
Labeling of surface GluN2A or GluN2B together with pre- and postsynaptic markers in hippocampal cultures: **A.** GluN2B (red)/PSD95 (green)/VGLUT (blue): triple staining reveals the differential distribution of GluN2B in synaptic (*) and extrasynaptic regions (**). **B.** GluN2A (red)/VGLUT (blue)/SAP102 (green): GluN2A is found as a partial perisynaptic ring around synaptic SAP102 (**). **C.** The first super-resolution microscopy image of NMDARs: synaptic GluN2A STED/SAP102 confocal. STED resolves ~50 nm synaptic or perisynaptic puncta (*) of GluN2A. Scale bars = 500 nm. Data from (Petralia et al., 2010)

Interactions between the extracellular domain of NMDARs and other proteins are also important for the subcellular localization of NMDARs. For example, activated Ephrin B2 receptors directly interact with GluN2B triggering the synaptic accumulation and stabilization of NMDARs (Dalva et al., 2000; Takasu et al., 2002; Nolt et al., 2011). The extracellular matrix protein reelin (Groc et al., 2007), as well as neuroligins and integrins have also been implicated in regulation of NMDAR subcellular localization (Jung et al., 2010).

In addition, the surface mobility of NMDARs also has a role in regulating NMDAR synaptic content and distribution (reviewed in Choquet and Triller, 2013). It is now well

accepted that NMDARs diffuse in and out of the PSD (Tovar and Westbrook, 2002), GluN2B-NMDARs with a higher rate compared to GluN2A-NMDARs which are more retained within the synapse (Groc et al., 2006). NMDAR mobility is regulated by neuronal development (Groc et al., 2006), protein kinase activity (Groc et al., 2004), and NMDAR protein interactions (Groc et al., 2007; Bard et al., 2010).

4.4.1. Synaptic versus extrasynaptic NMDAR controversy

Depending on the subcellular localization, NMDAR activation can lead to very different outcomes. Activation of synaptic NMDARs is associated with cell survival *via* activation of CREB (cyclic-AMP response element binding protein). In contrast, activation of extrasynaptic NMDARs most commonly leads to cell death *via* mitochondrial dysfunction, termed excitotoxicity (Hardingham and Bading, 2010), although some positive effects of extracellular NMDAR activation have been suggested, mainly during early development (reviewed in Petralia, 2012). An increase in extrasynaptic NMDAR activation has been implicated in several neurodegenerative diseases (reviewed in Hardingham and Bading, 2010; Petralia, 2012), although it is not known whether the GluN2 subunit expressed in extrasynaptic NMDARs defines the intracellular cascade triggered by activation of these receptors (Sanz-Clemente et al., 2013b).

4.5. GluN1/GluN2A/GluN2B triheteromers

Diheteromeric NMDARs containing either two GluN2A or two GluN2B subunits have been extensively studied regarding their physiology, pharmacology, structure and expression. However, little is known about the GluN1/GluN2A/GluN2B triheteromers while there is increasing evidence that they represent a substantial NMDAR population of the adult brain (Sheng et al., 1994; Luo et al., 1997; Al-Hallaq et al., 2007; Gray et al., 2011; Rauner and Köhr, 2011; Tovar et al., 2013). GluN1/GluN2A/GluN2B receptors are uniquely modulated by specific allosteric modulators of GluN2A (Zn^{2+}) and GluN2B (ifenprodil or Ro 25-6981) and exhibit gating kinetics distinct from either GluN2A- or GluN2B-NMDARs (Hansen et al., 2014; Stroebel et al., 2014; Cheriyan et al., 2016) but cannot be fully inhibited (Hatton and Paoletti, 2005). Surprisingly, GluN2A-specific antagonists inhibit recombinant GluN1/GluN2A/GluN2B receptors more efficiently compared to GluN2B inhibitors,

suggesting a predominance of GluN2A in the ion channel gating of triheteromeric complexes (Cheriyan et al., 2016). Consistent with this finding, a recent study, revealing the structure of triheteromeric NMDARs by cryogenic EM, demonstrates the closer interaction between the GluN1 and GluN2A subunits (Lü et al., 2017). Interestingly, NMDARs containing both GluN2A and GluN2B show similar internalization rates as GluN1/GluN2B diheteromers (Tang et al., 2010).

Despite all these findings, specific pharmacological and biochemical tools to directly analyze endogenous NMDAR triheteromers do not exist. The recent development of super-resolution imaging techniques may provide new ways to study the distribution and content of these receptors and shed light on their role in the CNS.

5. Super-resolution microscopy in the brain

In order to understand the functional architecture of the postsynaptic and extrasynaptic specialization of NMDARs, or other synaptic proteins, a higher-resolution structure of the PSD and its molecular underpinnings is needed. The recent advancement of super-resolution light microscopy techniques provides a useful tool to study the localization and mobility of PSD proteins, both *in vitro* and *in vivo*, at the nanometer scale.

5.1. Super-resolution light microscopy techniques

Optical microscopy has been a key tool in biological and medical fields by allowing us to image and investigate microorganisms, cells, tissues and organs, even under live conditions. Using suitable fluorescent probes, microscopic images provide information of the sample structure, cellular environment and ion/molecule distributions within cells. Light microscopy is highly non-invasive, does not require complicated sample preparation and provides a wide range of imaging modalities to study biological structures and events. However, the main limitation of optical microscopes is that the spatial resolution is limited to approximately half the wavelength of the excitation light as defined by Ernst Abbe in 1873 (Abbe, 1873). This means that structures, such as individual proteins, or events taking place below ~250 nm regions cannot be resolved. This means great limitations in the field of

neuroscience due to the small size of synapses (e.g. synaptic active zone = 300 ± 150 nm, synaptic vesicles = 30-40 nm, synaptic cleft = 20-30 nm [reviewed in Sauer and Heilemann, 2017]). 'The diffraction limit' of optical microscopes was first overcome by EM that uses electrons instead of light to observe subdiffraction structures and organelles. EM allows very high resolution (few nanometers); however, it requires complicated sample processing that entails severe damage. The recent development of super-resolution light microscopy techniques provides information of structural assemblies in a biological context. These approaches utilize different concepts (discussed below) to break the diffraction barrier and allow a resolution of up to tens of nanometers.

The current super-resolution techniques can be divided into two groups: 1) techniques that image an ensemble of fluorophores such as stimulated emission depletion (STED) (Hell and Wichmann, 1994; Klar et al., 2000) or structured illumination microscopy (SIM) (Gustafsson, 2005) and 2) techniques that image single molecules referred to as single-molecule localization microscopy (SMLM) such as stochastic optical reconstruction microscopy (STORM) (Rust et al., 2006; Bates et al., 2007), dSTORM (Heilemann et al., 2008) or photoactivated localization microscopy (PALM) (Betzig et al., 2006; Hess et al., 2006). Introducing all super-resolution imaging techniques is beyond the scope of this thesis, so further on I will focus on the techniques I used to study NMDAR localization (**Table 4, Figure 12**).

5.1.1. Stimulated emission depletion (STED) microscopy

The first technique to overcome the diffraction limit of light was STED microscopy, developed by Stefan W. Hell in 1994 (Hell and Wichmann, 1994). The main concept of this method is to improve the spatial resolution by quenching fluorescence emission on the periphery of the point spread function (PSF), so that emission can only occur from a diffraction limited spot inside the PSF (**Figure 12**). This is achieved by a special laser called the STED laser which, thanks to its unique doughnut-like shape, de-excites the outer fluorescent molecules to the ground state (S_0) by stimulated emission at a wavelength longer than that used for fluorescence excitation. Therefore, fluorescence emission only occurs from the center of the PSF which is detected by a photodetector. The image is generated by the spatial distribution of fluorescence signals detected at each position of the sample. Until now, the maximal resolution achieved was ~6 nm using diamond crystals (Rittweger et al., 2009) but the typical spatial resolution in biological samples varies between 30 and 70 nm (Chéreau et al., 2015).

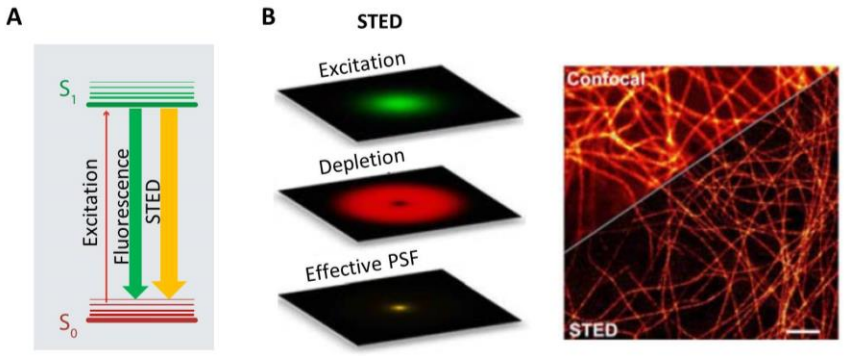

Figure 12. The principle of STED microscopy
A. Energy state diagram for STED microscopy: photon absorption excites the fluorophore from ground state (S_1) to the excited state (S_1) (red arrow). Fluorescence occurs from the spontaneous return of the molecule to S_0 (green arrow); however, fluorescence can be forcefully depleted *via* stimulated emission (yellow arrow) by light of a longer wavelength. As a result no fluorescence occurs in the depleted area. **B.** The concept of STED microscopy during image acquisition: top panel: excitation of the sample results fluorescence emission; middle panel: stimulated emission depletion of the outer part of the point spread function (PSF) resulting in a much smaller PSF (bottom panel). Higher resolution image is generated by scanning the sample (right panel). Scale bar = 2 µm. Adapted from (Stender et al., 2013)**.**

5.1.2. Direct stochastic optical reconstruction microscopy (dSTORM)

SMLM techniques are fundamentally different from STED in the sense that they image single molecules. The basic principle of these techniques is that the position of a single molecule can be identified with ~1 nm accuracy if sufficient photons are collected and there are no other similar emitters within ~200 nm (Bobroff, 1986). dSTORM (or ground state depletion followed by individual molecule return, GSDIM [Fölling et al., 2008]) utilizes the reversible switching of conventional fluorophores to achieve such sparse emission (Heilemann et al., 2008; van de Linde et al., 2008, 2011). The fluorophores are switched to triplet state (T_1) or another metastable dark state using a high excitation laser power while the fluorophores remaining or returning to the ground state (S_0) can be excited and detected (**Figure 13**) (Fölling et al., 2008; Heilemann et al., 2008). The switching of the fluorophores is controlled by a 'switching buffer' containing oxygen scavengers and reducing agents (Heilemann et al., 2008; van de Linde et al., 2008). The super-resolved image is reconstructed from a large number of conventional wide-field images (**Figure 13**), each containing the high-accuracy positional information of a subset of dispersed fluorescent molecules.

Table 4. Comparison of STED and dSTORM super-resolution microscopy techniques. Adapted from (Yamanaka et al., 2014; Sydor et al., 2015).

dSTORM versus STED super-resolution microscopy		
	STED	**dSTORM**
Principle	Reduction of PSF by stimulated emission depletion	Stochastic activation & determination of PSF centroid
Microscope type	Laser scanning	Wide-field
Number of required excitation wavelengths	2	1 to 2
Spatial resolution		
Lateral	20-70 nm	10-30 nm
Axial	40-150 nm	10-75 nm
Z-stack range	~20 µm	Few hundreds nm - few µm
Applicable fluorescent probe	Any if photostable	Photoswitchable fluorescent proteins/molecules
Photodamage	Moderate-high	Low-moderate
Photobleaching	Moderate-high	Low
Preparations	Fixed samples *In vitro* *In vivo*	Fixed samples *In vitro*

dSTORM is a powerful tool to study distribution and clustering patterns of endogenous cytoplasmic or membrane proteins; however, due to the high concentration of reducing agents (e.g. β-mercaptoethanol) of the 'switching buffer' its use in live cell imaging is quite limited (Heilemann et al., 2008). An additional limitation of dSTORM is the limited availability of fluorophores with good switching properties and high quantum yield (Fernández-Suárez and Ting, 2008; Ni et al., 2017), therefore, performing multicolor dSTORM can be challenging. In a comparative study, the best performing fluorophore was found to be Alexa Fluor 647 (Dempsey et al., 2011; Ni et al., 2017) with its following properties: $\lambda_{excitation}$ = 650 nm, $\lambda_{emission}$ = 665 nm, exctinction coeffient (ε_{Abs}) = 240 000 $M^{-1}cm^{-1}$, fluorescence quantum yield (η_{fl}) = 33 %, fluorescence lifetime (τ_{fl}) = 1.0 ns, number of detected photons per single molecule in each imaging cycle (N) = 6000 (Fernández-Suárez and Ting, 2008).

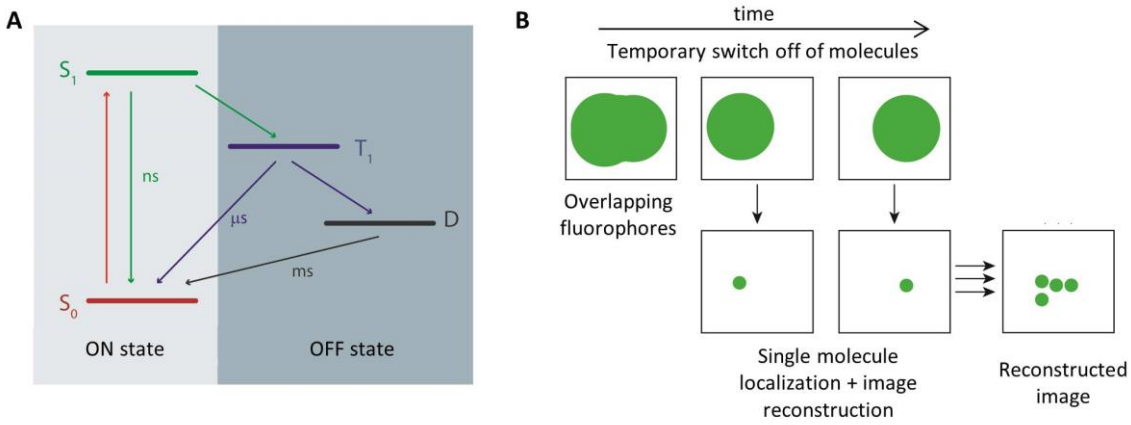

Figure 13. The principle of dSTORM
A. Schematic diagram demonstrating the molecular basis of dSTORM: photon absorption excites the fluorophore from ground state (S_1) to excited state (S_1) (red arrow). From S_1 the molecules can either spontaneously return to S_0 in a nanoseconds (ns) timescale while emitting fluorescence or they can reside in a metastable triplet (T_1) or dark (D) state for micro- (µs) or even milliseconds (ms) before relaxation to S_0 (no fluorescence emission occurs in this case). While in the off state (T_1 or D), the fluorophores cannot be excited, therefore only a limited amount of excitable fluorophores is available. **B.** Scheme demonstrating single-molecule detection in dSTORM: in order to detect single molecules, fluorophores are temporarily switched off. Image reconstruction is based on the centroid of the point spread function of individual localizations.

5.1.3. Use of super-resolution microscopy in neurobiology

STED microscopy has proven immensely useful in neurobiological studies due to its potential in imaging live cell dendritic spines (Nagerl et al., 2008; Urban et al., 2011) and synaptic vesicles (Westphal et al., 2008) at high depth penetration, optical sectioning and imaging speed, with a wide range of fluorophores available for sample labelling (reviewed in Tønnesen and Nägerl, 2013 and Chéreau et al., 2015), while dSTORM is a powerful tool to study distribution and clustering patterns of endogenous synaptic proteins in a quantitative manner (reviewed in Sigrist and Sabatini, 2012; Willig and Barrantes, 2014; MacGillavry and Hoogenraad, 2015; Sauer and Heilemann, 2017). Such techniques have been successfully applied to unveil the synaptic organization of important structural players in neurons as well as neurotransmitter receptors and other PSD proteins. An extensive study using three color 3D STORM characterized the organization of several pre- and postsynaptic proteins (Dani et al., 2010). They reported a sequential alignment of proteins along the longitudinal axis of the synapse, with neurotransmitter receptors being localized at the postsynaptic membrane, followed by PSD scaffold proteins (Dani et al., 2010). Super-resolution imaging revealed nano-sized clusters of both pre- and postsynaptic proteins. For example, proteins necessary

for neuronal exocytosis, such as syntaxin 1, SNAP-25 or tomosyn were found in ~90 nm size nanoclusters (Bar-On et al., 2012; Bielopolski et al., 2014). Quantitative dSTORM identified the unit-like organization of active zones with ~137 endogenous Bruchpilot molecules (a structural organizer of the presynapse) per unit, confirmed by electrophysiological data of neurotransmitter release, indicating the advantage of this method in revealing structure-function relationships at the molecular level (Ehmann et al., 2014). In the postsynaptic compartment, ~70-80 nm size domains (termed 'nanodomains') were found for both PSD95 and AMPARs in three parallel studies using complementary super-resolution techniques (Fukata et al., 2013; MacGillavry et al., 2013; Nair et al., 2013). A similar organization of the scaffold gephyrin and inhibitory GABAergic receptors was found in inhibitory synapses (Specht et al., 2013; Pennacchietti et al., 2017). These 'nanodomains' are dynamically regulated and have been proposed to play important roles in synaptic transmission through the alignment of pre- and postsynaptic processes (Tang et al., 2016).

Chapter 2: Aims

In this context, my main working hypothesis is that GluN2A- and GluN2B-NMDARs are differentially organized into nano-sized clusters in both synaptic and extrasynaptic sites and these nano-sized clusters, similarly to GluN2A and GluN2B expression, go through changes during development and can be differentially regulated by specific protein-protein interactions or posttranslational modifications. The aim of this project is to address several fundamental questions about the precise localization and nanoscale organization of two important NMDAR subtypes by taking advantage of super-resolution techniques such as dSTORM and STED microscopy. The project is divided into the following sections:

1. Visualization of the nanoscopic distribution of surface GluN2A- and GluN2B-NMDARs using dSTORM in mature (17 DIV) primary hippocampal cultures

2. Determination of nanoclustering of GluN2A- and GluN2B-NMDARs

3. Characterization of GluN2A- and GluN2B-NMDAR nanoscale organization in synaptic structures using PSD95 as a postsynaptic marker

4. Examination of changes in GluN2A- and GluN2B-NMDAR nano-organization during development

5. Investigation of the regulation of NMDAR nanoscale organization with special focus on interactions with PDZ scaffolds and CaMKII activity

Chapter 3: Materials and Methods

1. Neuronal cultures

Primary hippocampal cultures were prepared from 18 day embryonic Sprague-Dawley rats according to the protocol of Kaech and Banker (Kaech and Banker, 2006). Briefly, hippocampi were dissected and collected in Hanks' Balanced Salt Solution (HBSS; Gibco #14025-050) containing Penicillin-Streptomycin (PS; Gibco #15140-122) and HEPES (Gibco #14025-056). The tissue was dissociated with Trypsin-EDTA (Gibco #25300-054)/PS/HEPES and neurons were plated in minimum essential medium (MEM; Gibco #21090-022) supplemented with 10% horse serum (PAN Dutscher #500135A) on coverslips coated with 1 mg/ml poly-L-lisine (PLL; Sigma-Aldrich #P2636-1G) in 60 mm Petri dishes at a density of either 150.000, for immunostaining, or 250.000, for transfection, cells per dish. Following neuronal attachment to the surface, the coverslips were flipped on top of a glial cell monolayer in Neurobasal medium (Gibco #12348-017) supplemented with L-glutamine (PAA #M11-004) and SM1 (Stem Cell #05711). Cells were maintained in a humidified incubator at 36.5°C with 5% CO_2.

2. Transfection

Neurons were transfected at DIV 9-11 using the calcium-phosphate coprecipitation method (Jiang and Chen, 2006). Precipitates containing 1-1.5 µg plasmidic DNA were prepared using the following solutions: TE (1 mM Tris–HCl pH 7.3, 1 mM EDTA), $CaCl_2$ (2.5 M $CaCl_2$ in 10 mM HEPES, pH 7.2), 2× HEPES-buffered saline (HEBS; 12 mM dextrose, 50 mM HEPES, 10 mM KCl, 280 mM NaCl and 1.5 mM $Na_2HPO_4 \cdot 2H_2O$, pH 7.2). Coverslips containing neurons were moved to 12 well multiwell plates containing 200 µl/well of conditioned culture medium. The 50 µl precipitate solution was added to each well, in the presence of 2mM kynurenic acid (Sigma-Aldrich #K3375) and incubated for 1 h at 37 °C. Afterwards, cells were washed with unsupplemented Neurobasal medium containing 2 mM kynurenic acid and moved back to their original culture dish for 4 days of expression before use.

For STED imaging, cells were co-transfected with GluN1-GFP, GluN2A-HA and GluN2B-flag. 10 µM D-APV was added to the culture medium after transfection.

3. Antibodies and immunostaining

The following primary antibodies were used: anti-flag (Sigma-Aldrich #F1804, 2 µg/ml), anti-GluN2A (Agrobio, custom-made, epitope: GHSHDVTERELRN, 0.1 mg/ml, [Ferreira et al., 2017]), anti-GluN2B (Agrobio, custom-made, epitope: NTHEKRIYQSNMLNR, 0.1 mg/ml, [Ferreira et al., 2017]), anti-HA (Roche #11867423001, 0.5 µg/ml), anti-PSD95 (Thermo Scientific #7E3-1B8, 1 µg/ml), anti-SAP102 (Alomone labs #APZ-003, 4 µg/ml), anti-VGLUT (Merck #AB5905), anti-GFP (Thermo Scientific #A6455). All secondary antibodies were used at 0.1 mg/ml concentration: anti-guinea pig Alexa 647 (Thermo Scientific #A21450), anti-mouse Alexa 488 (Thermo Scientific #A11001), anti-mouse Alexa 532 (Thermo Scientific #A11002), anti-mouse Atto 647N (Sigma-Aldrich #50185), anti-rabbit Alexa 488 (Thermo Scientific #A11008), anti-rabbit Alexa 568 (Thermo Scientific #A11011), anti-rabbit Alexa 647 (Thermo Scientific #A21244), anti-rat Alexa 594 (Thermo Scientific # A21471).

Live neurons were surface stained for endogenous or overexpressed (GluN2A-HA, GluN2B-flag) GluN2A and/or GluN2B for 15 min at 37°C using specific antibodies. After fixation (4% paraformaldehyde/4% sucrose in PBS, 15 min) at room temperature (RT), neurons were permeabilized with 0.4% Triton X-100 (Sigma-Aldrich #T9284, 5 min) and treated with a blocking solution containing 1.5% bovine serum albumin (Sigma-Aldrich #A3059)/0.1% fish skin gelatin (Sigma-Aldrich #G7765)/0.1% Triton X-100 for 40 min. Cells were then successively incubated with the second primary antibody(ies), when indicated, for 45 min at RT. The secondary antibodies were used during 30 min incubation at RT and, after an additional wash, the cells were mounted in Mowiol. For dSTORM imaging, a second fixation was performed after incubation with the secondary antibodies and cells were kept in PBS at 4°C until imaging.

4. Peptides

For experiments using the NMDAR subunit-specific TAT peptides live cells were pre-incubated with 1 µM concentration of either $[TAT\text{-}GluN2A]_2$, $[TAT\text{-}GluN2B]_2$ or $[TAT\text{-}NS]_2$ peptide for 45 min at 37°C. For CaMKII inhibition, AIP-2 or its respective control, TAT-NS was used at 5 µM concentration for 15 min at 37°C. Afterwards, the cells were stained for endogenous surface GluN2A or GluN2B as described above.

5. dSTORM imaging

All imaging sessions were performed using a commercial Leica SR GSD 3D microscope (Leica Microsystems, Wetzlar, Germany) equipped with a Leica HC PL APO 160x/1.43 NA oil immersion TIRF objective enabling detection of single fluorophores and an EMCCD iXon camera (ANDOR, Belfast, UK). Samples were illuminated in total internal reflection fluorescence (TIRF) mode and images were obtained with an exposure time of 10.85ms with up to 100,000 consecutive frames. Imaging was carried out at room temperature in a closed Ludin chamber (Life Imaging Services, Switzerland) using a pH-adjusted extracellular solution containing oxygen scavengers and reducing agents (Heilemann et al., 2008; van de Linde et al., 2008). When the field of interest was chosen for proximal dendrites, a snapshot was taken of the epifluorescence labeling of NMDAR and PSD95. Image acquisition was controlled by the Leica LAS software. First, the ensemble fluorescence of Alexa 647 was converted into dark state using 50% of full power of the 642 nm laser (500 mW). Once the desired number of single fluorophores per frame was reached, the intensity of the 642 nm laser was reduced to 15% of full laser power and kept at this level during acquisition. In order to keep an optimal number of stochastically activated molecules per frame the intensity of the 405 nm laser (30 mW) was continuously adjusted reaching a maximum of 10% of full laser power. The particle detection threshold was set to 15 in the Leica LAS software. Multicolor fluorescent microspheres (#T7279 TetraSpeck, Life Technologies) were used for lateral drift correction.

6. Co-localization study of synaptic proteins

Fluorescence images were acquired using an Electron Multiplying Charged Coupled Device (EMCCD) Photometrics Quantem 512 camera and MetaMorph imaging software (Molecular Devices), on an inverted confocal spinning-disk microscope (Leica DMI6000B, Leica), with a Leica HCX PL APO CS 63x/1.4 oil objective. For each experiment, images in each channel (SPI lasers 488/568/647, quad simple filters) were captured using the same laser intensity and exposure time across all fixed cells; images were acquired as grey scale from individual channels and pseudocolor overlays were prepared using ImageJ. To quantify the immunocytochemistry data, 19-22 cells were selected. From each neuron, two to three dendrites were chosen for analysis. The images were subjected to a user-defined intensity threshold, for cluster selection and background subtraction. Number of clusters was measured for all selected regions and normalized to the dendrite length. Synaptic clusters were

determined as the postsynaptic clusters overlapping the thresholded image of PSD95 (postsynaptic) or VGLUT (presynaptic).

7. Calculation of localization precision

Theoretical localization precision was calculated from the integrated intensity of single PSFs using the methods of Thompson (Thompson et al., 2002) and Mortensen (Mortensen et al., 2010) implemented in the LAMA software (Malkusch and Heilemann, 2016a). Both of these methods utilize PSFs calculated based on a 'least-squares estimation' (LSE). Localization precision depends mainly on the number of detected photons (N) and the standard deviation of the PSF (σ), both of which depend on characteristics of the optical setup and the type of fluorescent labelling used. Additionally, localization precision depends also on the area imaged in one pixel of the camera chip (a) and the background signal (b). The Leica SR GSD 3D system, with AlexaFluor 647 labelling, had a σ value of 140 nm (σ) and a noise value of 8.4 (b).

8. dSTORM data analysis

Image-based analysis: Super-resolution images were reconstructed by the Leica LAS software using a fitting algorithm determining the centroid-coordinates of a single molecule and fitting the point-spread-function (PSF) of a distinct diffraction limited event to a Gaussian function. NMDAR or PSD95 clusters were identified on their respective epifluorescence images. GluN2A- or GluN2B-NMDAR nanodomain number, area and shape were quantified after segmentation of their respective dSTORM reconstructed images (MetaMorph software, Molecular Devices). Morphological features, such as surface area, length and shape of each segmented structure, were exported to calculate their respective distributions. The dimensions were computed by 2D anisotropic Gaussian fitting, from which the principal and the auxiliary axes were extracted as 2.3σ long and 2.3σ short, respectively. The shape factor was calculated as a ratio between the auxiliary and the principal axes. The epifluorescence image of PSD95 was superimposed on the NMDAR dSTORM image to identify the PSD95 positive (PSD95+) *versus* PSD95 negative (PSD95-) nanodomains.

Density-based analysis: the previously described density-based spatial clustering of applications with noise (DBSCAN) (Ester et al., 1996) algorithm, implemented in the LAMA software (Malkusch and Heilemann, 2016a), was used to calculate the area and molecule number of NMDAR clusters. The DBSCAN algorithm identifies localizations that reside

within the middle of a circle of the observation radius (ε) and enclose at least P_{min} (minimal cluster size) localizations. An ε of 14 nm was chosen which roughly corresponds to the radius of an NMDAR (6 nm [Lee et al., 2014]) with the antibody complex (~8 nm [Tan et al., 2008]) attached to it. The P_{min} was chosen based on the density-distribution of the localizations within ε; in our case the value was 6 in order to separate the localizations from noise but not too large to find sparse clusters. The cluster localizations were corrected for fluorophore blinking (**Figure 14**) and normalized to the corresponding image background to identify molecules per clusters.

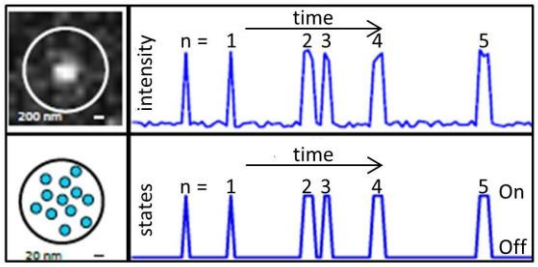

Figure 14. Characteristics of fluorophore blinking
Top left: image of single-molecule blinking events within a diffraction limited spot. Top right: intensity within the circular region (top left) measured over time showing 5 blinking events. Bottom left: DBSCAN analysis of all localizations from the top image reveals a cluster comprising 12 localizations. Bottom right: binary state trace of all cluster localizations against time shows the number of blinking events. Adapted from (Malkusch and Heilemann, 2016b)

9. Integrated morphometry analysis of PSD95 clusters

Epifluorescence images of PSD95 obtained by the Leica SR GSD 3D microscope were subjected to a user-defined threshold for cluster selection and background subtraction. Next, MetaMorph integrated morphometry analysis was used to identify the number and area of PSD95 clusters.

10. STED imaging and analysis

All STED imaging sessions were carried out on a Leica DMI6000 TCS SP8 X system equipped with two continuous wave STED lasers for excitation at 592 nm and 660 nm and a pulsed 775 nm depletion laser. A 40X/1.3 NA oil immersion objective was used to identify transfected cells, while a 100X/1.4 NA oil immersion objective lens was used for STED imaging. Fluorescence signals were passed through a pinhole size of 1 Airy unit. Image frame size was adjusted per image and acquired sequentially in line-scan mode using a scan speed of 400 Hz with a pixel size of 20 nm.

For STED image analysis, five NMDAR clusters expressing both GluN2A-HA and GluN2B-flag were selected per single STED image for a total of 22 images from two separate experiments. The selected clusters were subjected to a user-defined intensity threshold being the same in both channels and cluster area was measured afterwards.

11. Statistics

The statistical analysis was performed with the help of GraphPad Prism 5 software (GraphPad Software, Inc). The use of non-parametric statistical tests was implemented because of the non-Gaussian distribution of the datasets. The different statistical tests used (t test or ANOVA, depending on the number of datasets) are indicated in the results section at each experiment.

Chapter 4: Results

1. Nanoscopic map of surface GluN2A- and GluN2B-NMDARs

In order to precisely map the localization of NMDARs, we surface-labelled live hippocampal neurons at DIV 17 using custom-made GluN2A or GluN2B antibodies directed against their extracellular N-termini. At this age, both GluN2A- and GluN2B-NMDARs were highly expressed at the neuronal surface (**Figure 15**).

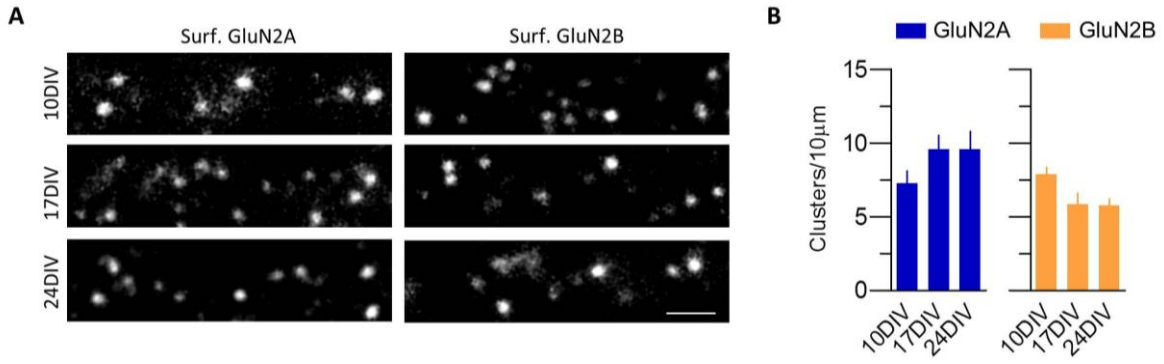

Figure 15. GluN2A and GluN2B expression during development in hippocampal cultures
A. Representative epifluorescence images of GluN2A- or GluN2B-NMDAR in neuronal cultures at DIV 10 (top), 17 (middle) or 24 (bottom). Scale bar = 10 µm. **B.** Changes in surface expression of NMDARs per 10 µm dendrite length represented as mean ± SEM values.

Diffraction-limited epifluorescence images of surface GluN2A- or GluN2B-NMDARs revealed a relatively homogenous distribution along the dendrite of both (**Figure 16A-B**). GluN2A- and GluN2B-NMDAR clusters appeared indistinguishable using this conventional approach; therefore,weapplied dSTORM, using Alexa Fluor 647 labeling, to visualize the distribution of GluN2A- or GluN2B-containing NMDARs at nanoscale. dSTORM is a single-molecule localization technique where the increase in resolution is achieved by localization of individual fluorescent molecules *via* stochastic activation. The reconstructed dSTORM images (**Figure 16B-C**) unveiled a nanoscopic distribution of surface NMDAR clusters with a localization precision of ~25 nm (**Figure 17A-B**). First, we used DBSCAN analysis to characterize NMDAR clusters. The DBSCAN algorithm utilizes the localization coordinates to identify cluster edges based on density (Ester et al., 1996). The two DBSCAN parameters, observation radius (ε) and minimal cluster size (P_{min}), were identified based on the radius of the NMDAR (ε=14 nm [Lee et al., 2014]) with the primary and secondary antibody labeling

and the minimal number of localizations within this radius (P_{min}=6) (**Figure 18**; for details, refer to Chapter 3. Section 8: dSTORM data analysis). DBSCAN analysis revealed that GluN2A-NMDAR nanoscale cluster area is 1.5x larger than that of GluN2B-NMDARs (**Figure 16C-D**). (For exact values, refer to **Table 5**).

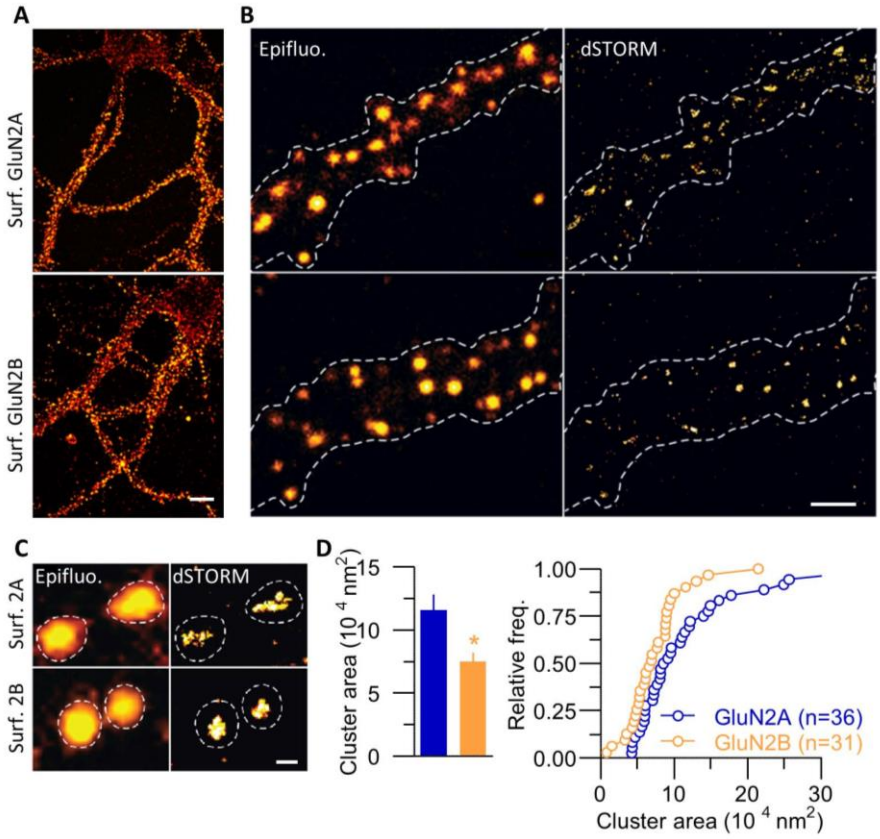

Figure 16. Nanoscopic surface distribution of GluN2A- and GluN2B-NMDARs in mature neurons
A. Epifluorescence images of surface immunostaining of endogenous surface GluN2A- (top) or surface GluN2B-NMDAR (bottom) at 17 DIV hippocampal neurons labelled with specific custom-made antibodies. Scale bar = 10 µm. **B.** Comparison between epifluorescence (left) and super-resolution dSTORM image (right, obtained by Leica LAS software) of a single dendrite stained for either GluN2A- (top) or GluN2B-NMDARs (bottom). Dotted line represents the border of the dendrite based on the epifluorescence image. Scale bar = 1 µm. **C.** Comparison of enlarged epifluorescence (left) and super-resolved (right, obtained by Leica LAS software) clusters of GluN2A- (top) or GluN2B-NMDAR (bottom). Dotted line represents the border of the cluster based on the epifluorescence image. Scale bar = 300 nm. **D.** Differences in the area of super-resolved GluN2A- and GluN2B-NMDAR clusters represented by mean ± SEM values and their relative distributions.

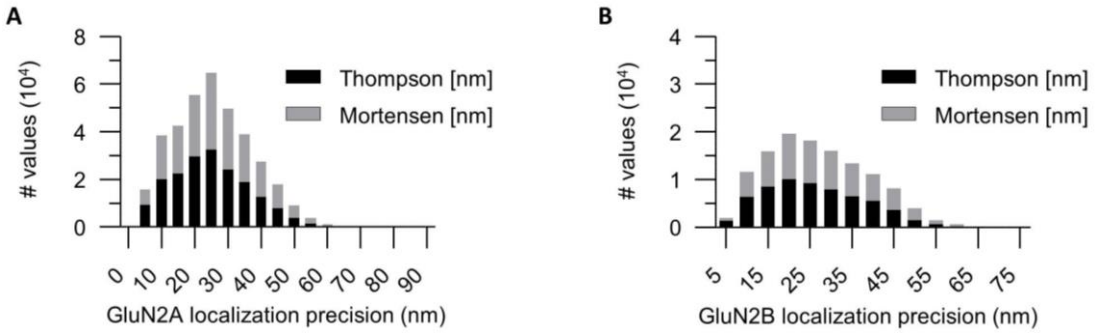

Figure 17. Localization precision of GluN2A- and GluN2B-NMDARs
A. Localization precision of GluN2A-NMDARs immunostained with specific GluN2A antibodies and AlexaFluor 647. **B.** Localization precision of GluN2B-NMDARs immunostained with specific GluN2B antibodies and AlexaFluor 647.

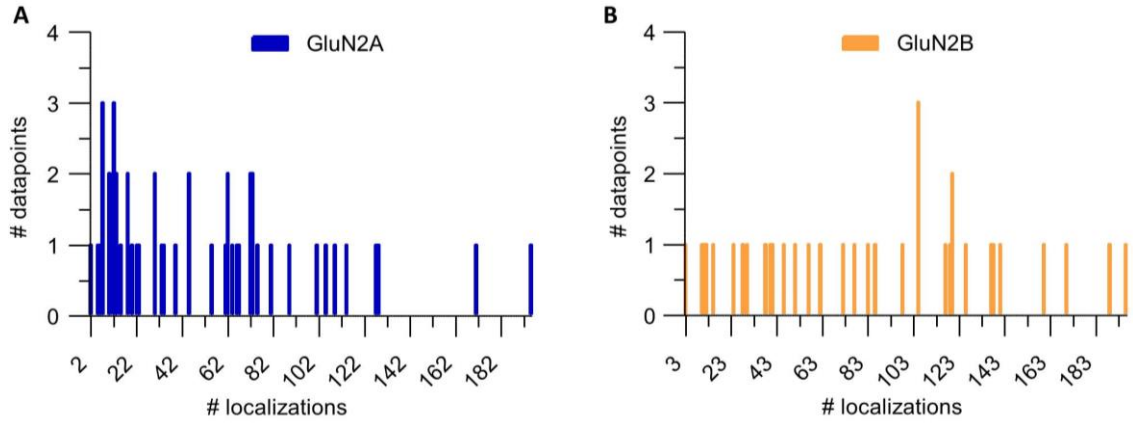

Figure 18. Calculation of P_{min} for DBSCAN analysis
A-B. Frequency distribution of the number of GluN2A (**A**) or GluN2B (**B**) localizations within 14 nm (radius of a single NMDAR with primary and secondary antibody labeling) radius of a central localization. The minimum number of localizations were 2 or 3, respectively. Therefore, a value of 6 localizations (=higher minimum value (3)*2) was chosen for the minimal cluster size in DBSCAN analysis.

Table 5. Results of NMDAR dSTORM cluster analysis

Parameter	Analysis method	Mean ± SEM	n	Statistical test	p value
2A cluster area	DBSCAN	11.56 ± 1.25 *10^4 nm^2	36 (8 cells/ 4 exp)	Mann Whitney	**0.0166**
2B cluster area		7.487 ± 0.72 *10^4 nm^2	31 (8 cells/ 4 exp)		
2A loc. precision	Thompson	24.5 ± 0.08	18236 localizations	NA	NA
	Mortensen	26.43 ± 0.09		NA	NA
2B loc. precision	Thompson	26.06±0.15	6080 localizations	NA	NA
	Mortensen	27.91±0.15		NA	NA

2. Nanoclustering of GluN2A- and GluN2B-NMDAR clusters

The dSTORM images of GluN2A- and GluN2B-NMDARs also revealed a non-uniform distribution of the clusters, which contain several nanodomains (**Figure 19A**). In order to characterize these nanodomains, we implemented an additional analysis method to overcome the limitation of DBSCAN when analyzing structures in close proximity (**Figure 20**). The lower number of nanodomains identified in DBSCAN compared to multidimensional image analysis (MIA) is due to the high density of localizations which cannot be corrected for in DBSCAN. Thus the need for MIA analysis to analyze different parameters of nanodomains.

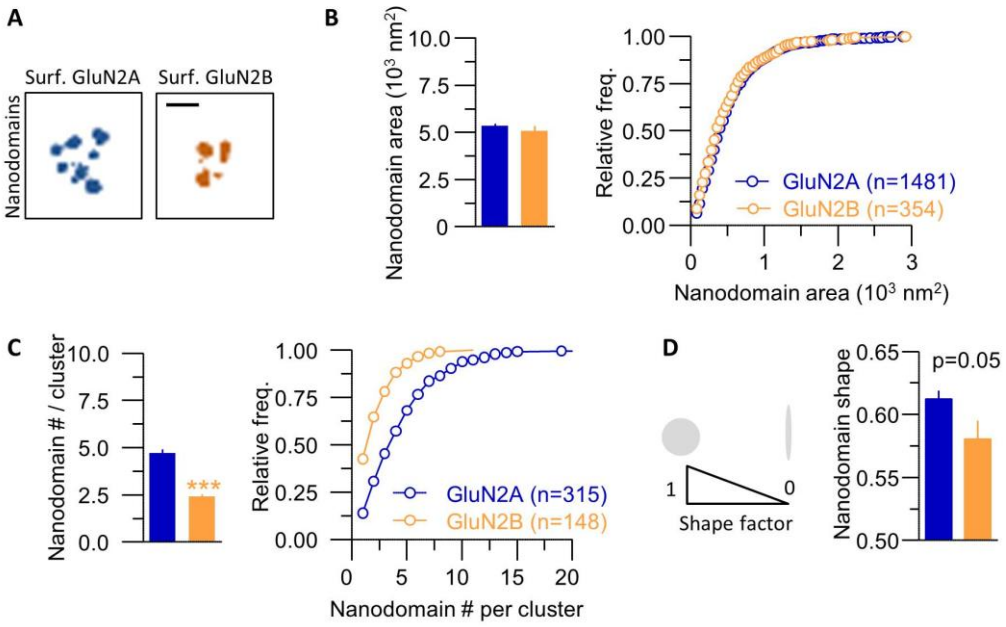

Figure 19. Nano-organization of GluN2A- and GluN2B-NMDARs in mature neurons
A. Enlarged single cluster of GluN2A- (left, blue) or GluN2B-NMDAR (right, orange), both composed of nanodomains (MIA analysis). Scale bar = 200 nm. **B-D.** Comparison between GluN2A- and GluN2B-NMDAR nanodomains: **B.** Mean ± SEM values (left) and relative distribution (right) of GluN2A and GluN2B-NMDAR nanodomain area. **C.** Mean ± SEM values (left) and relative distribution (right) of the number of nanodomains contained within a GluN2A- or GluN2B-NMDAR cluster. **D.** Differences in the shape of GluN2A- and GluN2B-NMDAR nanodomains. Schematic representation of the definition of the shape factor (left): a value between 0 and 1, with an object being circular at 1. Right, the bar graph represents the mean ± SEM values.

MIA analyis provided the following morphometric parameters of the nanodomains: area, number per cluster and shape (Nair et al., 2013). We report here that the area of GluN2A- and GluN2B-NMDAR nanodomains was similar (**Figure 19B**). However, their

number was significantly different, as GluN2A-NMDAR nanodomain number was 2-fold higher than that of GluN2B-NMDARs (**Figure 19C**). Furthermore, GluN2B-NMDAR nanodomains tend to be more elongated than GluN2A-NMDAR ones (**Figure 19D**), as evaluated by the shape factor (value between 0 and 1; the closer to 1 the more circular the structure is) (for exact results, refer to **Table 6**). Thus, both GluN2A- and GluN2B-NMDAR clusters are formed by nanodomains exhibiting subunit-specific characteristics.

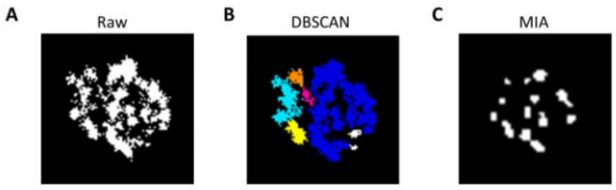

Figure 20. Comparison of DBSCAN and MIA analysis
A. An example of a single NMDAR cluster before analysis. Image was reconstructed with LAMA software. **B.** Same cluster as in (A) after DBSCAN analysis. The different colors correspond to all nanodomains identified within the cluster = 7. **C.** Same cluster as in (A) after MIA analysis. White objects correspond to all nanodomains identified within the cluster = 13.

Table 6. Results of NMDAR nanodomain analysis

Parameter	Analysis method	Mean ± SEM	n	Statistical test	p value
2A nanodomain area	MIA	5.3±1.2* 10^3 nm^2	1481 (16 cells/6 exp)	Mann Whitney	**0.0929**
2B nanodomain area		5.1±2.5* 10^3 nm^2	354 (14 cells/7 exp)		
2A nanodomain #	MIA	4.7±0.2	315 (16 cells/6 exp)	Mann Whitney	**<0.0001**
2B nanodomain #		2.4±0.15	148 (14 cells/7 exp)		
2A nanodomain shape	MIA	0.6122 ±0.007	1481 (16 cells/6 exp)	Mann Whitney	*0.0503*
2A nanodomain shape		0.5807 ±0.014	354 (14 cells/7 exp)		

3. GluN2A- and GluN2B-NMDAR nanoscale organization in synaptic structures

Although the surface density of GluN1-NMDAR (based on GluN1-SEP overexpression in 14 DIV neurons) clusters is similar to that of pre- (vGluT) and post-synapic markers (**Figure 21**), indicating that most surface GluN1-NMDAR clusters are embedded into the synapse, we investigated the nanoscale organization of GluN2A- and GluN2B-NMDAR in glutamate synapses labelled with the postsynaptic marker PSD95. Consistent with the literature, GluN2A-NMDAR were more co-localized with PSD95 when compared to GluN2B-NMDAR (**Figure 22A-B**). Most importantly, the above mentioned difference in surface NMDAR nanoscale organization was recapitualted in identified synapses (**Figure 22C-G**). In addition to differences in nanodomain number, the area of synaptic GluN2A-NMDAR nanodomains were also greater than that of GluN2B-NMDAR (**Figure 22E-G**) (for exact values, refer to **Table 7**). Thus, in identified glutamate synapses, the surface GluN2A- and GluN2B-NMDAR nanoscale organization is different.

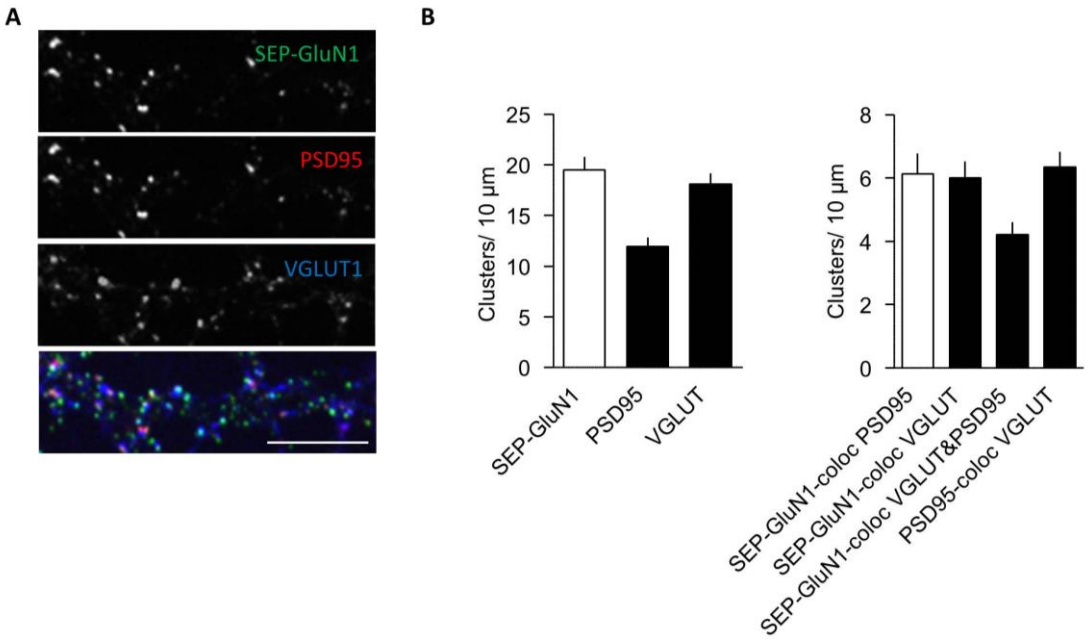

Figure 21. Linear density of GluN1 and its colocalization with pre- and postsynaptic proteins
A. Representative images of 14 DIV neurons with surface labelling of overexpressed GluN1-SEP, endogenous PSD95 or endogenous VGLUT and their merge (green: GluN1-SEP, red: PSD95, blue: VGLUT). Scale bar = 10 µm. **B.** Number of clusters (left) or colocalizing clusters (right) per 10 µm dendrite length (SEP-GluN1 with PSD95 or VGLUT or both; PSD95-VGLUT) (n=44 regions, 27 cells/1 experiment).

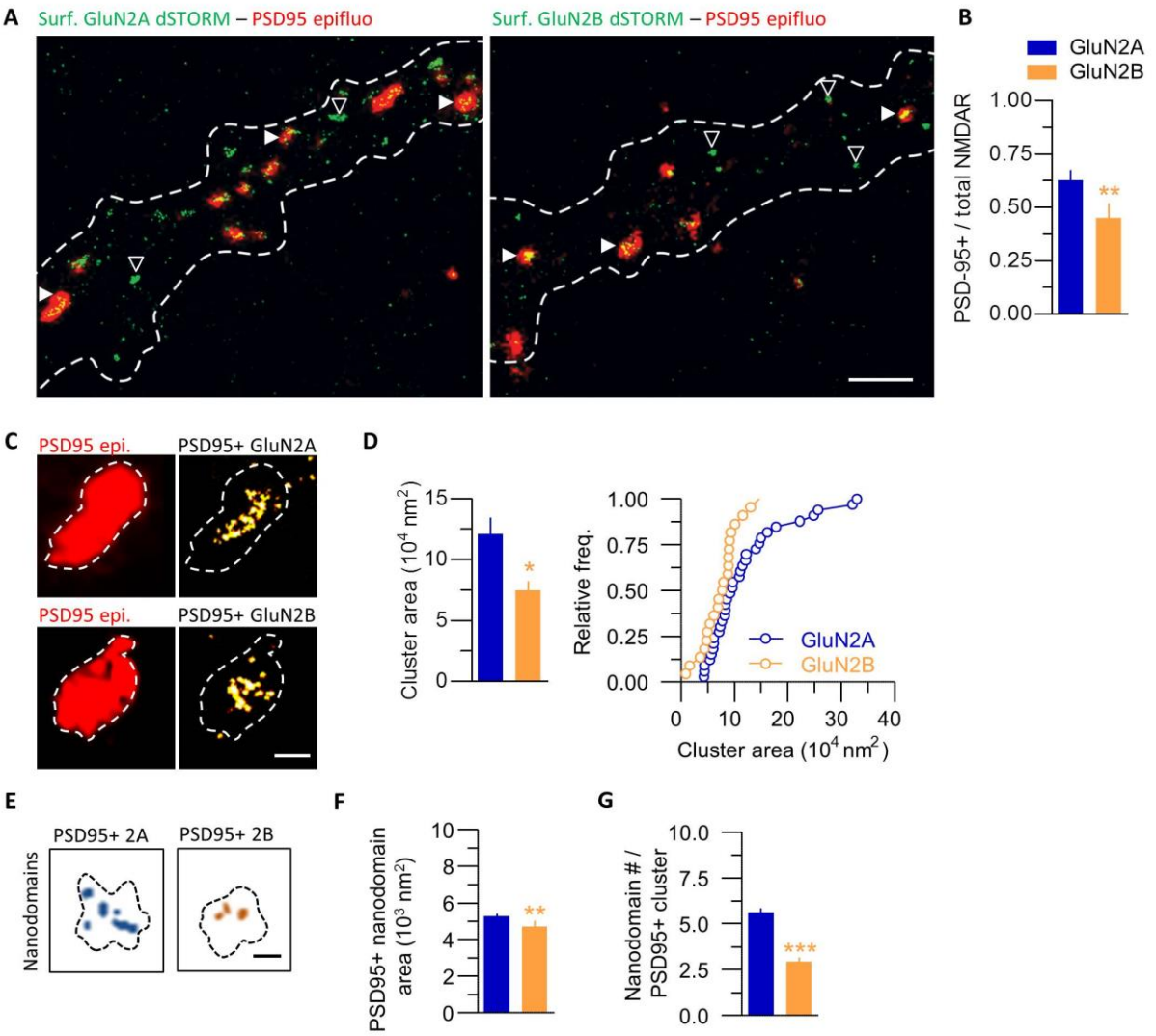

Figure 22. Comparison of PSD95 positive (PSD95+) NMDAR clusters and nanodomains in mature neurons

A. dSTORM image (obtained by Leica LAS software) of GluN2A- (left, green) or GluN2B-NMDAR (right, green) overlaid with the corresponding epifluorescence image of PSD95 (red). Dotted line represents the border of the dendrite based on the NMDAR epifluorescence image. Full arrowheads point to PSD95+ NMDAR clusters, while open arrowheads point to PSD95- (negative) NMDAR clusters. Scale bar = 2 µm. **B.** Ratio of PSD95+ GluN2A- and GluN2B-NMDAR over total surface clusters represented by mean ± SEM values **C.** Left, enlarged PSD95 clusters with dotted outline. Right, enlarged PSD95+ cluster of GluN2A- (top) or PSD95+ GluN2B-NMDAR (bottom). Scale bar = 300 nm. **D.** Differences in the area of PSD95+ GluN2A- and PSD95+ GluN2B-NMDAR clusters represented by the mean ± SEM values (left) and frequency distributions (right). **E-G.** Comparison between PSD95+ GluN2A- and PSD95+ GluN2B-NMDAR nanodomains: **E.** Representative images of enlarged PSD95+ GluN2A (left) or PSD95+ GluN2B nanodomains (MIA). Dotted line represents the border of the epifluorescence PSD95 cluster. Scale bar = 200 nm. **F.** Bar graph of mean ± SEM values of PSD95+ nanodomains. **G.** Bar graph of mean ± SEM values of the number of nanodomains contained within a PSD95+ GluN2A- or GluN2B-NMDAR cluster.

To further confirm these findings, we used another super-resolution imaging approach, i.e. STED microscopy, in neurons expressing tagged-GluN2A and GluN2B subunits. Schematically, GluN2A-HA and GluN2B-flag were overexpressed at 10 DIV, surface-labeled at 14 DIV using specific anti-HA and anti-flag antibodies in live hippocampal neurons, and imaged using STED microscopy in order to achieve similar image quality and spatial resolution for both receptors. GluN1-GFP was co-transfected to delineate NMDAR clusters. In confocal microscopy images GluN2A-HA and GluN2B-flag clusters overlapped without any discernable differences (**Figure 23A**). In contrast, STED images clearly resolved the protein distributions as only partially overlapping (**Figure 23A-B**). Similarly to the dSTORM data (**Figure 16C-D**), the area of GluN2A-NMDAR nanoscale clusters was larger than that of GluN2B-NMDARs (**Figure 23C**) (for exact values, refer to **Table 7**). More importantly, the vast majority, if not all, synapses contained both overexpressed GluN2A- and GluN2B-NMDAR to various relative amount (**Figure 23B-C**), indicating that mature synapses of hippocampal neurons contain a mixture of GluN2A- and GluN2B-NMDARs. Additionally, the STED images also suggest the existence of nanodomains (**Figure 23B**), alike dSTORM images (**Figure 19A**); however, the maximal achievable resolution in our STED setup does not allow the analysis of nanodomain parameters.

Table 7. Results of synaptic GluN2A- and GluN2B-NMDARs

Parameter	Analysis method	Mean ± SEM	n	Statistical test	p value
2A coloc with PSD95	Colocalization	0.63±0.04	16 cells/6 exp	Mann Whitney	**0.0086**
2B coloc with PSD95		0.44±0.07	12 cells/7 exp		
PSD95+ 2A cluster area	DBSCAN	12.07±1.3 $*10^4 nm^2$	33 (8 cells/4 exp)	Mann Whitney	**0.0273**
PSD95+ 2B cluster area		7.45±0.76 $*10^4 nm^2$	22 (6 cells/4 exp)		
PSD95+ 2A nanodomain area	MIA	5.2±0.1 $*10^3 nm^2$	1042 (16 cells/ 6 exp)	Mann Whitney	**0.0094**
PSD95+ 2B nanodomain area		4.7±0.3 $*10^3 nm^2$	189 (12 cells/7 exp)		
PSD95+ 2A nanodomain #	MIA	5.62±0.24	186 (16 cells/6 exp)	Mann Whitney	**0.0001**
PSD95+ 2B nanodomain #		2.93±0.24	69 (12 cells/7 exp)		
2A cluster area	STED	6.1 ±0.48 $*10^4 nm^2$	110 (22 cells/3 exp)	Paired t test	**<0.0001**
2B cluster area		2.7 ±0.24 $*10^4 nm^2$	110 (22 cells/3 exp)		

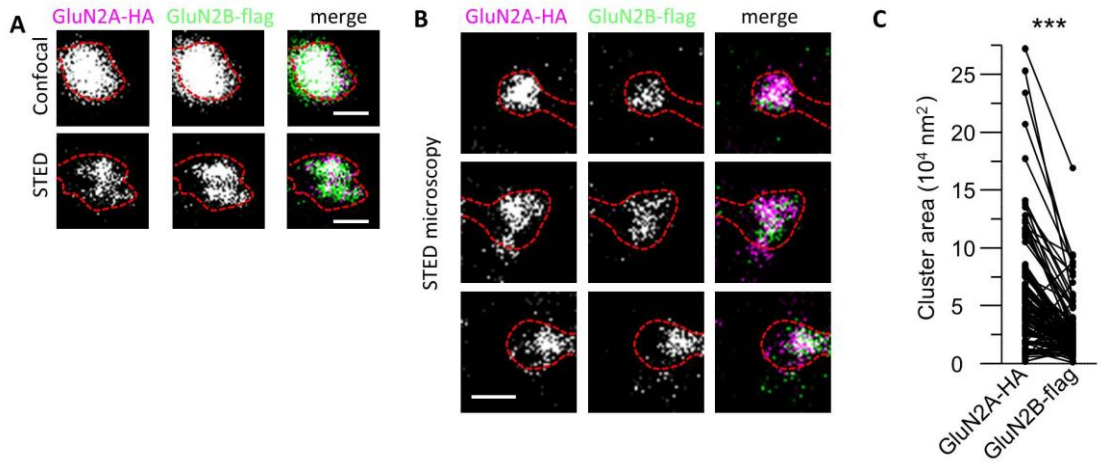

Figure 23. GluN2A- and GluN2B-NMDARs occupy the same synapse

A. Representative image of a cluster of overexpressed GluN2A-HA – AlexaFluor 594 (left), GluN2B-flag – Atto647N (middle), and the merge of the two (right; magenta: GluN2A, green: GluN2B-flag). Top panel: confocal microscopy images, bottom panel: STED microscopy images of same cluster shown in top panel. The red dotted line represents the outline of the spine morphology obtained from GluN1-GFP expression. Scale bar = 400 nm. **B.** Examples of NMDAR clusters obtained by STED imaging of NMDAR clusters expressing both GluN2A-HA (left, magenta), GluN2B-flag (middle) and the merge of the two (right; magenta: GluN2A, green: GluN2B). The red dotted line represents the outline of the spine morphology obtained from GluN1-GFP expression. Scale bar = 400 nm. **C.** Paired analysis of the cluster area of GluN2A-HA and GluN2B-flag (n = 110 clusters / 22 images / 3 experiments for both GluN2A-HA and GluN2B-flag) demonstrates the larger area of GluN2A relative to GluN2B within the same synapse.

4. Developmental changes in the nano-organization of GluN2A- and GluN2B-NMDARs

During brain development an evolution of NMDAR subunit composition can be observed. Schematically, GluN2B-NMDARs are highly expressed during early development and reach a peak around the second postnatal week in rodents, whereas GluN2A-NMDAR levels increase only after birth, exceeding GluN2B subunits by adulthood ([Monyer et al., 1994] for details, refer to Chapter 1. sections 3.1.1. and 4.2.). Whether this developmental subunit change results from a simple subunit swap in fixed nanodomains remains unknown. Therefore, we investigated the nano-organization of GluN2A- and GluN2B-NMDARs throughout development. First, we confirmed the developmental profile of PSD95-positive glutamate synapses in our hippocampal network, with the peak of glutamate synapse number at DIV 17 (**Figure 24, Table 8**), and the concomitant developmental switch of the GluN2A/B subunit enrichment (**Figure 15**). Next, GluN2A- or GluN2B-NMDARs were surface-labeled at 10, 17 and 24 DIV and dSTORM images were acquired of each. Strikingly, GluN2A-NMDAR clusters undergo a major reorganization during this period (**Figure 25**). All cluster parameters were affected, i.e. changes of the cluster area, molecule number (calculated with DBSCAN analysis), nanodomain area and number (**Figure 25**), revealing a major restructuration peak at DIV 17. The GluN2A-NMDAR cluster area expanded between DIV 10 and 17, followed by a reduction at DIV 24 (**Figure 25B**). These changes were paralleled by similar changes in the molecule number per cluster (**Figure 25C**). For GluN2B-NMDAR clusters, similar, though more subtle, changes were observed (**Figure 25**). GluN2B-NMDAR cluster area increased between DIV 10 to 17, and then remained stable (**Figure 25B**). The molecule number per GluN2B-NMDAR cluster was not correlated with this profile as it was highest at immature states (DIV 10), decreasing then over maturation (**Figure 25C**). Thus, the developmental profile of GluN2A- and GluN2B-NMDAR nanoscale organization is different.

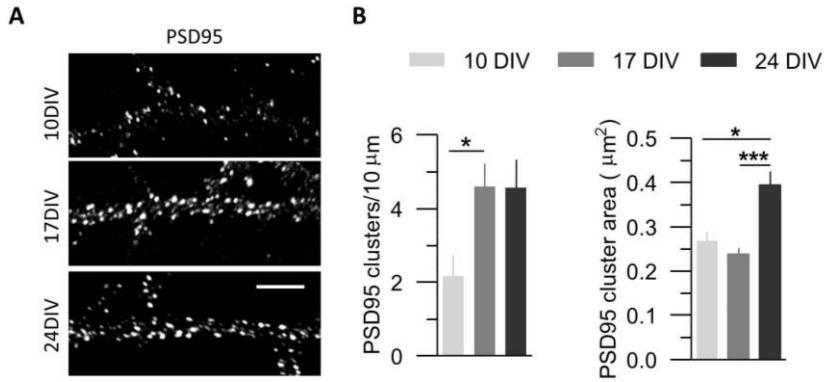

Figure 24. Development of hippocampal cultures
A. Conventional wide-field fluorescence images of the changes in PSD95 immunostaining during the development of neuronal cells. Scale bar = 10 µm. **B.** Bar graphs representing the changes in PSD95 expression during development (mean ± SEM values). Left: linear density of PSD95 clusters per 10 µm dendrite length. Right: PSD95 cluster area.

Table 8. Results of PSD95 cluster analysis during development

Parameter	Analysis method	Mean ± SEM	n	Statistical test	p value
PSD95 cluster#/10µm					
10 DIV	Integrated morphometry analysis	2.16±0.57	156 (30 cells/11 exp)	One-way Anova	*<0.01
17 DIV		4.58±0.63	215 (28/11 exp)		
24 DIV		4.56±0.76	222 (26/9 exp)		
PSD95 cluster area					
10 DIV	Integrated morphometry analysis	0.2677±0.02	156 (30 cells/11 exp)	One-way Anova	*<0.01, ***<0.0001
17 DIV		0.24±0.01	215 (28/11 exp)		
24 DIV		0.4±0.03	222 (26/9 exp)		

When exploring the morphometric characteristics of GluN2A- and GluN2B-NMDAR clusters during this period, a similar trend was observed. The nanodomain area of both NMDAR subtypes increased from DIV 10 to 17, followed by a reduction at DIV 24 (**Figure 25E**). The number of nanodomains also increased from 10 to 17 DIV and was maintained in the case of GluN2A-NMDARs whereas the number did not change until 24 DIV for GluN2B-NMDARs (**Figure 25F**). At all developmental stages, GluN2A-NMDAR clusters contained more nanodomains compared to GluN2B-NMDAR (**Figure 25F**) (for exact values, refer to **Table 9**). Together, our data indicate that NMDAR nano-organization is highly regulated throughout brain cell network development, with clear differences between GluN2A- or GluN2B-NMDARs, suggesting distinct regulatory processes.

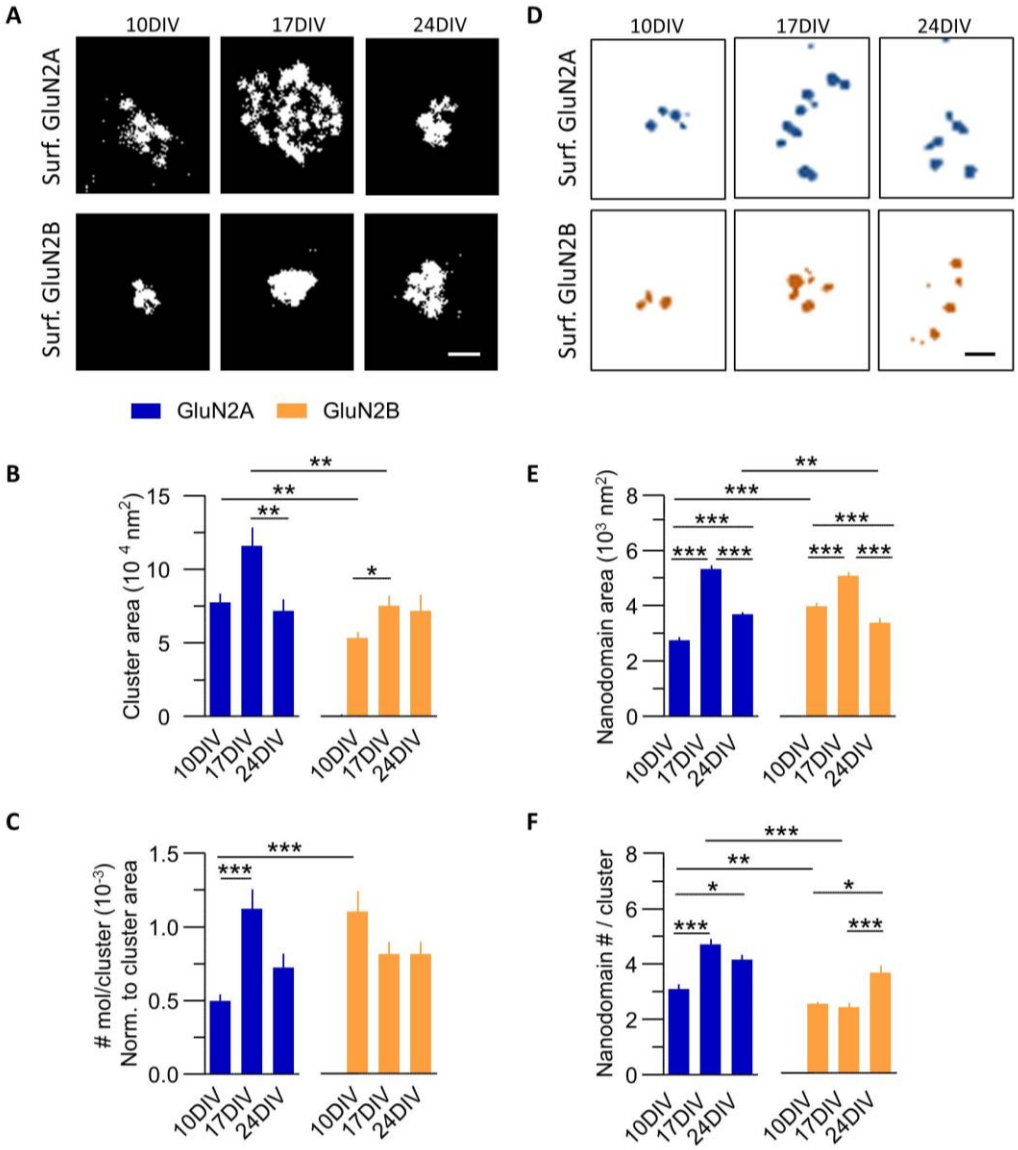

Figure 25. Nanoscopic re-organization of GluN2A- and GluN2B-NMDARs during development
A. Enlarged clusters of GluN2A- (top) or GluN2B-NMDAR (bottom) during development of neuronal cultures (obtained by LAMA software). Scale bar = 200 nm. **B.** Changes in the cluster area of GluN2A- or GluN2B-NMDAR during development. **C.** Developmental changes in the molecule number per GluN2A- or GluN2B-NMDAR. Values are normalized to the cluster area. **D.** Developmental changes in nanodomains of GluN2A- (top) or GluN2B-NMDAR (bottom) clusters (MIA). Scale bar = 100 nm. **E.** Changes in the nanodomain area of GluN2A- or GluN2B-NMDAR. **F.** Changes in the number of nanodomains within clusters of GluN2A- or GluN2B-NMDAR.

Table 9. Results of nano-organizational changes in GluN2A- and GluN2B-NMDARs during development

Parameter	Analysis method	Mean ± SEM	n	Statistical test	p value
2A cluster area					
10 DIV	DBSCAN	7.732±0.64*10^4nm^2	39 (8 cells/4 exp)	Kruskal-Wallis	*<0.01, **<0.001
17 DIV		11.56 ± 1.255*10^4nm^2	36 (8 cells/4 exp)		
24 DIV		7.138 ± 0.824*10^4nm^2	31 (8 cells/4 exp)		
2B cluster area					
10 DIV	DBSCAN	5.313±0.48*10^4nm^2	31 (8 cells/4 exp)	Kruskal-Wallis	*<0.01, **<0.001
17 DIV		7.487±0.72*10^4nm^2	31 (8 cells/4 exp)		
24 DIV		7.158±1.12*10^4nm^2	24 (8 cells/4 exp)		
2A mol #/cluster area					
10 DIV	DBSCAN	0.49±0.05*10^{-3}	39 (8 cells/4 exp)	Kruskal-Wallis	***<0.0001
17 DIV		0.1±0.3*10^{-3}	36 (8 cells/4 exp)		
24 DIV		0.7±0.09*10^{-3}	31 (8 cells/4 exp)		
2B mol #/cluster area					
10 DIV	DBSCAN	1.1±0.1*10^{-3}	31 (8 cells/4 exp)	Kruskal-Wallis	***<0.0001
17 DIV		0.8±0.08*10^{-3}	31 (8 cells/4 ex.)		
24 DIV		0.8±0.08*10^{-3}	24 (8 cells/4 exp)		
2A nanodomain area					
10 DIV	MIA	2.75±0.12*10^3nm^2	554 (12 cells/6 exp)	Kruskal-Wallis	**<0.001, ***<0.0001
17 DIV		5.34 ± 0.12*10^3nm^2	1481 (16 cells/6 exp)		
24 DIV		3.68±0.17*10^3nm^2	1481 (14 cells/5 exp)		
2B nanodomain area					
10 DIV	MIA	3.97±0.14*10^3nm^2	823 (18 cells/5 exp)	Kruskal-Wallis	**<0.001, ***<0.0001
17 DIV		5.08±0.25*10^3nm^2	354 (14 cells/7 exp)		
24 DIV		3.39±0.17*10^3nm^2	491 (12 cells/4 exp)		
2A nanodomain #					
10 DIV	MIA	3.1±0.17	180 (12 cells/6 exp)	Kruskal-Wallis	*<0.01, **<0.001, ***<0.0001
17 DIV		4.7±0.2	315 (16 cells/6 exp)		
24 DIV		4.1±0.26	287 (14 cells/5 exp)		
2B nanodomain #					
10 DIV	MIA	2.5±0.09	331 (18 cells/5 exp)	Kruskal-Wallis	*<0.01, **<0.001, ***<0.0001
17 DIV		2.4±0.14	148 (14 cells/7 exp)		
24 DIV		3.6±0.26	135 (12 cells/4 exp)		

5. Differential regulation of NMDAR nanoscale organization by PDZ scaffolds and CaMKII activity

Although numerous molecules have been shown to regulate NMDAR trafficking, their synaptic anchoring mostly relies on the protein-protein interactions and phosphorylation state of their long intracellular CTDs (Lau and Zukin, 2007; Sanz-Clemente et al., 2013b). The PDZ binding motif is critical for interaction with PSD-MAGUKs, and is also a site of regulation by protein kinases such as CaMKII. Thus, we challenged GluN2A- and GluN2B-NMDARs by altering their interactions with PDZ scaffold using well-described biomimetic competing peptides (Bard et al., 2010) and by blocking the activity of CaMKII. First, we used TAT-coupled divalent competitive peptides that interfere with the binding of the CTD of either GluN2A or GluN2B and their PDZ scaffold partners (Bard et al., 2010). Both the cluster area and molecule number of GluN2A-NMDARs were significantly decreased in the presence of $[TAT\text{-}GluN2A]_2$ when compared to the control condition (i.e. $[TAT\text{-}NS]_2$) (**Figure 26A-C**), whereas GluN2A-NMDAR nanodomain area and number remained stable (**Figure 26E, G**). Together, this leads to a significant reduction of GluN2A-NMDAR density in nanodomains (**Figure 26I**), consistent with the former observation that this competing peptide rapidly displaced GluN2A-NMDARs from synapses (Bard et al., 2010). Quite differently, disrupting the interaction between GluN2B-NMDARs and PDZ scaffolds ($[TAT\text{-}GluN2B]_2$ peptide) significantly increased the GluN2B-NMDAR nanodomain area (**Figure 26F, H**) without affecting cluster area or molecule number (**Figure 26B, D**). Thus, although this also leads to a significant reduction of GluN2B-NMDAR density in nanodomains (**Figure 26J**), consistent with the former observation (Bard et al., 2010), the topographical changes are dramatically different between GluN2A- and GluN2B-NMDARs (for exact values, refer to **Table 10**).

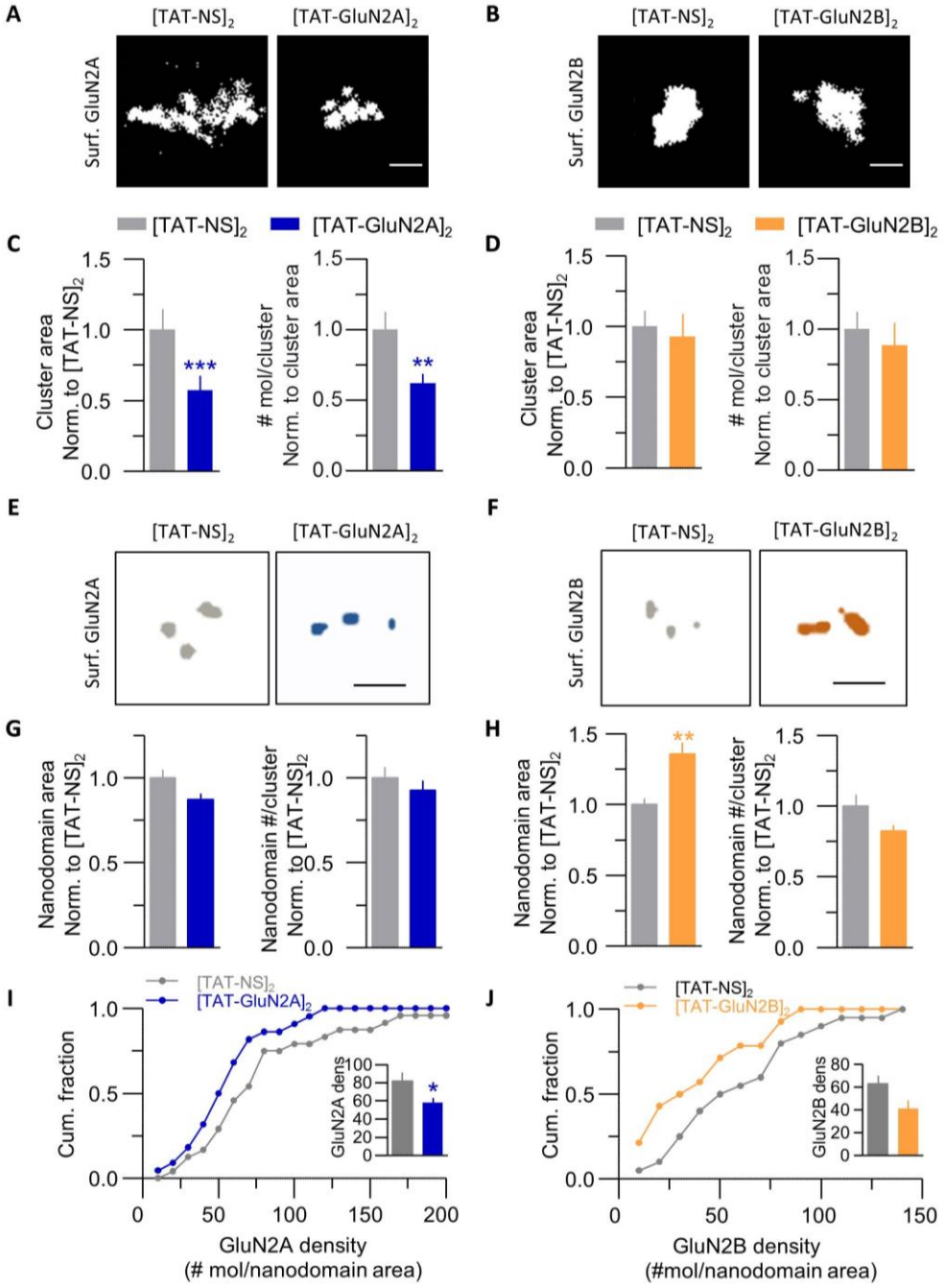

Figure 26. Effect of specific disrupting TAT peptides on GluN2A- and GluN2B-NMDAR organization
A-B. Enlarged dSTORM GluN2A- (**A**) or GluN2B-NMDAR (**B**) cluster (LAMA) after stimulation with either $[TAT\text{-}NS]_2$ or specific $[TAT\text{-}GluN2A]_2$ (**A**) or $[TAT\text{-}GluN2B]_2$ (**B**) peptide. **C.** Mean ± SEM values of GluN2A-NMDAR cluster area (left) and molecule number (right) in control ($[TAT\text{-}NS]_2$) and $[TAT\text{-}GluN2A]_2$ conditions. Values are normalized to $[TAT\text{-}NS]_2$. **D.** Mean ± SEM values of GluN2B-NMDAR cluster area (left) and molecule number (right) in control ($[TAT\text{-}NS]_2$) and $[TAT\text{-}GluN2B]_2$ conditions. Values are normalized to $[TAT\text{-}NS]_2$. **E-H.** Effect of TAT peptides on nanodomains: GluN2A- (**E**) or GluN2B-NMDAR (**F**) nanodomains (MIA) following treatment with either $[TAT\text{-}NS]_2$ or specific $[TAT\text{-}GluN2A]_2$ (**E**) or $[TAT\text{-}GluN2B]_2$ (**F**) peptide. **G.** Mean ± SEM values of GluN2A-NMDAR nanodomain area (left) and number (right). **H.** Mean ± SEM values of GluN2B-NMDAR nanodomain area (left) and number (right). **I-J.** Density of GluN2A- or GluN2B-NMDARs: relative frequency of GluN2A- (**I**) or GluN2B-NMDAR (**J**) molecule number per nanodomain area. Inset graphs represent respective mean ± SEM values. Scale bar = 200 nm.

Table 10. Results of the effect of specific disrupting peptides on the nano-organization of GluN2A- and GluN2B-NMDARs

Parameter	Analysis method	Mean ± SEM	n	Statistical test	p value
2A cluster area					
$[TAT\text{-}NS]_2$	DBSCAN	1.0±0.14	24 (6 cells/3 exp)	Mann Whitney	**0.0006**
$[TAT\text{-}GluN2A]_2$		0.57±0.1	22 (6 cells/3 exp)		
2A mol # / cluster area					
$[TAT\text{-}NS]_2$	DBSCAN	1.0±0.12	24 (6 cells/3 exp)	Mann Whitney	**0.0098**
$[TAT\text{-}GluN2A]_2$		0.62±0.06	22 (6 cells/3 exp)		
2A nanodomain area					
$[TAT\text{-}NS]_2$	MIA	1.0±0.05	359 (13 cells/4 exp)	Mann Whitney	0.29
$[TAT\text{-}GluN2A]_2$		0.87±0.03	393 (15 cells/4 exp)		
2A nanodomain #					
$[TAT\text{-}NS]_2$	MIA	1.0±0.06	107 (13 cells/4 exp)	Mann Whitney	0.25
$[TAT\text{-}GluN2A]_2$		0.92±0.06	129 (15 cells/4 exp)		
2A density	Mol # per nanodomain area				
$[TAT\text{-}NS]_2$		81.5±9.9	24 (6 cells/3 exp)	Unpaired t test	**0.046**
$[TAT\text{-}GluN2A]_2$		57.4±5.7	22 (6 cells/3 exp)		
2B cluster area					
$[TAT\text{-}NS]_2$	DBSCAN	1.0±0.11	20 (6 cells/3 exp)	Mann Whitney	0.61
$[TAT\text{-}GluN2B]_2$		0.93±0.16	14 (6 cells/3 exp)		
2B mol # / cluster area					
$[TAT\text{-}NS]_2$	DBSCAN	1.0±0.12	20 (6 cells/3 exp)	Mann Whitney	0.39
$[TAT\text{-}GluN2B]_2$		0.88±0.15	14 (6 cells/3 exp)		
2B nanodomain area					
$[TAT\text{-}NS]_2$	MIA	1.0±0.04	327 (11 cells/3 exp)	Mann Whitney	**0.0045**
$[TAT\text{-}GluN2B]_2$		1.36±0.08	214 (13 cells/3 exp)		
2B nanodomain #					
$[TAT\text{-}NS]_2$	MIA	1.0±0.08	133 (11 cells/3 exp)	Mann Whitney	0.44
$[TAT\text{-}GluN2B]_2$		0.82±0.04	104 (13 cells/3 exp)		
2B density	Mol # per nanodomain area				
$[TAT\text{-}NS]_2$		62.7±7.4	20 (6 cells/3 exp)	Unpaired t test	0.25
$[TAT\text{-}GluN2A]_2$		40.8±7.1	14 (6 cells/3 exp)		

Interestingly, the $[TAT\text{-}GluN2A]_2$ peptide increased the nanodomain number of GluN2B-NMDAR clusters without affecting the cluster area, molecule number or nanodomain (**Figure 27**, **Table 11**).

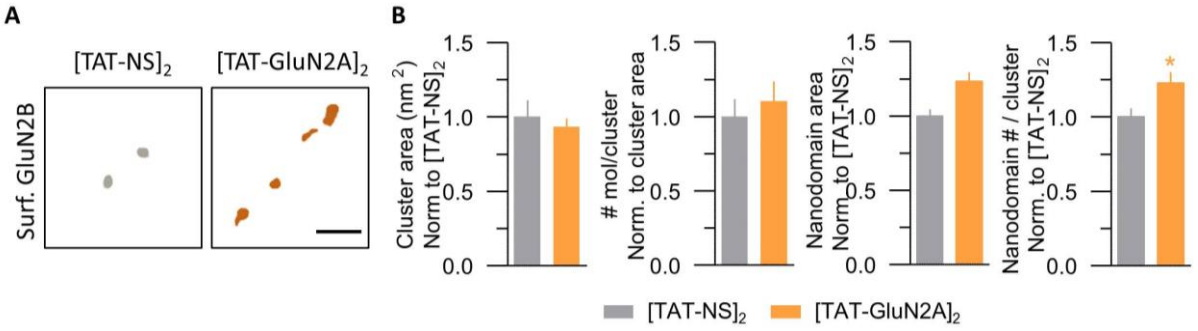

Figure 27. Effect of $[TAT\text{-}GluN2A]_2$ on GluN2B-NMDARs
A. Enlarged cluster (MIA) of GluN2B-NMDAR treated with either $[TAT\text{-}NS]_2$ (left) or $[TAT\text{-}GluN2A]_2$ (right); both clusters are composed of nanodomains. **B.** Effect of $[TAT\text{-}GluN2A]_2$ (orange) on GluN2B-NMDAR compared to control $[TAT\text{-}NS]_2$ (gray). Values represent mean ± SEM normalized to $[TAT\text{-}NS]_2$. Graphs from left to right: cluster area, molecule number per cluster, nanodomain area and nanodomain number per cluster. Scale bar = 200 nm.

Table 11. Results of the effect of $[TAT\text{-}GluN2A]_2$ on GluN2B-NMDAR nano-organization

Parameter	Analysis method	Mean ± SEM	n	Statistical test	p value
2B cluster area					
$[TAT\text{-}NS]_2$	DBSCAN	1.0±0.11	20 (6 cells/ 3 exp)	Mann Whitney	0.74
$[TAT\text{-}GluN2A]_2$		0.93±0.06	19 (4 cells/ 3 exp)		
2B mol #/cluster area					
$[TAT\text{-}NS]_2$	DBSCAN	1.0±0.12	20 (6 cells/ 3 exp)	Mann Whitney	0.53
$[TAT\text{-}GluN2A]_2$		1.1±0.13	19 (4 cells/ 3 exp)		
2B nanodomain area					
$[TAT\text{-}NS]_2$	MIA	1.0±0.05	90 (8 cells/ 3 exp)	Mann Whitney	0.061
$[TAT\text{-}GluN2A]_2$		1.23±0.13	100 (8 cells/ 3 exp)		
2B nanodomain #					
$[TAT\text{-}NS]_2$	MIA	1.0±0.06	90 (8 cells/ 3 exp)	Mann Whitney	**0.019**
$[TAT\text{-}GluN2A]_2$		1.23±0.07	100 (8 cells/ 3 exp)		

If different regulatory processes are involved in the nanoscale organization of these NMDAR subtypes, one may predict that altering the activity of CaMKII, a major regulator of GluN2-NMDAR synaptic content (Hell, 2014), will differentially impact GluN2A- and GluN2B-NMDAR nanoscale organization. To test this, we acutely blocked CaMKII activity using the autocamtide-2-related inhibitory peptide (AIP), a specific substrate competitive inhibitor of CaMKII, and examined its impact on NMDAR nanoscale distribution (**Figure**

28A, C). For GluN2A-NMDARs, AIP increased the density of GluN2A-NMDAR in nanodomains through an increase in the molecule number and no change in cluster and nanodomain topography (**Figure 28A-B, E-F, I**). In contrast, for GluN2B-NMDARs, AIP increased the area of GluN2B nanodomain (**Figure 28H**) without affecting the number of molecules or nanodomains (**Figure 28D, G-H, J**) (for exact values, refer to **Table 12**). Collectively, these data demonstrate that GluN2A- and GluN2B-NMDARs are differentially regulated by the alteration of their PDZ scaffold binding and CaMKII activity. The regulation of GluN2A-NMDARs mostly implicates changes in the number of receptors in fixed nanodomains, whereas the regulation of GluN2B-NMDARs mostly implicates changes in the nanodomain topography with fixed number of receptors.

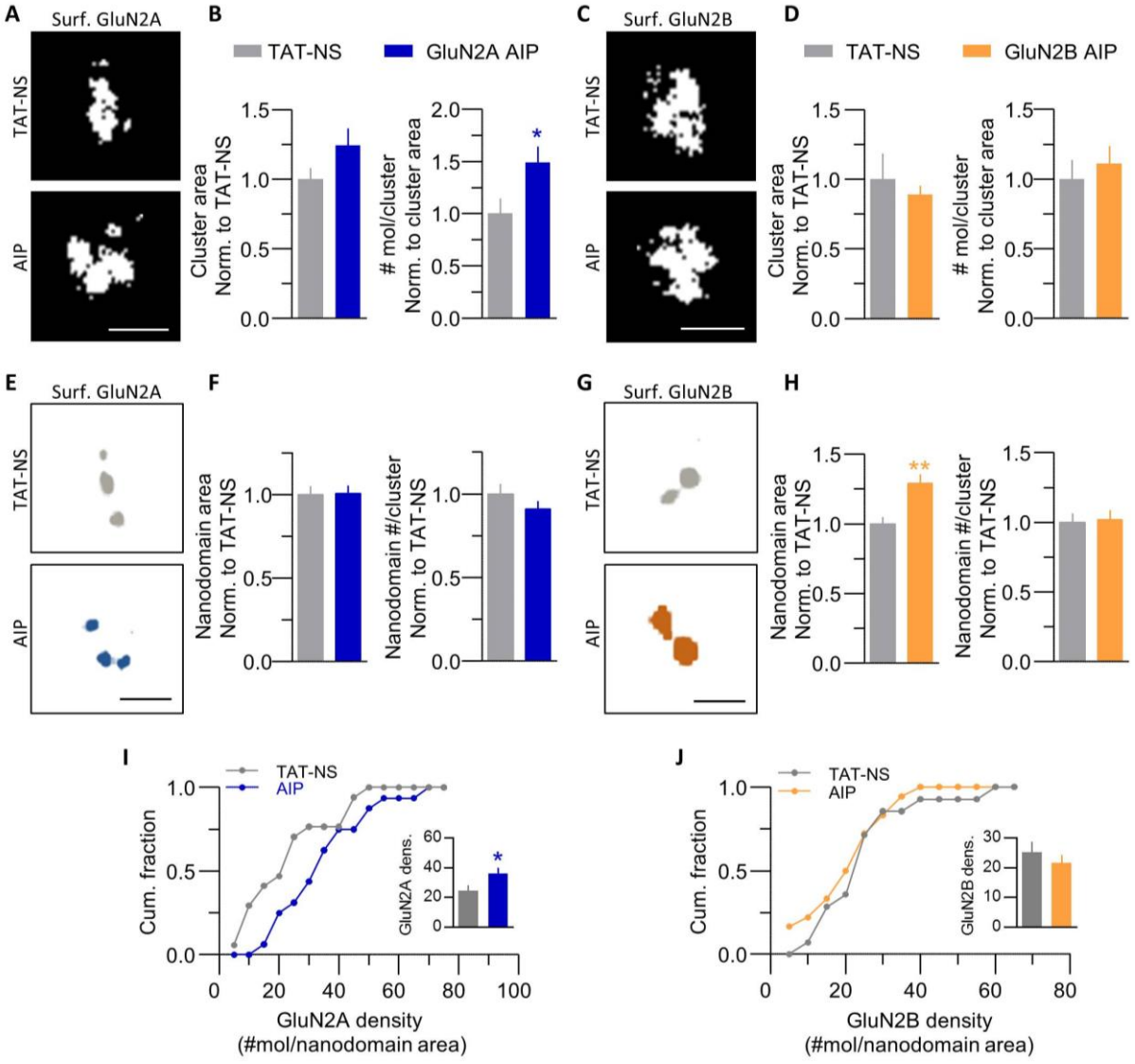

Figure 28. Effect of CaMKII inhibition on GluN2A- and GluN2B-NMDAR organization
A-D. Effect of AIP treatment on cluster area and molecule number: Enlarged dSTORM GluN2A (**A**) or GluN2B-NMDAR (**C**) cluster (LAMA) stimulated with either TAT-NS or AIP. **B.** Mean ± SEM values of

GluN2A-NMDAR cluster area (left) and cluster molecule number (right) in control (TAT-NS) and AIP conditions. Values are normalized to TAT-NS. D. Mean ± SEM values of GluN2B-NMDAR cluster area (left) and cluster molecule number (right) in control (TAT-NS) and AIP conditions. Values are normalized to TAT-NS. **E-H.** Effect of AIP treatment on the nano-organization of GluN2A- or GluN2B-NMDAR: GluN2A-NMDAR (**E**) or GluN2B-NMDAR (**G**) nanodomains (MIA) following treatment with either TAT-NS or AIP. **F.** Mean ± SEM values of GluN2A-NMDAR nanodomain area (left) and number (right). **H.** Mean ± SEM values of GluN2B-NMDAR nanodomain area (left) and number (right). **I-J.** Density of GluN2A- or GluN2B-NMDARs: relative frequency of GluN2A- (**I**) or GluN2B-NMDAR (**J**) molecule number per nanodomain area. Inset graphs represent respective mean ± SEM values. Scale bar = 200 nm.

Table 12. Results of the effect of CaMKII inhibition on the nano-organization of GluN2A- and GluN2B-NMDARs

Parameter	Analysis method	Mean ± SEM	n	Statistical test	p value
2A cluster area					
TAT-NS	DBSCAN	1.0±0.08	17 (5 cells/2 exp)	Mann Whitney	0.25
AIP		1.24±0.15	16 (5 cells/2 exp)		
2A mol # / cluster area					
TAT-NS	DBSCAN	1.0±0.15	17 (5 cells/2 exp)	Mann Whitney	**0.0244**
AIP		1.5±0.15	16 (5 cells/2 exp)		
2A nanodomain area					
TAT-NS	MIA	1.0±0.95	197 (9 cells/3 exp)	Mann Whitney	0.66
AIP		1.005±0.05	177 (9 cells/3 exp)		
2A nanodomain #					
TAT-NS	MIA	1.0±0.06	95 (9 cells/3 exp)	Mann Whitney	0.42
AIP		0.91±0.05	94 (9 cells/3 exp)		
2A density	Mol # per nanodomain area				
TAT-NS		24.24±3.56	17 (5 cells/2 exp)	Unpaired t test	**0.015**
AIP		35.9±3.75	16 (5 cells/2 exp)		
2B cluster area					
TAT-NS	DBSCAN	1.0±0.18	14 (5 cells/3 exp)	Mann Whitney	0.805
AIP		0.89±0.07	18 (5 cells/3 exp)		
2B mol # / cluster area					
TAT-NS	DBSCAN	1.0±0.14	14 (5 cells/3 exp)	Mann Whitney	0.31
AIP		1.11±0.13	18 (5 cells/3 exp)		
2B nanodomain area					
TAT-NS	MIA	1.0±0.05	143 (10 cells/4 exp)	Mann Whitney	**0.0035**
AIP		1.3±0.06	143 (9 cells/3 exp)		
2B nanodomain #					
TAT-NS	MIA	1.0±0.06	81 (10 cells/4 exp)	Mann Whitney	0.82
AIP		1.02±0.07	80 (10 cells/4 exp)		
2B density	Mol # per nanodomain area				
TAT-NS		25.1±3.4	14 (5 cells/3 exp)	Unpaired t test	0.2
AIP		21.64±2.4	18 (5 cells/3 exp)		

Chapter 5: Discussion and future perspectives

Here we used a combination of single-molecule imaging (dSTORM) and quantitative spatial analysis in rat hippocampal neurons to examine the surface organization of GluN2A- and GluN2B-NMDARs at nanoscale resolution. Although the distribution of individual molecules revealed a structured pattern of both NMDAR subtypes, we unveiled a clear difference in the number, area, and shape of their nanoscale structures (nanodomains). This differential organization was maintained in synaptic structures identified by PSD95. During development, the membrane organization of both NMDAR subtypes evolved, with marked changes for GluN2A-NMDAR topology. Preventing the interaction between GluN2 C-termini and PDZ scaffolds or blocking CaMKII activity differentially impacted their nanoscale organization. Indeed, these manipulations regulated the number of GluN2A-based individual molecules in an unchanged topography. In contrast, the number of GluN2B-based individual molecules remained constant in an altered topography. Thus, the nanoscale organization of surface GluN2A- and GluN2B-NMDARs in hippocampal neurons is structurally different and regulated by different processes, supporting the hypothesis that these NMDAR subtypes are engaged in distinct signaling complexes.

Excitatory synapses are mostly found in small dendritic protrusions called dendritic spines. The molecular architecture of dendritic spines defines the efficiency of signal transmission; therefore it is essential to understand the precise localization of neurotransmitter receptors, PSD scaffolds and signaling molecules, as well as the mechanisms involved in regulating their dynamic localization. The development of super-resolution microscopy has permitted to image beyond the diffraction limit of light, providing unprecedented insight into the subcellular organization of such complex structures (reviewed in Tønnesen and Nägerl, 2013; Willig and Barrantes, 2014; MacGillavry and Hoogenraad, 2015; Zhong, 2015). These techniques have revealed that the nanoscale organization of such neurotransmitter receptors, PSD scaffolds and signaling molecules (e.g. AMPARs, PSD95, and CaMKII) is structured in the postsynaptic compartment (Fukata et al., 2013; MacGillavry et al., 2013; Nair et al., 2013; Lu et al., 2014). Both AMPARs and PSD95 are clustered in 1-4 nanodomains of ~50-80 nm size in hippocampal synapses. These nanodomains are plastic entities as spine size and neuronal activity can directly affect their structure demonstrated by their increased number after blockade of neuronal activity (MacGillavry et al., 2013; Nair et al., 2013). Differential

nanoscale distributions of GluN2A- and GluN2B-NMDARs were previously suggested by the differential enrichment of these two subtypes in PSD95 clusters. Indeed, GluN2A-NMDARs were not, whereas GluN2B-NMDAR localizations were statistically enriched in PSD95 domains compared to the total PSD; however, this study did not distinguish between surface and intracellular receptors (MacGillavry et al., 2013). Here we provide the first surface mapping of GluN2A- and GluN2B-NMDARs at the nanoscale level, revealing the presence of 2 to 5 nanodomains per NMDAR cluster. The similarities between AMPARs, PSD95, and now NMDAR nanodomains in hippocampal synapses strengthen the view that the postsynaptic compartment is a highly compartmentalized structure. Interestingly, nano-sized clusters have also been identified for other, non-neuronal membrane proteins (reviewed in Garcia-Parajo et al., 2014); therefore, nanoclustering appears to be a dominant feature of protein organization which potentially represents a mode of spatiotemporal orchestration of biochemical reactions as suggested by liquid-liquid phase transitions (Li et al., 2012; Banjade and Rosen, 2014). In eukaryotic cells, specific chemical reactions occur in multiple isolated compartments surrounded by membrane bilayers (e.g. nucleus, ER, mitochondria, etc.). However, not all cellular compartments are wrapped in membranes, especially when rapid and dynamic reactions to the changing environment are required, where membranes could actually function as rate-limiting factors. Examples of well-recognized membrane-lacking cellular compartments include ribonucleoprotein enriched granules, Cajal bodies and PML (promyelocytic leukemia) nuclear bodies, centrosomes, and stress or germ granules in the cytoplasm (Hyman et al., 2014; Banani et al., 2017) which usually have irregular architecture and are enriched with specific sets of components with varying stoichiometry (Hyman et al., 2014; Banani et al., 2017). Compartmentalization is even more critical for the postsynaptic terminal, where concentrating components together can increase reaction kinetics for proper reception, interpretation, and storage of signals transmitted by the presynaptic neuron. PSD95 and SynGAP have been shown to spontaneously undergo phase transition, forming condensed, membrane-lacking compartments *in vitro* (Zeng et al., 2016). The key requirements for phase transition (*in vitro*), are multivalent protein–protein interactions and high (submillimolar) local protein concentration (Li et al., 2012) which can be accomplished within the PSD. Therefore the nanoscale structures observed in neurons likely serve as important neurotransmission units, as suggested by their alignment with the presynaptic machinery (Tang et al., 2016). The differential nanoscale organization of GluN2A- and GluN2B-NMDARs suggests the presence of distinct transmission units. It is noteworthy, that GluN1/GluN2A/GluN2B triheteromers have been proposed to compose a variable fraction of

synaptic NMDARs (Al-Hallaq et al., 2007; Rauner and Köhr, 2011). Our super-resolved surface mapping supports a model in which postsynaptic NMDAR clusters of mature neurons are composed of a heterogeneous mixture of diheteromeric GluN2A- and GluN2B-containing NMDARs (non-overlapping nanoscale areas) and, possibly, triheteromeric GluN1/GluN2A/GluN2B-NMDARs (overlapping nanoscale area).

Although both GluN2A and GluN2B display a relatively broad expression throughout the CNS, a developmental evolution of NMDAR subunit composition can be observed in many brain regions. GluN2B levels are high during embryonic and early postnatal development (Monyer et al., 1994; Sans et al., 2000; Sheng et al., 1994) which is required for spine growth, stabilization of synaptic connections and hippocampus-dependent learning (von Engelhardt et al., 2008; Lee et al., 2010). However, GluN2B expression can inhibit the synaptic incorporation of AMPARs (Hall et al., 2007; Ferreira et al., 2011; Gray et al., 2011) and reduce the threshold for LTP (Lee, 2010; Xu et al., 2009; Yashiro & Philpot, 2008) which is overcome by a developmental switch from synaptic GluN2B-containing NMDARs to synaptic GluN2A-containing NMDARs. GluN2A expression gradually increases after birth and becomes abundant in adulthood (Monyer et al., 1994; Sans et al., 2000; Sheng et al., 1994). This raises the question whether the developmental switch is also observed at the nanoscopic level. If yes, are there differences in the nano-organization between GluN2A and GluN2B during development? Here we show that GluN2A-NMDAR clusters and nanodomains undergo a major reorganization during the evolution of hippocampal cultures with a major restructuration peak at 17 DIV, whereas similar, although more discrete changes occur in GluN2B-NMDAR nanodomains. This data, together with the observation that GluN2A-NMDAR clusters contained more nanodomains at all developmental stages compared to GluN2B-NMDARs indicates that NMDAR nano-organization is highly regulated throughout brain cell network development, with clear differences between GluN2A- and GluN2B-NMDARs.

In addition to the subdiffraction topological information given by super-resolution imaging, single-molecule imaging techniques taking advantage of fluorophore switching, such as dSTORM and PALM, also carry the potential of providing valuable quantitative information of the protein of interest. Single-molecule data is collected by temporally resolving individual fluorophores. The precise position of a single molecule is calculated with up to ~10 nm accuracy for the current available fluorophores (Bobroff, 1986; Patrizio and

Specht, 2016). The coordinate information belonging to the imaged fluorophores is then combined to obtain a super-resolved pointillist image. Precise analysis of synaptic protein copies is of particular interest in studying neurotransmission, since the efficiency of this process is correlated to the availability of receptors as well as the rapid changes in receptor numbers. Such quantifications for AMPARs demonstrated a relationship between AMPAR nanodomain content and the amplitude of synaptic transmission (MacGillavry et al., 2013; Nair et al., 2013). However, the direct use of localization number as molecule number does not take into account fluorophore blinking properties. Therefore, we implemented a localization density-based analysis (DBSCAN [Ester et al., 1996]) to identify the number of molecules per NMDAR cluster with a fluorophore blinking correction included (Malkusch and Heilemann, 2016a). Both GluN2A and GluN2B were localized with ~25 nm precision. The developmental changes in the molecule number per GluN2A-NMDAR cluster matched the changes observed in cluster organization. In contrast, an inverse correlation can be observed between GluN2B-NMDAR cluster area and molecule number, further supporting a differential hierarchical organization of these distinct NMDAR subtypes.

Over the past few decades, the mechanisms underlying the trafficking and synaptic anchoring of GluN2A- and GluN2B-NMDARs have been the subject of intense investigation (Lau and Zukin, 2007; Sanz-Clemente et al., 2013b). A well-established working model proposes that the binding of GluN2A or GluN2B subunits to different PSD-MAGUK proteins, *via* the interaction between the C-terminus of GluN2A/GluN2B subunits and PDZ domains of MAGUKs, plays an important role in the localization of synaptic NMDARs. This functional interaction is further regulated by phosphorylation events mediated by various kinases such as CaMKII and CK2 (Sanz-Clemente et al., 2010). In this study, both surface endogenous GluN2A- and GluN2B-NMDARs were acutely challenged by alterations of either scaffold binding or CaMKII-dependent phosphorylation, and changes in their surface nano-organization were monitored using super-resolution imaging. As expected, the nanoscale organization of both GluN2A- and GluN2B-NMDARs was altered by these molecular challenges, consistent with the role of PDZ scaffolds and CaMKII regulation of NMDAR-mediated transmission (Lau and Zukin, 2007; Sanz-Clemente et al., 2013b). However, the nanoscale modifications were strikingly different for GluN2A- and GluN2B-NMDARs. Preventing the interaction between GluN2A-NMDARs and PDZ scaffolds decreased the density of receptors within nanodomains by reducing the number of receptors within unaltered nanodomains (i.e. topology). In contrast, preventing the interaction between

GluN2B-NMDARs and PDZ scaffolds decreased the density of receptors within nanodomains by altering their topology without changing the receptor number. These data support thus a model in which PDZ scaffolds control GluN2-NMDARs *via* two distinct mechanisms. The GluN2A-NMDARs are potentially anchored through their PDZ interactions in stable nanodomains, controlling most of their synaptic content. By contrast, GluN2B-NMDARs are possibly redistributed between different nanodomains, depending on the type of engaged interactions. Interestingly, it has been recently reported that *in vivo* NMDARs are partitioned into discrete populations of ~0.8 MDa complexes composed only of NMDAR subunits and ~1.5 MDa supercomplexes containing additional PSD scaffolds (Frank et al., 2016). These complexes and supercomplexes could actually enclose multiple GluN2A- and GluN2B-NMDARs and it has been proposed that a neurotransmitter nanocluster can accommodate between 30 to 60 supercomplexes (Frank and Grant, 2017). Interestingly, disrupting the interaction between PSD-MAGUK proteins and GluN2B-NMDARs, but not GluN2A-NMDARs, dismantles NMDAR supercomplexes (1.5 MDa). This is consistent with our findings, suggesting a specific role of GluN2B-NMDARs in structuring different nanoscale complexes in the postsynaptic density whereas GluN2A does not appear to be an organizer in this compartmentalization. The differential effect of CaMKII blockade on the nanoscale organization between NMDAR subtypes also fuels this model. The identified protein composition of supercomplexes further supports the idea that receptor nanoclustering serves to compartmentalize specific postsynaptic functions, through spatial localization, in order to increase regulation efficiency.

Conclusions and future perspectives

My project aimed to investigate the precise localization and architecture of two major NMDAR subtypes at the nanometer level with special focus on the regulation of this organization. In conclusion, we here provide the first nanoscale topographical map of native GluN2A- and GluN2B-NMDARs in rat hippocampal neurons. Additionally, we unveil that these key NMDAR subtypes are differentially organized in basal conditions and under synaptic remodeling processes and that the regulation of their nano-organization is achieved at different hierarchical levels.

We demonstrate that both NMDAR subtypes are organized in nanoscale structures (nanodomains) that differ in their number, area, and shape. However, the biological functions underlying the physical parameters of these nanodomains are not fully understood. It appears that GluN2B, in contrast to GluN2A, is important for nanodomain structuration. Still, are there other factors controlling nanodomain organization? PSD scaffold proteins, for instance, seem to be logical candidates, especially because of their important role in anchoring and trafficking of NMDARs to the synapse. This also raises the question whether nanodomains are assembled in the cellular membrane from individual components or are they trafficked to the membrane as a whole? Can individual receptors pass in between distinct nanodomains? Based on our data on GluN2A nano-organizational changes, it appears to be the case; nonetheless, additional, live single-molecule imaging is required to confirm this. Such techniques would also provide information on the dynamic properties of nanodomains. It would be interesting to examine whether nanodomains also move in and out of the synapse, similarly to receptors.

Here we studied the organization of individual GluN2A- and GluN2B-containing NMDARs. The STED images suggest that both GluN2A- and GluN2B-NMDARs occupy the same synaptic area; however, it does not confirm, whether both NMDAR subtypes are present in the same nanodomains. Do distinct nanodomains activate specific intracellular signaling cascades? Could the different nanodomains explain the selective effects of co-agonists on GluN2A- and GluN2B-NMDARs? Moreover, how are the nanodomains co-organized with other neurotransmitter receptors such as AMPARs that also form nanoclusters in synapses? Multi-color single-molecule imaging techniques and developing labeling strategies can help us tackle this question. Live imaging methods could also provide information on how these structures evolve together during synaptic maturation and plasticity changes.

Based on the results we present here, the nano-organization of either GluN2A- or GluN2B-NMDARs is similar throughout the dendritic surface (synaptic and extrasynaptic regions). Therefore, the regulation of the subcellular localization of these two NMDAR subtypes still remains an open question. One could think that if other interacting partners participate in structuring the nanodomains, such as scaffold proteins, then these interacting partners are potentially different in synaptic and extrasynaptic compartments.

Differential changes in the surface expression of GluN2A- or GluN2B-NMDARs have been reported in a number of CNS disorders. What is the significance of nanodomains in these pathological conditions? Investigation of the potential changes in the physical parameters of nanodomains in different diseases could not only lead us closer to understanding their biological function but also provide new insights in potential therapeutic targets.

References

Abbe E (1873) Ueber einen neuen Beleuchtungsapparat am Mikroskop. Arch für Mikroskopische Anat 9:469–480.

Abe M (2004) NMDA Receptor GluR /NR2 Subunits Are Essential for Postsynaptic Localization and Protein Stability of GluR 1/NR1 Subunit. J Neurosci 24:7292–7304.

Akashi K, Kakizaki T, Kamiya H, Fukaya M, Yamasaki M, Abe M, Natsume R, Watanabe M, Sakimura K (2009) NMDA Receptor GluN2B (GluR 2/NR2B) Subunit Is Crucial for Channel Function, Postsynaptic Macromolecular Organization, and Actin Cytoskeleton at Hippocampal CA3 Synapses. J Neurosci 29:10869–10882.

Akazawa C, Shigemoto R, Bessho Y, Nakanishi S, Mizuno N (1994) Differential expression of five N-methyl-D-aspartate receptor subunit mRNAs in the cerebellum of developing and adult rats. J Comp Neurol 347:150–160.

Al-Hallaq RA, Conrads TP, Veenstra TD, Wenthold RJ (2007) NMDA Di-Heteromeric Receptor Populations and Associated Proteins in Rat Hippocampus. J Neurosci 27:8334–8343.

Al-Hallaq RA, Yasuda RP, Wolfe BB (2001) Enrichment of N-methyl-D-aspartate NR1 splice variants and synaptic proteins in rat postsynaptic densities. J Neurochem 77:110–119.

Aoki C, Venkatesan C, Go C-G, Mong JA, Dawson TM (1994) Cellular and Subcellular localization of NMDA-R1 subunit immunoreactivity in the visual cortex of adult and neonatal rats. J Neurosci 14:5202–5222.

Atlason PT, Garside ML, Meddows E, Whiting P, McIlhinney RAJ (2007) N-Methyl-D-aspartate (NMDA) receptor subunit NR1 forms the substrate for oligomeric assembly of the NMDA receptor. J Biol Chem 282:25299–25307.

Banani SF, Lee HO, Hyman AA, Rosen MK (2017) Biomolecular condensates: organizers of cellular biochemistry. Nat Rev Mol Cell Biol 18:285–298.

Banerjee A, Larsen RS, Philpot BD, Paulsen O (2016) Roles of presynaptic NMDA receptors in neurotransmission and plasticity. Trends Neurosci 39:26–39.

Banjade S, Rosen MK (2014) Phase transitions of multivalent proteins can promote clustering of membrane receptors. Elife 3:1–24.

Bar-On D, Wolter S, van de Linde S, Heilemann M, Nudelman G, Nachliel E, Gutman M, Sauer M, Ashery U (2012) Super-resolution Imaging Reveals the Internal Architecture of Nano-sized Syntaxin Clusters. J Biol Chem 287:27158–27167.

Bard L, Groc L (2011) Glutamate receptor dynamics and protein interaction: Lessons from the NMDA receptor. Mol Cell Neurosci 48:298–307.

Bard L, Sainlos M, Bouchet D, Cousins S, Mikasova L, Breillat C, Stephenson FA, Imperiali B, Choquet D, Groc L (2010) Dynamic and specific interaction between synaptic NR2-NMDA receptor and PDZ proteins. Proc Natl Acad Sci U S A 107:19561–19566.

Barria A, Malinow R (2005) NMDA receptor subunit composition controls synaptic plasticity by regulating binding to CaMKII. Neuron 48:289–301.

Bates M, Huang B, Dempsey GT, Zhuang X (2007) Multicolor Super-Resolution Imaging with Photo-Switchable Fluorescent Probes. Science (80-) 317:1749–1753.

Baucum AJ (2017) Proteomic Analysis of Postsynaptic Protein Complexes Underlying Neuronal

Plasticity. ACS Chem Neurosci 8:689–701.

Bayer KU, De Koninck P, Leonard a S, Hell JW, Schulman H (2001) Interaction with the NMDA receptor locks CaMKII in an active conformation. Nature 411:801–805.

Bayer KU, LeBel E, McDonald GL, O'Leary H, Schulman H, De Koninck P (2006) Transition from reversible to persistent binding of CaMKII to postsynaptic sites and NR2B. J Neurosci 26:1164–1174.

Bayés À, Collins MO, Croning MDR, van de Lagemaat LN, Choudhary JS, Grant SGN (2012) Comparative Study of Human and Mouse Postsynaptic Proteomes Finds High Compositional Conservation and Abundance Differences for Key Synaptic Proteins Dunaevsky A, ed. PLoS One 7:e46683.

Bayés À, van de Lagemaat LN, Collins MO, Croning MDR, Whittle IR, Choudhary JS, Grant SGN (2011) Characterization of the proteome, diseases and evolution of the human postsynaptic density. Nat Neurosci 14:19–21.

Béïque J-C, Lin D-T, Kang M-G, Aizawa H, Takamiya K, Huganir RL (2006) Synapse-specific regulation of AMPA receptor function by PSD-95. Proc Natl Acad Sci 103:19535–19540.

Bellone C, Nicoll RA (2007) Rapid Bidirectional Switching of Synaptic NMDA Receptors. Neuron 55:779–785.

Benson DL (1997) Dendritic compartmentation of NMDA receptor mRNA in cultured hippocampal neurons. Neuroreport 8:823–828.

Berretta N, Jones RS (1996) Tonic facilitation of glutamate release by presynaptic N-methyl-D-aspartate autoreceptors in the entorhinal cortex. Neuroscience 75:339–344.

Betzig E, Patterson GH, Sougrat R, Lindwasser OW, Olenych S, Bonifacino JS, Davidson MW, Lippincott-Schwartz J, Hess HF (2006) Imaging Intracellular Fluorescent Proteins at Nanometer Resolution. Science (80-) 313:1642–1645.

Bidoret C, Ayon A, Barbour B, Casado M (2009) Presynaptic NR2A-containing NMDA receptors implement a high-pass filter synaptic plasticity rule. Proc Natl Acad Sci U S A 106:14126–14131.

Bielopolski N, Lam AD, Bar-On D, Sauer M, Stuenkel EL, Ashery U (2014) Differential Interaction of Tomosyn with Syntaxin and SNAP25 Depends on Domains in the WD40 β-Propeller Core and Determines Its Inhibitory Activity. J Biol Chem 289:17087–17099.

Blanpied TA, Scott DB, Ehlers MD (2002) Dynamics and Regulation of Clathrin Coats at Specialized Endocytic Zones of Dendrites and Spines. Neuron 36:435–449.

Bobroff N (1986) Position measurement with a resolution and noise-limited instrument. Rev Sci Instrum 57:1152–1157.

Bosch M, Hayashi Y (2012) Structural plasticity of dendritic spines. Curr Opin Neurobiol 22:383–388.

Bouvier G, Bidoret C, Casado M, Paoletti P (2015) Presynaptic NMDA receptors: Roles and rules. Neuroscience 311:322–340.

Bozic M, Valdivielso JM (2015) The potential of targeting NMDA receptors outside the CNS. Expert Opin Ther Targets 19:399–413.

Brasier DJ, Feldman DE (2008) Synapse-specific expression of functional presynaptic NMDA receptors in rat somatosensory cortex. J Neurosci 28:2199–2211.

Brenman JE, Christopherson KS, Craven SE, McGee AW, Bredt DS (1996) Cloning and characterization of postsynaptic density 93, a nitric oxide synthase interacting protein. J Neurosci 16:7407–7415.

Brickley SG, Misra C, Mok MHS, Mishina M, Cull-Candy SG (2003) NR2B and NR2D Subunits Coassemble in Cerebellar Golgi Cells to Form a Distinct NMDA Receptor Subtype Restricted to Extrasynaptic Sites. J Neurosci 23:4958–4966.

Brigman JL, Wright T, Talani G, Prasad-Mulcare S, Jinde S, Seabold GK, Mathur P, Davis MI, Bock R, Gustin RM, Colbran RJ, Alvarez VA, Nakazawa K, Delpire E, Lovinger DM, Holmes A (2010) Loss of GluN2B-Containing NMDA Receptors in CA1 Hippocampus and Cortex Impairs Long-Term Depression, Reduces Dendritic Spine Density, and Disrupts Learning. J Neurosci 30:4590–4600.

Burnashev N, Zhou Z, Neher E, Sakmann B (1995) Fractional calcium currents through recombinant GluR channels of the NMDA, AMPA and kainate receptor subtypes. J Physiol 485:403–418.

Cao J, Viholainen JI, Dart C, Warwick HK, Leyland ML, Courtney MJ (2005) The PSD95-nNOS interface: a target for inhibition of excitotoxic p38 stress-activated protein kinase activation and cell death. J Cell Biol 168:117–126.

Carlin RK, Grab DJ, Cohen RS, Siekevitz P (1980) Isolation and characterization of postsynaptic densities from various brain regions: Enrichment of different types of postsynaptic densities. J Cell Biol 86:831–843.

Cathala L, Misra C, Cull-Candy S (2000) Developmental profile of the changing properties of NMDA receptors at cerebellar mossy fiber-granule cell synapses. J Neurosci 20:5899–5905

Chater TE, Goda Y (2014) The role of AMPA receptors in postsynaptic mechanisms of synaptic plasticity. Front Cell Neurosci 8:401.

Chavis P, Westbrook G (2001) Integrins mediate functional pre- and postsynaptic maturation at a hippocampal synapse. Nature 411:317–321.

Chazot PL, Stephenson FA (1997a) Biochemical evidence for the existence of a pool of unassembled C2 exon-containing NR1 subunits of the mammalian forebrain NMDA receptor. J Neurochem 68:507–516.

Chazot PL, Stephenson FA (1997b) Molecular dissection of native mammalian forebrain NMDA receptors containing the NR1 C2 exon: direct demonstration of NMDA receptors comprising NR1, NR2A, and NR2B subunits within the same complex. J Neurochem 69:2138–2144.

Chen B-S, Thomas E V, Sanz-Clemente A, Roche KW (2011) NMDA receptor-dependent regulation of dendritic spine morphology by SAP102 splice variants. J Neurosci 31:89–96.

Chen BS, Gray JA, Sanz-Clemente A, Wei Z, Thomas E V., Nicoll R a., Roche KW (2012) SAP102 Mediates Synaptic Clearance of NMDA Receptors. Cell Rep 2:1120–1128.

Chen HJ, Rojas-Soto M, Oguni A, Kennedy MB (1998) A synaptic Ras-GTPase activating protein (p135 SynGAP) inhibited by CaM kinase II. Neuron 20:895–904.

Chen L, Cooper NGF, Mower GD (2000) Developmental changes in the expression of NMDA receptor subunits (NR1, NR2A, NR2B) in the cat visual cortex and the effects of dark rearing. Mol Brain Res 78:196–200.

Chen N, Luo T, Raymond LA (1999) Subtype-dependence of NMDA receptor channel open probability. J Neurosci 19:6844–6854.

Chen S, Diamond JS (2002) Synaptically released glutamate activates extrasynaptic NMDA receptors on cells in the ganglion cell layer of rat retina. J Neurosci 22:2165–2173.

Chen X, Vinade L, Leapman RD, Petersen JD, Nakagawa T, Phillips TM, Sheng M, Reese TS (2005) Mass of the postsynaptic density and enumeration of three key molecules. Proc Natl Acad Sci U S A 102:11551–11556.

Chen X, Winters C, Azzam R, Li X, Galbraith JA, Leapman RD, Reese TS (2008) Organization of the core structure of the postsynaptic density. Proc Natl Acad Sci U S A 105:4453–4458.

Cheng D, Hoogenraad CC, Rush J, Ramm E, Schlager MA, Duong DM, Xu P, Wijayawardana SR, Hanfelt J, Nakagawa T, Sheng M, Peng J (2006) Relative and Absolute Quantification of Postsynaptic Density Proteome Isolated from Rat Forebrain and Cerebellum. Mol Cell Proteomics 5:1158–1170.

Chéreau R, Tønnesen J, Nägerl UV (2015) STED microscopy for nanoscale imaging in living brain slices. Methods 88:57–66.

Cheriyan J, Balsara RD, Hansen KB, Castellino FJ (2016) Pharmacology of triheteromeric N -Methyl-d -Aspartate Receptors. Neurosci Lett 617:240–246.

Choquet D, Triller A (2013) The dynamic synapse. Neuron 80:691–703.

Christopherson KS (2003) Lipid- and protein-mediated multimerization of PSD-95: implications for receptor clustering and assembly of synaptic protein networks. J Cell Sci 116:3213–3219.

Chung HJ, Huang YH, Lau L-F, Huganir RL (2004) Regulation of the NMDA Receptor Complex and Trafficking by Activity-Dependent Phosphorylation of the NR2B Subunit PDZ Ligand. J Neurosci 24:10248–10259.

Ciabarra A, Sullivan J, Gahn L, Pecht G, Heinemann S, Sevarino K (1995) Cloning and characterization of chi-1: a developmentally regulated member of a novel class of the ionotropic glutamate receptor family. J Neurosci 15: 6498-6508.

Colledge M, Snyder EM, Crozier RA, Soderling JA, Jin Y, Langeberg LK, Lu H, Bear MF, Scott JD (2003) Ubiquitination regulates PSD-95 degradation and AMPA receptor surface expression. Neuron 40:595–607.

Collingridge GL, Peineau S, Howland JG, Wang YT (2010) Long-term depression in the CNS. Nat Rev Neurosci 11:459–473.

Collins MO, Husi H, Yu L, Brandon JM, Anderson CNG, Blackstock WP, Choudhary JS, Grant SGN (2006) Molecular characterization and comparison of the components and multiprotein complexes in the postsynaptic proteome. J Neurochem 97:16–23.

Collins MO, Yu L, Coba MP, Husi H, Campuzano I, Blackstock WP, Choudhary JS, Grant SGN (2005) Proteomic Analysis of in Vivo Phosphorylated Synaptic Proteins. J Biol Chem 280:5972–5982.

Corbel C, Hernandez I, Wu B, Kosik KS (2015) Developmental attenuation of N-methyl-D-aspartate receptor subunit expression by microRNAs. Neural Dev 10:20.

Cotman CW, Banker G, Churchill L, Taylor D (1974) Isolation of postsynaptic densities from rat brain. J Cell Biol 63:441-455.

Cousins SL, Kenny AV, Stephenson FA (2009) Delineation of additional PSD-95 binding domains within NMDA receptor NR2 subunits reveals differences between NR2A/PSD-95 and NR2B/PSD-95 association. Neuroscience 158:89–95.

Cousins SL, Papadakis M, Rutter AR, Stephenson FA (2008) Differential interaction of NMDA receptor subtypes with the post-synaptic density-95 family of membrane associated guanylate kinase proteins. J Neurochem 104:903–913.

Cousins SL, Stephenson FA (2012) Identification of N- Methyl-d-aspartic Acid (NMDA) Receptor Subtype-specific Binding Sites That Mediate Direct Interactions with Scaffold Protein PSD-95. J Biol Chem 287:13465–13476.

Cull-Candy SG, Leszkiewicz DN (2004) Role of Distinct NMDA Receptor Subtypes at Central Synapses. Sci Signal 2004:re16-re16.

Dalmau J, Gleichman AJ, Hughes EG, Rossi JE, Peng X, Lai M, Dessain SK, Rosenfeld MR, Balice-Gordon R, Lynch DR (2008) Anti-NMDA-receptor encephalitis: case series and analysis of the effects of antibodies. Lancet Neurol 7:1091–1098.

Dalva MB, Takasu MA, Lin MZ, Shamah SM, Hu L, Gale NW, Greenberg ME (2000) EphB Receptors Interact with NMDA Receptors and Regulate Excitatory Synapse Formation. Cell 103:945–956.

Dani A, Huang B, Bergan J, Dulac C, Zhuang X (2010) Superresolution Imaging of Chemical Synapses in the Brain. Neuron 68:843–856.

Dempsey GT, Vaughan JC, Chen KH, Bates M, Zhuang X (2011) Evaluation of fluorophores for optimal performance in localization-based super-resolution imaging. Nat Methods 8:1027–1036.

Dingledine R, Borges K, Bowie D, Traynelis SF (1999) The glutamate receptor ion channels. Pharmacol Rev 51:7–61.

Dosemeci A, Tao-Cheng J-H, Vinade L, Jaffe H (2006) Preparation of postsynaptic density fraction from hippocampal slices and proteomic analysis. Biochem Biophys Res Commun 339:687–694.

Duguid IC, Smart TG (2004) Retrograde activation of presynaptic NMDA receptors enhances GABA release at cerebellar interneuron–Purkinje cell synapses. Nat Neurosci 7:525–533.

Dumas TC (2005) Developmental regulation of cognitive abilities: Modified composition of a molecular switch turns on associative learning. Prog Neurobiol 76:189–211.

Dunah AW, Luo J, Wang Y-H, Yasuda RP, Wolfe BB (1998) Subunit Composition ofN-Methyl-d-aspartate Receptors in the Central Nervous System that Contain the NR2D Subunit. Mol Pharmacol 53:429–437.

Dunah AW, Standaert DG (2001) Dopamine D1 receptor-dependent trafficking of striatal NMDA glutamate receptors to the postsynaptic membrane. J Neurosci 21:5546–5558.

Dupuis JP, Ladepeche L, Seth H, Bard L, Varela J, Mikasova L, Bouchet D, Rogemond V, Honnorat J, Hanse E, Groc L (2014) Surface dynamics of GluN2B-NMDA receptors controls plasticity of maturing glutamate synapses. EMBO J 33:842–861.

Ehmann N, van de Linde S, Alon A, Ljaschenko D, Keung XZ, Holm T, Rings A, DiAntonio A, Hallermann S, Ashery U, Heckmann M, Sauer M, Kittel RJ (2014) Quantitative super-resolution imaging of Bruchpilot distinguishes active zone states. Nat Commun 5:4650.

El-Husseini AE-D, Schnell E, Dakoji S, Sweeney N, Zhou Q, Prange O, Gauthier-Campbell C, Aguilera-Moreno A, Nicoll RA, Bredt DS (2002) Synaptic strength regulated by palmitate cycling on PSD-95. Cell 108:849–863.

El-Husseini AE, Craven SE, Chetkovich DM, Firestein BL, Schnell E, Aoki C, Bredt DS (2000a) Dual Palmitoylation of PSD-95 Mediates Its Vesiculotubular Sorting, Postsynaptic Targeting, and Ion

Channel Clustering. J Cell Biol 148:159–172.

El-Husseini AE, Schnell E, Chetkovich DM, Nicoll RA, Bredt DS (2000b) PSD-95 involvement in maturation of excitatory synapses. Science (80-) 290:1364–1368.

El-Husseini AE, Topinka JR, Lehrer-Graiwer JE, Firestein BL, Craven SE, Aoki C, Bred DS (2000c) Ion channel clustering by membrane-associated guanylate kinases: Differential regulation by N-terminal lipid and metal binding motifs. J Biol Chem. 275:23904-23910

Elias GM, Elias LAB, Apostolides PF, Kriegstein AR, Nicoll RA (2008) Differential trafficking of AMPA and NMDA receptors by SAP102 and PSD-95 underlies synapse development. Proc Natl Acad Sci 105:20953–20958.

Elias GM, Funke L, Stein V, Grant SG, Bredt DS, Nicoll RA (2006) Synapse-Specific and Developmentally Regulated Targeting of AMPA Receptors by a Family of MAGUK Scaffolding Proteins. Neuron 52:307–320.

Elias GM, Nicoll RA (2007) Synaptic trafficking of glutamate receptors by MAGUK scaffolding proteins. Trends Cell Biol 17:343–352.

Espinosa JS, Wheeler DG, Tsien RW, Luo L (2009) Uncoupling Dendrite Growth and Patterning: Single-Cell Knockout Analysis of NMDA Receptor 2B. Neuron 62:205–217.

Ester M, Kriegel H, Sander J, Xu X (1996) A density-based algorithm for discovering clusters in large spacial databases with noise. Proc Second Int Conf Knowl Discov Data Min 96:226–231.

Farrant M, Feldmeyer D, Takahashi T, Cull-Candy SG (1994) NMDA-receptor channel diversity in the developing cerebellum. Nature 368:335–339.

Fernández-Suárez M, Ting AY (2008) Fluorescent probes for super-resolution imaging in living cells. Nat Rev Mol Cell Biol 9:929–943.

Ferreira JS, Papouin T, Ladépêche L, Yao A, Langlais VC, Bouchet D, Dulong J, Mothet J-P, Sacchi S, Pollegioni L, Paoletti P, Oliet SHR, Groc L (2017) Co-agonists differentially tune GluN2B-NMDA receptor trafficking at hippocampal synapses. Elife 6:1-22.

Ferreira JS, Rooyakkers A, She K, Ribeiro L, Carvalho AL, Craig AM (2011) Activity and protein kinase C regulate synaptic accumulation of N-methyl-D-aspartate (NMDA) receptors independently of GluN1 splice variant. J Biol Chem 286:28331–28342.

Ferreira JS, Schmidt J, Rio P, Aguas R, Rooyakkers A, Li KW, Smit AB, Craig AM, Carvalho AL (2015) GluN2B-Containing NMDA Receptors Regulate AMPA Receptor Traffic through Anchoring of the Synaptic Proteasome. J Neurosci 35:8462–8479.

Fink CC, Meyer T (2002) Molecular mechanisms of CaMKII activation in neuronal plasticity. Curr Opin Neurobiol 12:293–299.

Flint AC, Maisch US, Weishaupt JH, Kriegstein AR, Monyer H (1997) NR2A subunit expression shortens NMDA receptor synaptic currents in developing neocortex. J Neurosci 17:2469–2476.

Fölling J, Bossi M, Bock H, Medda R, Wurm CA, Hein B, Jakobs S, Eggeling C, Hell SW (2008) Fluorescence nanoscopy by ground-state depletion and single-molecule return. Nat Methods 5:943–945.

Frank RA, Grant SG (2017) Supramolecular organization of NMDA receptors and the postsynaptic density. Curr Opin Neurobiol 45:139–147.

Frank RAW, Komiyama NH, Ryan TJ, Zhu F, O'Dell TJ, Grant SGN (2016) NMDA receptors are

selectively partitioned into complexes and supercomplexes during synapse maturation. Nat Commun 7:11264.

Fukata Y, Dimitrov A, Boncompain G, Vielemeyer O, Perez F, Fukata M (2013) Local palmitoylation cycles define activity-regulated postsynaptic subdomains. J Cell Biol 202:145–161.

Furukawa H, Gouaux E (2003) Mechanisms of activation, inhibition and specificity: Crystal structures of the NMDA receptor NR1 ligand-binding core. EMBO J 22:2873–2885.

Furukawa H, Singh SK, Mancusso R, Gouaux E (2005) Subunit arrangement and function in NMDA receptors. Nature 438:185–192.

Fux CM, Krug M, Dityatev A, Schuster T, Schachner M (2003) NCAM180 and glutamate receptor subtypes in potentiated spine synapses: an immunogold electron microscopic study. Mol Cell Neurosci 24:939–950.

Gaertner TR, Kolodziej SJ, Wang D, Kobayashi R, Koomen JM, Stoops JK, Waxham MN (2004) Comparative Analyses of the Three-dimensional Structures and Enzymatic Properties of α, β, γ, and δ Isoforms of Ca 2+ -Calmodulin-dependent Protein Kinase II. J Biol Chem 279:12484–12494.

Gambrill AC, Barria A (2011) NMDA receptor subunit composition controls synaptogenesis and synapse stabilization. Proc Natl Acad Sci U S A 108:5855–5860.

Garcia-Parajo MF, Cambi A, Torreno-Pina JA, Thompson N, Jacobson K (2014) Nanoclustering as a dominant feature of plasma membrane organization. J Cell Sci 127:4995–5005.

Gardoni F, Bellone C, Cattabeni F, Di Luca M (2001a) Protein kinase C activation modulates alpha-calmodulin kinase II binding to NR2A subunit of N-methyl-D-aspartate receptor complex. J Biol Chem 276:7609–7613.

Gardoni F, Caputi A, Cimino M, Pastorino L, Cattabeni F, Di Luca M (1998) Calcium/calmodulin-dependent protein kinase II is associated with NR2A/B subunits of NMDA receptor in postsynaptic densities. J Neurochem 71:1733–1741.

Gardoni F, Marcello E, Di Luca M (2009) Postsynaptic density-membrane associated guanylate kinase proteins (PSD-MAGUKs) and their role in CNS disorders. Neuroscience 158:324–333.

Gardoni F, Mauceri D, Fiorentini C, Bellone C, Missale C, Cattabeni F, Luca M Di (2003) CaMKII-dependent Phosphorylation Regulates SAP97/NR2A Interaction. J Biol Chem 278:44745–44752.

Gardoni F, Picconi B, Ghiglieri V, Polli F, Bagetta V, Bernardi G, Cattabeni F, Di Luca M, Calabresi P (2006a) A Critical Interaction between NR2B and MAGUK in L-DOPA Induced Dyskinesia. J Neurosci 26:2914–2922.

Gardoni F, Polli F, Cattabeni F, Di Luca M (2006b) Calcium-calmodulin-dependent protein kinase II phosphorylation modulates PSD-95 binding to NMDA receptors. Eur J Neurosci 24:2694–2704.

Gardoni F, Schrama LH, Kamal A, Gispen WH, Cattabeni F, Di Luca M (2001b) Hippocampal synaptic plasticity involves competition between Ca2+/calmodulin-dependent protein kinase II and postsynaptic density 95 for binding to the NR2A subunit of the NMDA receptor. J Neurosci 21:1501–1509.

Gardoni F, Schrama LH, Van Dalen JJW, Gispen WH, Cattabeni F, Di Luca M (1999) αCaMKII binding to the C-terminal tail of NMDA receptor subunit NR2A and its modulation by autophosphorylation. FEBS Lett 456:394–398.

Gardoni F, Sgobio C, Pendolino V, Calabresi P, Di Luca M, Picconi B (2012) Targeting NR2A-

containing NMDA receptors reduces L-DOPA-induced dyskinesias. Neurobiol Aging 33:2138–2144.

Genever PG, Skerry TM (2000) Non-neuronal glutamate signalling pathways. Emerg Ther Targets 4:333–345.

Georgiev D, Taniura H, Kambe Y, Takarada T, Yoneda Y (2008) A critical importance of polyamine site in NMDA receptors for neurite outgrowth and fasciculation at early stages of P19 neuronal differentiation. Exp Cell Res 314:2603–2617.

Gereau RW, Swanson GT (2008) The Glutamate Receptors (Gereau RW, Swanson GT, eds). Humana Press.

Grant ER, Bacskai BJ, Anegawa NJ, Pleasure DE, Lynch DR (1998) Opposing contributions of NR1 and NR2 to protein kinase C modulation of NMDA receptors. J Neurochem 71:1471–1481.

Gray EG (1959a) Axo-somatic and axo-dendritic synapses of the cerebral cortex: an electron microscope study. J Anat 93:420–433.

Gray EG (1959b) Electron Microscopy of Synaptic Contacts on Dendrite Spines of the Cerebral Cortex. Nature 183:1592–1593.

Gray JA, Shi Y, Usui H, During MJ, Sakimura K, Nicoll RA (2011) Distinct Modes of AMPA Receptor Suppression at Developing Synapses by GluN2A and GluN2B: Single-Cell NMDA Receptor Subunit Deletion In Vivo. Neuron 71:1085–1101.

Groc L, Bard L, Choquet D (2009) Surface trafficking of N-methyl-D-aspartate receptors: physiological and pathological perspectives. Neuroscience 158:4–18.

Groc L, Choquet D, Stephenson FA, Verrier D, Manzoni OJ, Chavis P (2007) NMDA Receptor Surface Trafficking and Synaptic Subunit Composition Are Developmentally Regulated by the Extracellular Matrix Protein Reelin. J Neurosci 27:10165–10175.

Groc L, Heine M, Cognet L, Brickley K, Stephenson FA, Lounis B, Choquet D (2004) Differential activity-dependent regulation of the lateral mobilities of AMPA and NMDA receptors. Nat Neurosci 7:695–696.

Groc L, Heine M, Cousins SL, Stephenson FA, Lounis B, Cognet L, Choquet D (2006) NMDA receptor surface mobility depends on NR2A-2B subunits. Proc Natl Acad Sci 103:18769–18774.

Grosshans DR, Browning MD (2001) Protein kinase C activation induces tyrosine phosphorylation of the NR2A and NR2B subunits of the NMDA receptor. J Neurochem 76:737–744.

Guillaud L, Setou M, Hirokawa N (2003) KIF17 dynamics and regulation of NR2B trafficking in hippocampal neurons. J Neurosci 23:131–140.

Gustafsson MGL (2005) Nonlinear structured-illumination microscopy: Wide-field fluorescence imaging with theoretically unlimited resolution. Proc Natl Acad Sci 102:13081–13086.

Hall BJ, Ripley B, Ghosh A (2007) NR2B Signaling Regulates the Development of Synaptic AMPA Receptor Current. J Neurosci 27:13446–13456.

Hansen KB, Furukawa H, Traynelis SF (2010) Control of assembly and function of glutamate receptors by the amino-terminal domain. Mol Pharmacol 78:535–549.

Hansen KB, Ogden KK, Yuan H, Traynelis SF (2014) Distinct Functional and Pharmacological Properties of Triheteromeric GluN1/GluN2A/GluN2B NMDA Receptors. Neuron 81:1084–1096.

Hardingham GE, Bading H (2010) Synaptic versus extrasynaptic NMDA receptor signalling: implications for neurodegenerative disorders. Nat Rev Neurosci 11:682–696.

Harney SC, Jane DE, Anwyl R (2008) Extrasynaptic NR2D-Containing NMDARs Are Recruited to the Synapse during LTP of NMDAR-EPSCs. J Neurosci 28:11685–11694.

Harris AZ, Pettit DL (2007) Extrasynaptic and synaptic NMDA receptors form stable and uniform pools in rat hippocampal slices. J Physiol 584:509–519.

Harris KM, Weinberg RJ, Verrall AW (2012) Ultrastructure of synapses in the mammalian brain. Cold Spring Harb Perspect Biol 4:a005587-a005587.

Hatton CJ, Paoletti P (2005) Modulation of triheteromeric NMDA receptors by N-terminal domain ligands. Neuron 46:261–274.

Hayashi T, Thomas GM, Huganir RL (2009) Dual Palmitoylation of NR2 Subunits Regulates NMDA Receptor Trafficking. Neuron 64:213–226.

Heilemann M, van de Linde S, Schüttpelz M, Kasper R, Seefeldt B, Mukherjee A, Tinnefeld P, Sauer M (2008) Subdiffraction-Resolution Fluorescence Imaging with Conventional Fluorescent Probes. Angew Chemie Int Ed 47:6172–6176.

Hell JW (2014) CaMKII: Claiming Center Stage in Postsynaptic Function and Organization. Neuron 81:249–265.

Hell SW, Wichmann J (1994) Breaking the diffraction resolution limit by stimulated emission: stimulated-emission-depletion fluorescence microscopy. Opt Lett 19:780–782.

Heng MY, Detloff PJ, Wang PL, Tsien JZ, Albin RL (2009) In Vivo Evidence for NMDA Receptor-Mediated Excitotoxicity in a Murine Genetic Model of Huntington Disease. J Neurosci 29:3200–3205.

Henley JM, Wilkinson KA (2016) Synaptic AMPA receptor composition in development, plasticity and disease. Nat Rev Neurosci advance on:337–350.

Henson MA, Roberts AC, Pérez-Otaño I, Philpot BD (2010) Influence of the NR3A subunit on NMDA receptor functions. Prog Neurobiol 91:23–37.

Hering H, Sheng M (2001) Dendritic spines: structure, dynamics and regulation. Nat Rev Neurosci 2:880–888.

Hess ST, Girirajan TPK, Mason MD (2006) Ultra-High Resolution Imaging by Fluorescence Photoactivation Localization Microscopy. Biophys J 91:4258–4272.

Higgs MH, Lukasiewicz PD (1999) Glutamate uptake limits synaptic excitation of retinal ganglion cells. J Neurosci 19:3691–3700.

Hirao K, Hata Y, Ide N, Takeuchi M, Irie M, Yao I, Deguchi M, Toyoda A, Sudhof TC, Takai Y (1998) A novel multiple PDZ domain-containing molecule interacting with N-methyl-D-aspartate receptors and neuronal cell adhesion proteins. J Biol Chem 273:21105–21110.

Hlushchenko I, Koskinen M, Hotulainen P (2016) Dendritic spine actin dynamics in neuronal maturation and synaptic plasticity. Cytoskeleton 73:435–441.

Hogan-Cann AD, Anderson CM (2016) Physiological Roles of Non-Neuronal NMDA Receptors. Trends Pharmacol Sci 37:750–767.

Hollmann M, Heinemann S (1994) Cloned Glutamate Receptors. Annu Rev Neurosci 17:31–108.

Hoover BR, Reed MN, Su J, Penrod RD, Kotilinek LA, Grant MK, Pitstick R, Carlson GA, Lanier LM, Yuan L-L, Ashe KH, Liao D (2010) Tau Mislocalization to Dendritic Spines Mediates Synaptic Dysfunction Independently of Neurodegeneration. Neuron 68:1067–1081.

Horak M, Petralia RS, Kaniakova M, Sans N (2014) ER to synapse trafficking of NMDA receptors. Front Cell Neurosci 8:1–18.

Howard MA, Elias GM, Elias LAB, Swat W, Nicoll RA (2010) The role of SAP97 in synaptic glutamate receptor dynamics. Proc Natl Acad Sci 107:3805–3810.

Hu J-L, Liu G, Li Y-C, Gao W-J, Huang Y-Q (2010) Dopamine D1 receptor-mediated NMDA receptor insertion depends on Fyn but not Src kinase pathway in prefrontal cortical neurons. Mol Brain 3.

Hughes EG, Peng X, Gleichman AJ, Lai M, Zhou L, Tsou R, Parsons TD, Lynch DR, Dalmau J, Balice-Gordon RJ (2010) Cellular and synaptic mechanisms of anti-NMDA receptor encephalitis. J Neurosci 30:5866–5875.

Huh KH, Wenthold RJ (1999) Turnover analysis of glutamate receptors identifies a rapidly degraded pool of the N-methyl-D-aspartate receptor subunit, NR1, in cultured cerebellar granule cells. J Biol Chem 274:151–157.

Hyman AA, Weber CA, Ulicher F (2014) Liquid-Liquid Phase Separation in Biology. Annu Rev Cell Dev Biol 30:39–58.

Irie M, Hata Y, Takeuchi M, Ichtchenko K, Toyoda A, Hirao K, Takai Y, Rosahl TW, Südhof TC (1997) Binding of neuroligins to PSD-95. Science 277:1511–1515.

Ishii T, Moriyoshi K, Sugihara H, Sakurada K, Kadotani H, Yokoi M, Akazawa C, Shigemoto R, Mizuno N, Masu M (1993) Molecular characterization of the family of the N-methyl-D-aspartate receptor subunits. J Biol Chem 268:2836–2843.

Ivanov A, Pellegrino C, Rama S, Dumalska I, Salyha Y, Ben-Ari Y, Medina I (2006) Opposing role of synaptic and extrasynaptic NMDA receptors in regulation of the extracellular signal-regulated kinases (ERK) activity in cultured rat hippocampal neurons. J Physiol 572:789–798.

Iwamoto T, Yamada Y, Hori K, Watanabe Y, Sobue K, Inui M (2004) Differential modulation of NR1-NR2A and NR1-NR2B subtypes of NMDA receptor by PDZ domain-containing proteins. J Neurochem 89:100–108.

Jeyifous O, Lin EI, Chen X, Antinone SE, Mastro R, Drisdel R, Reese TS, Green WN (2016) Palmitoylation regulates glutamate receptor distributions in postsynaptic densities through control of PSD95 conformation and orientation. Proc Natl Acad Sci 113:E8482–E8491.

Jiang M, Chen G (2006) High Ca2+-phosphate transfection efficiency in low-density neuronal cultures. Nat Protoc 1:695–700.

Johnson JW, Ascher P (1987) Glycine potentiates the NMDA response in cultured mouse brain neurons. Nature 325:529–531.

Jourdain P, Bergersen LH, Bhaukaurally K, Bezzi P, Santello M, Domercq M, Matute C, Tonello F, Gundersen V, Volterra A (2007) Glutamate exocytosis from astrocytes controls synaptic strength. Nat Neurosci 10:331–339.

Jung S-Y, Kim J-H, Kwon O Bin, Jung JH, An K, Jeong AY, Lee CJ, Choi Y-B, Bailey CH, Kandel ER, Kim J-H (2010) Input-specific synaptic plasticity in the amygdala is regulated by neuroligin-1 via postsynaptic NMDA receptors. Proc Natl Acad Sci 107:4710–4715.

Jurd R, Thornton C, Wang J, Luong K, Phamluong K, Kharazia V, Gibb SL, Ron D (2008) Mind bomb-2 is an E3 ligase that ubiquitinates the N-methyl-D-aspartate receptor NR2B subunit in a phosphorylation-dependent manner. J Biol Chem 283:301–310.

Kaech S, Banker G (2006) Culturing hippocampal neurons. Nat Protoc 1:2406–2415.

Kalia L V, Pitcher GM, Pelkey KA, Salter MW (2006) PSD-95 is a negative regulator of the tyrosine kinase Src in the NMDA receptor complex. EMBO J 25:4971–4982.

Karakas E, Simorowski N, Furukawa H (2009) Structure of the zinc-bound amino-terminal domain of the NMDA receptor NR2B subunit. EMBO J 28:3910–3920.

Karakas E, Simorowski N, Furukawa H (2011) Subunit arrangement and phenylethanolamine binding in GluN1/GluN2B NMDA receptors. Nature 475:249–253.

Kato A, Rouach N, Nicoll RA, Bredt DS (2005) Activity-dependent NMDA receptor degradation mediated by retrotranslocation and ubiquitination. Proc Natl Acad Sci 102:5600–5605.

Keifer J, Zheng Z (2010) AMPA receptor trafficking and learning. Eur J Neurosci 32:269–277.

Kennedy MB (2013) Synaptic Signaling in Learning and Memory. Cold Spring Harb Perspect Biol 8:a016824.

Kennedy MB, Bennett MK, Erondu NE (1983) Biochemical and immunochemical evidence that the "major postsynaptic density protein" is a subunit of a calmodulin-dependent protein kinase. Proc Natl Acad Sci U S A 80:7357–7361.

Kew JN, Richards JG, Mutel V, Kemp JA (1998) Developmental changes in NMDA receptor glycine affinity and ifenprodil sensitivity reveal three distinct populations of NMDA receptors in individual rat cortical neurons. J Neurosci 18:1935–1943.

Kim E, Cho KO, Rothschild A, Sheng M (1996) Heteromultimerization and NMDA receptor-clustering activity of Chapsyn-110, a member of the PSD-95 family of proteins. Neuron 17:103–113.

Kim E, Naisbitt S, Hsueh YP, Rao A, Rothschild A, Craig AM, Sheng M (1997) GKAP, a novel synaptic protein that interacts with the guanylate kinase-like domain of the PSD-95/SAP90 family of channel clustering molecules. J Cell Biol 136:669–678.

Kim E, Sheng M (2004) PDZ domain proteins of synapses. Nat Rev Neurosci 5:771–781.

Kim JH, Liao D, Lau LF, Huganir RL (1998) SynGAP: a synaptic RasGAP that associates with the PSD-95/SAP90 protein family. Neuron 20:683–691.

Kim MJ, Dunah AW, Wang YT, Sheng M (2005) Differential Roles of NR2A- and NR2B-Containing NMDA Receptors in Ras-ERK Signaling and AMPA Receptor Trafficking. Neuron 46:745–760.

Kim MJ, Futai K, Jo J, Hayashi Y, Cho K, Sheng M (2007) Synaptic Accumulation of PSD-95 and Synaptic Function Regulated by Phosphorylation of Serine-295 of PSD-95. Neuron 56:488–502.

Kiraly DD, Lemtiri-Chlieh F, Levine ES, Mains RE, Eipper BA (2011) Kalirin binds the NR2B subunit of the NMDA receptor, altering its synaptic localization and function. J Neurosci 31:12554–12565.

Klar TA, Jakobs S, Dyba M, Egner A, Hell SW (2000) Fluorescence microscopy with diffraction resolution barrier broken by stimulated emission. Proc Natl Acad Sci U S A 97:8206–8210.

Kleckner N, Dingledine R (1988) Requirement for glycine in activation of NMDA-receptors expressed in Xenopus oocytes. Science (80-) 241:835–837.

Klemann CJHM, Roubos EW (2011) The gray area between synapse structure and function-Gray's synapse types I and II revisited. Synapse 65:1222–1230.

Kneussel M (2005) Postsynaptic scaffold proteins at non-synaptic sites. EMBO Rep 6:22–27.

Knox R, Zhao C, Miguel-Perez D, Wang S, Yuan J, Ferriero D, Jiang X (2013) Enhanced NMDA receptor tyrosine phosphorylation and increased brain injury following neonatal hypoxia–ischemia in mice with neuronal Fyn overexpression. Neurobiol Dis 51:113–119.

Ko J, Kim S, Chung HS, Kim K, Han K, Kim H, Jun H, Kaang B-K, Kim E (2006) SALM Synaptic Cell Adhesion-like Molecules Regulate the Differentiation of Excitatory Synapses. Neuron 50:233–245.

Kolodziej SJ, Hudmon A, Waxham MN, Stoops JK (2000) Three-dimensional reconstructions of calcium/calmodulin-dependent (CaM) kinase IIalpha and truncated CaM kinase IIalpha reveal a unique organization for its structural core and functional domains. J Biol Chem 275:14354–14359.

Kornau HC, Schenker LT, Kennedy MB, Seeburg PH (1995) Domain interaction between NMDA receptor subunits and the postsynaptic density protein PSD-95. Science 269:1737–1740.

Krapivinsky G, Krapivinsky L, Manasian Y, Ivanov A, Tyzio R, Pellegrino C, Ben-Ari Y, Clapham DE, Medina I (2003) The NMDA Receptor Is Coupled to the ERK Pathway by a Direct Interaction between NR2B and RasGRF1 NR1 subunits of the NMDAR, interacts in vivo and in vitro with RasGRF1. Neuron 40:775–784.

Kuner T, Schoepfer R (1996) Multiple structural elements determine subunit specificity of Mg2+ block in NMDA receptor channels. J Neurosci 16:3549–3558.

Kutsuwada T, Sakimura K, Manabe T, Takayama C, Katakura N, Kushiya E, Natsume R, Watanabe M, Inoue Y, Yagi T, Aizawa S, Arakawa M, Takahashi T, Nakamura Y, Mori H, Mishina M (1996) Impairment of suckling response, trigeminal neuronal pattern formation, and hippocampal LTD in NMDA receptor epsilon 2 subunit mutant mice. Neuron 16:333–344.

Ladepeche L, Dupuis JP, Bouchet D, Doudnikoff E, Yang L, Campagne Y, Bézard E, Hosy E, Groc L (2013) Single-molecule imaging of the functional crosstalk between surface NMDA and dopamine D1 receptors. Proc Natl Acad Sci U S A 110:18005–18010.

Lan J, Skeberdis VA, Jover T, Grooms SY, Lin Y, Araneda RC, Zheng X, Bennett MVL, Zukin RS (2001) Protein kinase C modulates NMDA receptor trafficking and gating. Nat Neurosci 4:382–390.

Lau CG, Zukin RS (2007) NMDA receptor trafficking in synaptic plasticity and neuropsychiatric disorders. Nat Rev Neurosci 8:413–426.

Lau LF, Mammen A, Ehlers MD, Kindler S, Chung WJ, Garner CC, Huganir RL (1996) Interaction of the N-methyl-D-aspartate receptor complex with a novel synapse-associated protein, SAP102. J Biol Chem 271:21622–21628.

Laurie DJ, Seeburg PH (1994) Regional and developmental heterogeneity in splicing of the rat brain NMDAR1 mRNA. J Neurosci 14:3180–3194.

Lavezzari G, McCallum J, Dewey CM, Roche KW (2004) Subunit-specific regulation of NMDA receptor endocytosis. J Neurosci 24:6383–6391.

Law AJ, Deakin JF (2001) Asymmetrical reductions of hippocampal NMDAR1 glutamate receptor mRNA in the psychoses. Neuroreport 12:2971–2974.

Le Meur K, Galante M, Angulo MC, Audinat E (2007) Tonic activation of NMDA receptors by ambient glutamate of non-synaptic origin in the rat hippocampus. J Physiol 580:373–383.

Lee C-H, Lü W, Michel JC, Goehring A, Du J, Song X, Gouaux E (2014) NMDA receptor structures reveal subunit arrangement and pore architecture. Nature 511:191–197.

Lee FJS, Liu F (2004) Direct interactions between NMDA and D1 receptors: a tale of tails. Biochem Soc Trans 32:1032–1036.

Lee FJS, Xue S, Pei L, Vukusic B, Chéry N, Wang Y, Wang YT, Niznik HB, Yu X, Liu F (2002) Dual regulation of NMDA receptor functions by direct protein-protein interactions with the dopamine D1 receptor. Cell 111:219–230.

Lee M-C, Yasuda R, Ehlers MD (2010) Metaplasticity at Single Glutamatergic Synapses. Neuron 66:859–870.

Leonard AS, Lim IA, Hemsworth DE, Horne MC, Hell JW (1999) Calcium/calmodulin-dependent protein kinase II is associated with the N-methyl-D-aspartate receptor. Proc Natl Acad Sci 96:3239–3244.

Levinson JN, Chéry N, Huang K, Wong TP, Gerrow K, Kang R, Prange O, Wang YT, El-Husseini A (2005) Neuroligins mediate excitatory and inhibitory synapse formation: involvement of PSD-95 and neurexin-1beta in neuroligin-induced synaptic specificity. J Biol Chem 280:17312–17319.

Li B, Otsu Y, Murphy TH, Raymond LA (2003) Developmental decrease in NMDA receptor desensitization associated with shift to synapse and interaction with postsynaptic density-95. J Neurosci 23:11244–11254.

Li BS, Sun MK, Zhang L, Takahashi S, Ma W, Vinade L, Kulkarni AB, Brady RO, Pant HC (2001) Regulation of NMDA receptors by cyclin-dependent kinase-5. Proc Natl Acad Sci U S A 98:12742–12747.

Li P, Banjade S, Cheng H-C, Kim S, Chen B, Guo L, Llaguno M, Hollingsworth J V, King DS, Banani SF, Russo PS, Jiang Q-X, Nixon BT, Rosen MK (2012) Phase transitions in the assembly of multivalent signalling proteins. Nature 483:336–340.

Liao GY, Kreitzer MA, Sweetman BJ, Leonard JP (2000) The postsynaptic density protein PSD-95 differentially regulates insulin- and Src-mediated current modulation of mouse NMDA receptors expressed in Xenopus oocytes. J Neurochem 75:282–287.

Lichnerova K, Kaniakova M, Park SP, Skrenkova K, Wang Y-X, Petralia RS, Suh YH, Horak M (2015) Two N -glycosylation Sites in the GluN1 Subunit Are Essential for Releasing N -methyl-d-aspartate (NMDA) Receptors from the Endoplasmic Reticulum. J Biol Chem 290:18379–18390.

Lin Y-C, Redmond L (2009) Neuronal CaMKII acts as a structural kinase. Commun Integr Biol 2:40–41.

Lin Y, Jover-Mengual T, Wong J, Bennett MVL, Zukin RS (2006) PSD-95 and PKC converge in regulating NMDA receptor trafficking and gating. Proc Natl Acad Sci 103:19902–19907.

Lin Y, Skeberdis V, Francesconi A, Bennett M, Zukin RS (2004) Postsynaptic Density Protein-95 Regulates NMDA Channel Gating and Surface Expression. J Neurosci 24:10138–10148.

Lisman J, Schulman H, Cline H (2002) The molecular basis of CaMKII function in synaptic and behavioural memory. Nat Rev Neurosci 3:175–190.

Liu X-B, Murray K, Jones E (2004) Switching of NMDA Receptor 2A and 2B Subunits at Thalamic

and Cortical Synapses during Early Postnatal Development. J Neurosci 24:8885–8895.

Losi G, Prybylowski K, Fu Z, Luo J, Wenthold R, Vicini S (2003) PSD-95 regulates NMDA receptors in developing cerebellar granule neurons of the rat. J Physiol 548:21–29.

Lu HE, MacGillavry HD, Frost NA, Blanpied TA (2014) Multiple Spatial and Kinetic Subpopulations of CaMKII in Spines and Dendrites as Resolved by Single-Molecule Tracking PALM. J Neurosci 34:7600–7610.

Lü W, Du J, Goehring A, Gouaux E (2017) Cryo-EM structures of the triheteromeric NMDA receptor and its allosteric modulation. Science (80-) 355:eaal3729.

Luo J, Wang Y, Yasuda RP, Dunah AW, Wolfe BB (1997) The majority of N-methyl-D-aspartate receptor complexes in adult rat cerebral cortex contain at least three different subunits (NR1/NR2A/NR2B). Mol Pharmacol 51:79–86.

MacGillavry HD, Hoogenraad CC (2015) The internal architecture of dendritic spines revealed by super-resolution imaging: What did we learn so far? Exp Cell Res 335:180–186.

MacGillavry HD, Song Y, Raghavachari S, Blanpied TA (2013) Nanoscale Scaffolding Domains within the Postsynaptic Density Concentrate Synaptic AMPA Receptors. Neuron 78:615–622.

Maglione M, Sigrist SJ (2013) Seeing the forest tree by tree: super-resolution light microscopy meets the neurosciences. Nat Neurosci 16:790–797.

Malenka RC, Bear MF (2004) Review LTP and LTD: An Embarrassment of Riches useful to conceptualize LTP and LTD as a general class of cellular/synaptic phenomena. Just as different neu- rons express different complements of ion channels to. Neuron 44:5–21.

Malenka RC, Kauer JA, Perkel DJ, Mauk MD, Kelly PT, Nicoll RA, Waxham MN (1989) An essential role for postsynaptic calmodulin and protein kinase activity in long-term potentiation. Nature 340:554–557.

Malkusch S, Heilemann M (2016a) Extracting quantitative information from single-molecule super-resolution imaging data with LAMA – LocAlization Microscopy Analyzer. Sci Rep 6:34486.

Malkusch S, Heilemann M (2016b) Lama: The LocAlization Microscopy Analyzer (Documentation) (publication in the works). :1–42.

Masdeu JC, Dalmau J, Berman KF (2016) NMDA Receptor Internalization by Autoantibodies: A Reversible Mechanism Underlying Psychosis? Trends Neurosci 39:300–310.

Matsuda K, Kamiya Y, Matsuda S, Yuzaki M (2002) Cloning and characterization of a novel NMDA receptor subunit NR3B: a dominant subunit that reduces calcium permeability. Brain Res Mol Brain Res 100:43–52.

Matsui K (2005) High-Concentration Rapid Transients of Glutamate Mediate Neural-Glial Communication via Ectopic Release. J Neurosci 25:7538–7547.

Mattison HA, Hayashi T, Barria A (2012) Palmitoylation at Two Cysteine Clusters on the C-Terminus of GluN2A and GluN2B Differentially Control Synaptic Targeting of NMDA Receptors. PLoS One 7:e49089.

Mauceri D, Gardoni F, Marcello E, Di Luca M (2007) Dual role of CaMKII-dependent SAP97 phosphorylation in mediating trafficking and insertion of NMDA receptor subunit NR2A. J Neurochem 100:1032–1046.

Mayer ML (2006) Glutamate receptors at atomic resolution. Nature 440:456–462.

Mayer ML, Westbrook GL, Guthrie PB (1984) Voltage-dependent block by Mg2+ of NMDA responses in spinal cord neurones. Nature 309:261–263.

McAllister AK (2007) Dynamic Aspects of Synapse Formation. Annu Rev Neurosci 30:425–450.

Meddows E, Le Bourdellès B, Grimwood S, Wafford K, Sandhu S, Whiting P, McIlhinney RAJ (2001) Identification of Molecular Determinants That Are Important in the Assembly of N-Methyl-D-aspartate Receptors. J Biol Chem 276:18795–18803.

Melamed O, Levav-Rabkin T, Zukerman C, Clarke G, Cryan JF, Dinan TG, Grossman Y, Golan HM (2014) Long-lasting glutamatergic modulation induced by neonatal GABA enhancement in mice. Neuropharmacology 79:616–625.

Mikasova L, De Rossi P, Bouchet D, Georges F, Rogemond V, Didelot A, Meissirel C, Honnorat J, Groc L (2012) Disrupted surface cross-talk between NMDA and Ephrin-B2 receptors in anti-NMDA encephalitis. Brain 135:1606–1621.

Milnerwood AJ, Gladding CM, Pouladi MA, Kaufman AM, Hines RM, Boyd JD, Ko RWY, Vasuta OC, Graham RK, Hayden MR, Murphy TH, Raymond LA (2010) Early Increase in Extrasynaptic NMDA Receptor Signaling and Expression Contributes to Phenotype Onset in Huntington's Disease Mice. Neuron 65:178–190.

Minatohara K, Ichikawa S-H, Seki T, Fujiyoshi Y, Doi T (2013) Ligand binding of PDZ domains has various roles in the synaptic clustering of SAP102 and PSD-95. Neurosci Lett 533:44–49.

Monyer H, Burnashev N, Laurie DJ, Sakmann B, Seeburg PH (1994) Developmental and regional expression in the rat brain and functional properties of four NMDA receptors. Neuron 12:529–540.

Monyer H, Sprengel R, Schoepfer R, Herb A, Higuchi M, Lomeli H, Burnashev N, Sakmann B, Seeburg PH (1992) Heteromeric NMDA receptors: molecular and functional distinction of subtypes. Science 256:1217–1221.

Morabito MA, Sheng M, Tsai L-H (2004) Cyclin-Dependent Kinase 5 Phosphorylates the N-Terminal Domain of the Postsynaptic Density Protein PSD-95 in Neurons. J Neurosci 24:865–876.

Moriyoshi K, Masu M, Ishii T, Shigemoto R, Mizuno N, Nakanishi S (1991) Molecular cloning and characterization of the rat NMDA receptor. Nature 354:31–37.

Moroni F, Luzzi S, Franchi-Micheli S, Zilletti L (1986) The presence of N-methyl-D-aspartate-type receptors for glutamic acid in the guinea pig myenteric plexus. Neurosci Lett 68:57–62.

Mortensen KI, Churchman LS, Spudich JA, Flyvbjerg H (2010) Optimized localization analysis for single-molecule tracking and super-resolution microscopy. Nat Methods 7:377-381.

Moss SJ, Smart TG (2001) Constructing the inhibitory synapse. Nat Rev Neurosci 2:240–250.

Mothet JP, Parent AT, Wolosker H, Brady RO, Linden DJ, Ferris CD, Rogawski MA, Snyder SH (2000) D-serine is an endogenous ligand for the glycine site of the N-methyl-D-aspartate receptor. Proc Natl Acad Sci U S A 97:4926–4931.

Müller BM, Kistner U, Kindler S, Chung WJ, Kuhlendahl S, Fenster SD, Lau LF, Veh RW, Huganir RL, Gundelfinger ED, Garner CC (1996) SAP102, a novel postsynaptic protein that interacts with NMDA receptor complexes in vivo. Neuron 17:255–265.

Na CH, Jones DR, Yang Y, Wang X, Xu Y, Peng J (2012) Synaptic protein ubiquitination in rat brain revealed by antibody-based ubiquitome analysis. J Proteome Res 11:4722–4732.

Nada S, Shima T, Yanai H, Husi H, Grant SGN, Okada M, Akiyama T (2003) Identification of PSD-93 as a substrate for the Src family tyrosine kinase Fyn. J Biol Chem 278:47610–47621.

Nagerl U V., Willig KI, Hein B, Hell SW, Bonhoeffer T (2008) Live-cell imaging of dendritic spines by STED microscopy. Proc Natl Acad Sci 105:18982–18987.

Nair D, Hosy E, Petersen JD, Constals A, Giannone G, Choquet D, Sibarita J-B (2013) Super-resolution imaging reveals that AMPA receptors inside synapses are dynamically organized in nanodomains regulated by PSD95. J Neurosci 33:13204–13224.

Nase G, Weishaupt J, Stern P, Singer W, Monyer H (1999) Genetic and epigenetic regulation of NMDA receptor expression in the rat visual cortex. Eur J Neurosci 11:4320–4326.

Newpher TM, Ehlers MD (2008) Glutamate Receptor Dynamics in Dendritic Microdomains. Neuron 58:472–497.

Newpher TM, Ehlers MD (2009) Spine microdomains for postsynaptic signaling and plasticity. Trends Cell Biol 19:218–227.

Ng D, Pitcher GM, Szilard RK, Sertié A, Kanisek M, Clapcote SJ, Lipina T, Kalia L V, Joo D, McKerlie C, Cortez M, Roder JC, Salter MW, McInnes RR (2009) Neto1 is a novel CUB-domain NMDA receptor-interacting protein required for synaptic plasticity and learning. Nestler E, ed. PLoS Biol 7:e41.

Ni M, Zhuo S, So PTC, Yu H (2017) Fluorescent probes for nanoscopy: four categories and multiple possibilities. J Biophotonics 10:11–23.

Niethammer M, Kim E, Sheng M (1996) Interaction between the C Terminus of NMDA Receptor Subunits and Multiple Members of the PSD-95 Family of Membrane-Associated Guanylate Kinases. J Neurosci 76:2157–2163.

Nishikawa T, Morita K, Kinjo K, Tsujimoto A (1982) Stimulation of catecholamine release from isolated adrenal glands by some amino acids. Jpn J Pharmacol 32:291–297.

Niswender CM, Conn PJ (2010) Metabotropic Glutamate Receptors: Physiology, Pharmacology, and Disease. Annu Rev Pharmacol Toxicol 50:295–322.

Nolt MJ, Lin Y, Hruska M, Murphy J, Sheffler-Colins SI, Kayser MS, Passer J, Bennett MVL, Zukin RS, Dalva MB (2011) EphB Controls NMDA Receptor Function and Synaptic Targeting in a Subunit-Specific Manner. J Neurosci 31:5353–5364.

Nong Y, Huang Y-Q, Salter MW (2004) NMDA receptors are movin' in. Curr Opin Neurobiol 14:353–361.

O'Rourke NA, Weiler NC, Micheva KD (2012) Deep molecular diversity of mammalian synapses: why it matters and how to measure it. Nat Rev Neurosci 13:365-379.

Omkumar R V, Kiely MJ, Rosenstein AJ, Min KT, Kennedy MB (1996) Identification of a phosphorylation site for calcium/calmodulindependent protein kinase II in the NR2B subunit of the N-methyl-D-aspartate receptor. J Biol Chem 271:31670–31678.

Palay SL (1956) Synapses in the central nervous system. J Biophys Biochem Cytol 2:193–201.

Palay SL, Palade GE (1955) The fine structure of neurons. J Cell Biol 1:69–88.

Paoletti P (2011) Molecular basis of NMDA receptor functional diversity. Eur J Neurosci 33:1351–1365.

Paoletti P, Bellone C, Zhou Q (2013) NMDA receptor subunit diversity: impact on receptor properties,

synaptic plasticity and disease. Nat Rev Neurosci 14:383–400.

Paoletti P, Neyton J (2007) NMDA receptor subunits: function and pharmacology. Curr Opin Pharmacol 7:39–47.

Papadakis M, Hawkins LM, Stephenson FA (2004) Appropriate NR1-NR1 disulfide-linked homodimer formation is requisite for efficient expression of functional, cell surface N-methyl-D-aspartate NR1/NR2 receptors. J Biol Chem 279:14703–14712.

Papouin T, Ladépêche L, Ruel J, Sacchi S, Labasque M, Hanini M, Groc L, Pollegioni L, Mothet JP, Oliet SHR (2012) Synaptic and extrasynaptic NMDA receptors are gated by different endogenous coagonists. Cell 150:633–646.

Patrizio A, Specht CG (2016) Counting numbers of synaptic proteins: absolute quantification and single molecule imaging techniques. Neurophotonics 3:41805.

Peng J, Kim MJ, Cheng D, Duong DM, Gygi SP, Sheng M (2004) Semiquantitative Proteomic Analysis of Rat Forebrain Postsynaptic Density Fractions by Mass Spectrometry. J Biol Chem 279:21003–21011.

Pennacchietti F, Vascon S, Nieus T, Rosillo C, Das S, Tyagarajan SK, Diaspro A, Del Bue A, Petrini EM, Barberis A, Cella Zanacchi F (2017) Nanoscale Molecular Reorganization of the Inhibitory Postsynaptic Density Is a Determinant of GABAergic Synaptic Potentiation. J Neurosci 37:1747–1756.

Pérez-Otaño I, Ehlers MD (2004) Learning from NMDA receptor trafficking: clues to the development and maturation of glutamatergic synapses. Neurosignals 13:175–189.

Pérez-Otaño I, Larsen RS, Wesseling JF (2016) Emerging roles of GluN3-containing NMDA receptors in the CNS. Nat Rev Neurosci 17:623–635.

Perroy J, Raynaud F, Homburger V, Rousset M-C, Telley L, Bockaert J, Fagni L (2008) Direct interaction enables cross-talk between ionotropic and group I metabotropic glutamate receptors. J Biol Chem 283:6799–6805.

Petralia RS (2012) Distribution of Extrasynaptic NMDA Receptors on Neurons. Sci World J 2012:1–11.

Petralia RS, Sans N, Wang YX, Wenthold RJ (2005) Ontogeny of postsynaptic density proteins at glutamatergic synapses. Mol Cell Neurosci 29:436–452.

Petralia RS, Wang YX, Hua F, Yi Z, Zhou a., Ge L, Stephenson F a., Wenthold RJ (2010) Organization of NMDA receptors at extrasynaptic locations. Neuroscience 167:68–87.

Petralia RS, Wang YX, Wenthold RJ (2003) Internalization at glutamatergic synapses during development. Eur J Neurosci 18:3207–3217.

Philpot BD, Sekhar AK, Shouval HZ, Bear MF (2001) Visual Experience and Deprivation Bidirectionally Modify the Composition and Function of NMDA Receptors in Visual Cortex. Neuron 29:157–169.

Pierce JP, Mayer T, McCarthy JB (2001) Evidence for a satellite secretory pathway in neuronal dendritic spines. Curr Biol 11:351–355.

Prybylowski K, Chang K, Sans N, Kan L, Vicini S, Wenthold RJ (2005) The synaptic localization of NR2B-containing NMDA receptors is controlled by interactions with PDZ proteins and AP-2. Neuron 47:845–857.

Prybylowski K, Wenthold RJ (2004) N-Methyl-D-aspartate Receptors: Subunit Assembly and Trafficking to the Synapse. J Biol Chem 279:9673–9676.

Qiu S, Hua Y-L, Yang F, Chen Y-Z, Luo J-H (2005) Subunit assembly of N-methyl-d-aspartate receptors analyzed by fluorescence resonance energy transfer. J Biol Chem 280:24923–24930.

Quinlan EM, Olstein DH, Bear MF (1999) Bidirectional, experience-dependent regulation of N-methyl-D-aspartate receptor subunit composition in the rat visual cortex during postnatal development. Proc Natl Acad Sci U S A 96:12876–12880.

Ramírez OA, Couve A (2011) The endoplasmic reticulum and protein trafficking in dendrites and axons. Trends Cell Biol 21:219–227.

Rauner C, Köhr G (2011) Triheteromeric NR1/NR2A/NR2B Receptors Constitute the Major N -Methyl-d-aspartate Receptor Population in Adult Hippocampal Synapses. J Biol Chem 286:7558–7566.

Raveendran R, Devi Suma Priya S, Mayadevi M, Steephan M, Santhoshkumar TR, Cheriyan J, Sanalkumar R, Pradeep KK, James J, Omkumar R V. (2009) Phosphorylation status of the NR2B subunit of NMDA receptor regulates its interaction with calcium/calmodulin-dependent protein kinase II. J Neurochem 110:92–105.

Rittweger E, Han KY, Irvine SE, Eggeling C, Hell SW (2009) STED microscopy reveals crystal colour centres with nanometric resolution. Nat Photonics 3:144–147.

Roberts EB, Ramoa AS (1999) Enhanced NR2A subunit expression and decreased NMDA receptor decay time at the onset of ocular dominance plasticity in the ferret. J Neurophysiol 81:2587–2591.

Robison AJ, Bartlett RK, Bass MA, Colbran RJ (2005) Differential Modulation of Ca 2+ /Calmodulin-dependent Protein Kinase II Activity by Regulated Interactions with N -Methyl-D-aspartate Receptor NR2B Subunits and α-Actinin. J Biol Chem 280:39316–39323.

Roche KW, Standley S, McCallum J, Dune Ly C, Ehlers MD, Wenthold RJ (2001) Molecular determinants of NMDA receptor internalization. Nat Neurosci 4:794–802.

Rodenas-Ruano A, Chávez AE, Cossio MJ, Castillo PE, Zukin RS (2012) REST-dependent epigenetic remodeling promotes the developmental switch in synaptic NMDA receptors. Nat Neurosci 10:1382-1390.

Rust MJ, Bates M, Zhuang X (2006) Sub-diffraction-limit imaging by stochastic optical reconstruction microscopy (STORM). Nat Methods 3:793–796.

Ryan TJ, Emes RD, Grant SG, Komiyama NH (2008) Evolution of NMDA receptor cytoplasmic interaction domains: implications for organisation of synaptic signalling complexes. BMC Neurosci 9:6.

Sakimura K, Kutsuwada T, Ito I, Manabe T, Takayama C, Kushiya E, Yagi T, Aizawa S, Inoue Y, Sugiyama H, Mishina M (1995) Reduced hippocampal LTP and spatial learning in mice lacking NMDA receptor epsilon 1 subunit. Nature 373:151–155.

Salter MW, Kalia L V. (2004) Src kinases: a hub for NMDA receptor regulation. Nat Rev Neurosci 5:317–328.

Sans N, Petralia RS, Wang YX, Blahos J, Hell JW, Wenthold RJ (2000) A developmental change in NMDA receptor-associated proteins at hippocampal synapses. J Neurosci 20:1260–1271.

Sans N, Prybylowski K, Petralia RS, Chang K, Wang Y-X, Racca C, Vicini S, Wenthold RJ (2003)

NMDA receptor trafficking through an interaction between PDZ proteins and the exocyst complex. Nat Cell Biol 5:520–530.

Sanz-Clemente A, Gray JA, Ogilvie KA, Nicoll RA, Roche KW (2013a) Activated CaMKII couples GluN2B and casein kinase 2 to control synaptic NMDA receptors. Cell Rep 3:607–614.

Sanz-Clemente A, Matta JA, Isaac JTR, Roche KW (2010) Casein Kinase 2 Regulates the NR2 Subunit Composition of Synaptic NMDA Receptors. Neuron 67:984–996.

Sanz-Clemente A, Nicoll RA, Roche KW (2013b) Diversity in NMDA receptor composition: many regulators, many consequences. Neuroscientist 19:62–75.

Sato Y, Tao Y-X, Su Q, Johns RA (2008) Post-synaptic density-93 mediates tyrosine-phosphorylation of the N-methyl-d-aspartate receptors. Neuroscience 153:700–708.

Sattler R, Xiong Z, Lu WY, Hafner M, MacDonald JF, Tymianski M (1999) Specific coupling of NMDA receptor activation to nitric oxide neurotoxicity by PSD-95 protein. Science 284:1845–1848.

Sauer M, Heilemann M (2017) Single-Molecule Localization Microscopy in Eukaryotes. Chem Rev 11:7478-7509.

Schell MJ, Molliver ME, Snyder SH (1995) D-serine, an endogenous synaptic modulator: localization to astrocytes and glutamate-stimulated release. Proc Natl Acad Sci U S A 92:3948–3952.

Schneggenburger R (1996) Simultaneous measurement of Ca2+ influx and reversal potentials in recombinant N-methyl-D-aspartate receptor channels. Biophys J 70:2165–2174.

Schorge S, Colquhoun D (2003) Studies of NMDA receptor function and stoichiometry with truncated and tandem subunits. J Neurosci 23:1151–1158.

Schüler T, Mesic I, Madry C, Bartholomäus I, Laube B (2008) Formation of NR1/NR2 and NR1/NR3 heterodimers constitutes the initial step in N-methyl-D-aspartate receptor assembly. J Biol Chem 283:37–46.

Scimemi A, Fine A, Kullmann DM, Rusakov DA (2004) NR2B-Containing Receptors Mediate Cross Talk among Hippocampal Synapses. J Neurosci 24:4767–4777.

Scott DB, Blanpied TA, Swanson GT, Zhang C, Ehlers MD (2001) An NMDA receptor ER retention signal regulated by phosphorylation and alternative splicing. J Neurosci 21:3063–3072.

Setou M, Nakagawa T, Seog DH, Hirokawa N (2000) Kinesin superfamily motor protein KIF17 and mLin-10 in NMDA receptor-containing vesicle transport. Science (80-) 288:1796–1802.

Sgambato-Faure V, Cenci MA (2012) Glutamatergic mechanisms in the dyskinesias induced by pharmacological dopamine replacement and deep brain stimulation for the treatment of Parkinson's disease. Prog Neurobiol 96:69–86.

Shen K, Meyer T (1999) Dynamic Control of CaMKII Translocation and Localization in Hippocampal Neurons by NMDA Receptor Stimulation. Science 284:162–167.

Sheng M (2001) Molecular organization of the postsynaptic specialization. Proc Natl Acad Sci U S A 98:7058–7061.

Sheng M, Cummings J, Roldan LA, Jan YN, Jan LY (1994) Changing subunit composition of heteromeric NMDA receptors during development of rat cortex. Nature 368:144–147.

Sheng M, Hoogenraad CC (2007) The postsynaptic architecture of excitatory synapses: a more quantitative view. Annu Rev Biochem 76:823–847.

Sheng M, Kim E (2011) The postsynaptic organization of synapses. Cold Spring Harb Perspect Biol 3:1–20.

Sheng M, Kim M (2002) Postsynaptic Signaling and Plasticity Mechanisms. Science (80-) 298:776–780.

Shinohara Y, Hirase H, Watanabe M, Itakura M, Takahashi M, Shigemoto R (2008) Left-right asymmetry of the hippocampal synapses with differential subunit allocation of glutamate receptors. Proc Natl Acad Sci U S A 105:19498–19503.

Shipton OA, Paulsen O (2014) GluN2A and GluN2B subunit-containing NMDA receptors in hippocampal plasticity. Philos Trans R Soc Lond B Biol Sci 369:20130163.

Siegel SJ, Broset N, Janssen WG, Gasict GP, Jahnt R, Heinemannt SF, Morrison JH (1994) Regional, cellular, and ultrastructural distribution of N-methyl-D-aspartate receptor subunit 1 in monkey hippocampus. Neurobiology 91:564–568.

Sigrist SJ, Sabatini BL (2012) Optical super-resolution microscopy in neurobiology. Curr Opin Neurobiol 22:86–93.

Sin WC, Haas K, Ruthazer ES, Cline HT (2002) Dendrite growth increased by visual activity requires NMDA receptor and Rho GTPases. Nature 419:475–480.

Siu CR, Beshara SP, Jones DG, Murphy KM (2017) Development of Glutamatergic Proteins in Human Visual Cortex across the Lifespan. J Neurosci 37:6031–6042.

Sjöström PJ, Turrigiano GG, Nelson SB (2003) Neocortical LTD via coincident activation of presynaptic NMDA and cannabinoid receptors. Neuron 39:641–654.

Snyder EM, Nong Y, Almeida CG, Paul S, Moran T, Choi EY, Nairn AC, Salter MW, Lombroso PJ, Gouras GK, Greengard P (2005) Regulation of NMDA receptor trafficking by amyloid-β. Nat Neurosci 8:1051–1058.

Sobczyk A, Scheuss V, Svoboda K (2005) NMDA Receptor Subunit-Dependent [Ca2+] Signaling in Individual Hippocampal Dendritic Spines. J Neurosci 25:6037–6046.

Song JY, Ichtchenko K, Südhof TC, Brose N (1999) Neuroligin 1 is a postsynaptic cell-adhesion molecule of excitatory synapses. Proc Natl Acad Sci U S A 96:1100–1105.

Sornarajah L, Vasuta OC, Zhang L, Sutton C, Li B, El-Husseini A, Raymond LA (2008) NMDA Receptor Desensitization Regulated by Direct Binding to PDZ1-2 Domains of PSD-95. J Neurophysiol 99:3052–3062.

Specht CG, Izeddin I, Rodriguez PC, El Beheiry M, Rostaing P, Darzacq X, Dahan M, Triller A (2013) Quantitative Nanoscopy of Inhibitory Synapses: Counting Gephyrin Molecules and Receptor Binding Sites. Neuron 79:308–321.

Standley S, Petralia RS, Gravell M, Hamilton R, Wang YX, Schubert M, Wenthold RJ (2012) Trafficking of the NMDAR2B receptor subunit distal cytoplasmic tail from endoplasmic reticulum to the synapse. PLoS One 7: e39585.

Standley S, Roche KW, McCallum J, Sans N, Wenthold RJ (2000) PDZ domain suppression of an ER retention signal in NMDA receptor NR1 splice variants. Neuron 28:887–898.

Steigerwald F, Schulz TW, Schenker LT, Kennedy MB, Seeburg PH, Köhr G (2000) C-Terminal truncation of NR2A subunits impairs synaptic but not extrasynaptic localization of NMDA receptors. J Neurosci 20:4573–4581.

Stender AS, Marchuk K, Liu C, Sander S, Meyer MW, Smith EA, Neupane B, Wang G, Li J, Cheng J-X, Huang B, Fang N (2013) Single Cell Optical Imaging and Spectroscopy. Chem Rev 113:2469–2527.

Stern-Bach Y, Bettler B, Hartley M, Sheppard PO, O'Hara PJ, Heinemann SF (1994) Agonist selectivity of glutamate receptors is specified by two domains structurally related to bacterial amino acid-binding proteins. Neuron 13:1345–1357.

Stern P, Béhé P, Schoepfer R, Colquhoun D (1992) Single-channel conductances of NMDA receptors expressed from cloned cDNAs: comparison with native receptors. Proceedings Biol Sci 250:271–277.

Steward O, Schuman EM (2003) Compartmentalized synthesis and degradation of proteins in neurons. Neuron 40:347–359.

Storey GP, Opitz-Araya X, Barria A (2011) Molecular determinants controlling NMDA receptor synaptic incorporation. J Neurosci 31:6311–6316.

Strack S, Choi S, Lovinger DM, Colbran RJ (1997) Translocation of autophosphorylated calcium/calmodulin-dependent protein kinase II to the postsynaptic density. J Biol Chem 272:13467–13470.

Strack S, Colbran RJ (1998) Autophosphorylation-dependent targeting of calcium/ calmodulin-dependent protein kinase II by the NR2B subunit of the N-methyl- D-aspartate receptor. J Biol Chem 273:20689–20692.

Strack S, McNeill RB, Colbran RJ (2000) Mechanism and regulation of calcium/calmodulin-dependent protein kinase II targeting to the NR2B subunit of the N-methyl-D-aspartate receptor. J Biol Chem 275: 23798-23806.

Stroebel D, Carvalho S, Grand T, Zhu S, Paoletti P (2014) Controlling NMDA Receptor Subunit Composition Using Ectopic Retention Signals. J Neurosci 34: 16630-16636.

Sucher NJ, Akbarian S, Chi CL, Leclerc CL, Awobuluyi M, Deitcher DL, Wu MK, Yuan JP, Jones EG, Lipton SA (1995) Developmental and regional expression pattern of a novel NMDA receptor-like subunit (NMDAR-L) in the rodent brain. J Neurosci 15:6509–6520.

Sun Y, Chen Y, Zhan L, Zhang L, Hu J, Gao Z (2015) The role of non-receptor protein tyrosine kinases in the excitotoxicity induced by the overactivation of NMDA receptors. Rev Neurosci 27:283–289.

Sun Y, Cheng X, Zhang L, Hu J, Chen Y, Zhan L, Gao Z (2017) The Functional and Molecular Properties, Physiological Functions, and Pathophysiological Roles of GluN2A in the Central Nervous System. Mol Neurobiol 54:1008–1021.

Swanger SA, He YA, Richter JD, Bassell GJ (2013) Dendritic GluN2A Synthesis Mediates Activity-Induced NMDA Receptor Insertion. J Neurosci 33:8898–8908.

Swanwick CC, Shapiro ME, Yi Z, Chang K, Wenthold RJ (2009) NMDA receptors interact with flotillin-1 and -2, lipid raft-associated proteins. FEBS Lett 583:1226–1230.

Sydor AM, Czymmek KJ, Puchner EM, Mennella V (2015) Super-Resolution Microscopy: From Single Molecules to Supramolecular Assemblies. Trends Cell Biol 25:730–748.

Takasu MA, Dalva MB, Zigmond RE, Greenberg ME (2002) Modulation of NMDA Receptor-Dependent Calcium Influx and Gene Expression Through EphB Receptors. Science (80-) 295:491–495.

Tan Y, Liu M, Noltin B, Go J, Gervay-Hague J, Liu G (2008) A Nanoengineering Approach for Investigation and Regulation of Protein Immobilization. ACS Nano 2:2374–2384.

Tang A-H, Chen H, Li TP, Metzbower SR, MacGillavry HD, Blanpied TA (2016) A trans-synaptic nanocolumn aligns neurotransmitter release to receptors. Nature 536:210–214.

Tang L-J, Li C, Hu S-Q, Wu Y-P, Zong Y-Y, Sun C-C, Zhang F, Zhang G-Y (2012) S-nitrosylation of c-Src via NMDAR-nNOS module promotes c-Src activation and NR2A phosphorylation in cerebral ischemia/reperfusion. Mol Cell Biochem 365:363–377.

Tang TTT, Badger JD, Roche P a., Roche KW (2010) Novel approach to probe subunit-specific contributions to N-Methyl-D-aspartate (NMDA) receptor trafficking reveals a dominant role for NR2B in receptor recycling. J Biol Chem 285:20975–20981.

Tang YP, Shimizu E, Dube GR, Rampon C, Kerchner GA, Zhuo M, Liu G, Tsien JZ (1999) Genetic enhancement of learning and memory in mice. Nature 401:63–69.

Tezuka T, Umemori H, Akiyama T, Nakanishi S, Yamamoto T, Stevens CF (1999) PSD-95 promotes Fyn-mediated tyrosine phosphorylation of the N-methyl-D-aspartate receptor subunit NR2A. Biochemistry 96:435–440.

Thomas CG, Miller AJ, Westbrook GL (2006) Synaptic and Extrasynaptic NMDA Receptor NR2 Subunits in Cultured Hippocampal Neurons. J Neurophysiol 95:1727–1734.

Thompson RE, Larson DR, Webb WW (2002) Precise Nanometer Localization Analysis for Individual Fluorescent Probes. Biophys J 82:2775–2783.

Tønnesen J, Nägerl UV (2013) Superresolution imaging for neuroscience. Exp Neurol 242:33–40.

Tovar KR, McGinley MJ, Westbrook GL (2013) Triheteromeric NMDA Receptors at Hippocampal Synapses. J Neurosci 33:9150–9160.

Tovar KR, Westbrook GL (1999) The incorporation of NMDA receptors with a distinct subunit composition at nascent hippocampal synapses in vitro. J Neurosci 19:4180–4188.

Tovar KR, Westbrook GL (2002) Mobile NMDA receptors at hippocampal synapses. Neuron 34:255–264.

Traynelis SF, Wollmuth LP, McBain CJ, Menniti FS, Vance KM, Ogden KK, Hansen KB, Yuan H, Myers SJ, Dingledine R (2010) Glutamate Receptor Ion Channels: Structure, Regulation, and Function. Pharmacol Rev 62:405–496.

Triller A, Choquet D (2005) Surface trafficking of receptors between synaptic and extrasynaptic membranes: and yet they do move! Trends Neurosci 28:133–139.

Tsui J, Malenka RC (2006) Substrate localization creates specificity in calcium/calmodulin-dependent protein kinase II signaling at synapses. J Biol Chem 281:13794–13804.

Urban NT, Willig KI, Hell SW, Nägerl UV (2011) STED Nanoscopy of Actin Dynamics in Synapses Deep Inside Living Brain Slices. Biophys J 101:1277–1284.

Vallejo D, Codocedo JF, Inestrosa NC (2017) Posttranslational Modifications Regulate the Postsynaptic Localization of PSD-95. Mol Neurobiol 54:1759–1776.

van de Linde S, Löschberger A, Klein T, Heidbreder M, Wolter S, Heilemann M, Sauer M (2011) Direct stochastic optical reconstruction microscopy with standard fluorescent probes. Nat Protoc 6:991–1009.

van de Linde S, Sauer M, Heilemann M (2008) Subdiffraction-resolution fluorescence imaging of

proteins in the mitochondrial inner membrane with photoswitchable fluorophores. J Struct Biol 164:250–254.

van Rossum D, Kuhse J, Betz H (1999) Dynamic interaction between soluble tubulin and C-terminal domains of N-methyl-D-aspartate receptor subunits. J Neurochem 72:962–973.

van Zundert B, Yoshii A, Constantine-Paton M (2004) Receptor compartmentalization and trafficking at glutamate synapses: a developmental proposal. Trends Neurosci 27:428–437.

Vasefi MS, Yang K, Li J, Kruk JS, Heikkila JJ, Jackson MF, MacDonald JF, Beazely MA (2013) Acute 5-HT7 receptor activation increases NMDA-evoked currents and differentially alters NMDA receptor subunit phosphorylation and trafficking in hippocampal neurons. Mol Brain 6:24.

Vicini S, Wang JF, Li JH, Zhu WJ, Wang YH, Luo JH, Wolfe BB, Grayson DR (1998) Functional and pharmacological differences between recombinant N-methyl-D-aspartate receptors. J Neurophysiol 79:555–566.

Vogl AM, Brockmann MM, Giusti SA, Maccarrone G, Vercelli CA, Bauder CA, Richter JS, Roselli F, Hafner A-S, Dedic N, Wotjak CT, Vogt-Weisenhorn DM, Choquet D, Turck CW, Stein V, Deussing JM, Refojo D (2015) Neddylation inhibition impairs spine development, destabilizes synapses and deteriorates cognition. Nat Neurosci 18:239–251.

Volianskis A, France G, Jensen MS, Bortolotto ZA, Jane DE, Collingridge GL (2015) Long-term potentiation and the role of N-methyl-D-aspartate receptors. Brain Res 1621:5–16.

von Engelhardt J, Doganci B, Jensen V, Hvalby Ø, Göngrich C, Taylor A, Barkus C, Sanderson DJ, Rawlins JNP, Seeburg PH, Bannerman DM, Monyer H (2008) Contribution of Hippocampal and Extra-Hippocampal NR2B-Containing NMDA Receptors to Performance on Spatial Learning Tasks. Neuron 60:846–860.

Wagner SA, Beli P, Weinert BT, Schölz C, Kelstrup CD, Young C, Nielsen ML, Olsen J V, Brakebusch C, Choudhary C (2012) Proteomic analyses reveal divergent ubiquitylation site patterns in murine tissues. Mol Cell Proteomics 11:1578–1585.

Wang C-Y, Chang K, Petralia RS, Wang Y-X, Seabold GK, Wenthold RJ (2006) A novel family of adhesion-like molecules that interacts with the NMDA receptor. J Neurosci 26:2174–2183.

Wang JQ, Guo M-L, Jin D-Z, Xue B, Fibuch EE, Mao L-M (2014) Roles of subunit phosphorylation in regulating glutamate receptor function. Eur J Pharmacol 728:183–187.

Wang PY, Petralia RS, Wang Y-X, Wenthold RJ, Brenowitz SD (2011) Functional NMDA receptors at axonal growth cones of young hippocampal neurons. J Neurosci 31:9289–9297.

Washbourne P, Bennett JE, McAllister AK (2002) Rapid recruitment of NMDA receptor transport packets to nascent synapses. Nat Neurosci 5:751–759.

Washbourne P, Liu X-B, Jones EG, McAllister AK (2004) Cycling of NMDA Receptors during Trafficking in Neurons before Synapse Formation. J Neurosci 24: 8253-8264.

Watanabe M, Inoue Y, Sakimura K, Mishina M (1992) Developmental changes in distribution of NMDA receptor channel subunit mRNAs. Neuroreport 3:1138–1140.

Wechsler A, Teichberg VI (1998) Brain spectrin binding to the NMDA receptor is regulated by phosphorylation, calcium and calmodulin. EMBO J 17:3931–3939.

Wee KSL, Zhang Y, Khanna S, Low CM (2008) Immunolocalization of NMDA receptor subunit NR3B in selected structures in the rat forebrain, cerebellum, and lumbar spinal cord. J Comp

Neurol 509:118–135.

Wenthold R, Petralia R, Blahos J I, Niedzielski A (1996) Evidence for multiple AMPA receptor complexes in hippocampal CA1/CA2 neurons. J Neurosci 16:1982–1989.

Wenthold RJ, Prybylowski K, Standley S, Sans N, Petralia RS (2003) Trafficking of NMDA receptors. Annu Rev Pharmacol Toxicol 43:335–358.

Westphal V, Rizzoli SO, Lauterbach MA, Kamin D, Jahn R, Hell SW (2008) Video-Rate Far-Field Optical Nanoscopy Dissects Synaptic Vesicle Movement. Science (80-) 320:246–249.

Wheeler D, Knapp E, Bandaru VVR, Wang Y, Knorr D, Poirier C, Mattson MP, Geiger JD, Haughey NJ (2009) Tumor necrosis factor-alpha-induced neutral sphingomyelinase-2 modulates synaptic plasticity by controlling the membrane insertion of NMDA receptors. J Neurochem 109:1237–1249.

Williams K, Min Shen Y, Molinoff PB (1993) Developmental Switch in the Expression of NMDA Receptors Occurs In Vivo and In Vitro. Neuron 10:267–278.

Willig KI, Barrantes FJ (2014) Recent applications of superresolution microscopy in neurobiology. Curr Opin Chem Biol 20:16–21.

Won H, Lee H-R, Gee HY, Mah W, Kim J-I, Lee J, Ha S, Chung C, Jung ES, Cho YS, Park S-G, Lee J-S, Lee K, Kim D, Bae YC, Kaang B-K, Lee MG, Kim E (2012) Autistic-like social behaviour in Shank2-mutant mice improved by restoring NMDA receptor function. Nature 486:261–265.

Won S, Incontro S, Nicoll RA, Roche KW (2016) PSD-95 stabilizes NMDA receptors by inducing the degradation of STEP 61. Proc Natl Acad Sci 113:E4736–E4744.

Won S, Levy JM, Nicoll RA, Roche KW (2017) MAGUKs: multifaceted synaptic organizers. Curr Opin Neurobiol 43:94–101.

Wyszynski M, Lin J, Rao A, Nigh E, Beggs AH, Craig AM, Sheng M (1997) Competitive binding of alpha-actinin and calmodulin to the NMDA receptor. Nature 385:439–442.

Xiao X, Levy AD, Rosenberg BJ, Higley MJ, Koleske AJ (2016) Disruption of Coordinated Presynaptic and Postsynaptic Maturation Underlies the Defects in Hippocampal Synapse Stability and Plasticity in Abl2/Arg-Deficient Mice. J Neurosci 36:6778–6791.

Xu H, Smith BN (2015) Presynaptic ionotropic glutamate receptors modulate GABA release in the mouse dorsal motor nucleus of the vagus. Neuroscience 308:95–105.

Xu Z, Chen R-Q, Gu Q-H, Yan J-Z, Wang S-H, Liu S-Y, Lu W (2009) Metaplastic Regulation of Long-Term Potentiation/Long-Term Depression Threshold by Activity-Dependent Changes of NR2A/NR2B Ratio. J Neurosci 29:8764–8773.

Yamada Y, Chochi Y, Ko JA, Sobue K, Inui M (1999) Activation of channel activity of the NMDA receptor-PSD-95 complex by guanylate kinase-associated protein (GKAP). FEBS Lett 458:295–298.

Yamada Y, Iwamoto T, Watanabe Y, Sobue K, Inui M (2002) PSD-95 eliminates Src-induced potentiation of NR1/NR2A-subtype NMDA receptor channels and reduces high-affinity zinc inhibition. J Neurochem 81:758–764.

Yamanaka M, Smith NI, Fujita K (2014) Introduction to super-resolution microscopy. Reprod Syst Sex Disord 63:177–192.

Yan Y-G, Zhang J, Xu S-J, Luo J-H, Qiu S, Wang W (2014) Clustering of surface NMDA receptors is

mainly mediated by the C-terminus of GluN2A in cultured rat hippocampal neurons. Neurosci Bull 30:655–666.

Yang E, Schulman H (1999) Structural examination of autoregulation of multifunctional calcium/calmodulin-dependent protein kinase II. J Biol Chem 274:26199–26208.

Yang J, Woodhall GL, Jones RSG (2006) Tonic Facilitation of Glutamate Release by Presynaptic NR2B-Containing NMDA Receptors Is Increased in the Entorhinal Cortex of Chronically Epileptic Rats. J Neurosci 26: 406-410.

Yao Y, Harrison CB, Freddolino PL, Schulten K, Mayer ML (2008) Molecular mechanism of ligand recognition by NR3 subtype glutamate receptors. EMBO J 27:2158–2170.

Yao Y, Mayer M (2006) Characterization of a Soluble Ligand Binding Domain of the NMDA Receptor Regulatory Subunit NR3A. J Neurosci 26:4559–4566.

Yashiro K, Philpot BD (2008) Regulation of NMDA receptor subunit expression and its implications for LTD, LTP, and metaplasticity. Neuropharmacology 55:1081–1094.

Yi Z, Petralia RS, Fu Z, Swanwick CC, Wang Y-X, Prybylowski K, Sans N, Vicini S, Wenthold RJ (2007) The role of the PDZ protein GIPC in regulating NMDA receptor trafficking. J Neurosci 27:11663–11675.

Yoshimura Y, Yamauchi Y, Shinkawa T, Taoka M, Donai H, Takahashi N, Isobe T, Yamauchi T (2003) Molecular constituents of the postsynaptic density fraction revealed by proteomic analysis using multidimensional liquid chromatography-tandem mass spectrometry. J Neurochem 88:759–768.

Yuan H, Hansen KB, Vance KM, Ogden KK, Traynelis SF (2009) Control of NMDA Receptor Function by the NR2 Subunit Amino-Terminal Domain. J Neurosci 29:12045–12058.

Zeng M, Shang Y, Araki Y, Guo T, Huganir RL, Zhang M (2016) Phase Transition in Postsynaptic Densities Underlies Formation of Synaptic Complexes and Synaptic Plasticity. Cell 166: 1163-1175.e12.

Zhang F, Li C, Wang R, Han D, Zhang Q-G, Zhou C, Yu H-M, Zhang G-Y (2007) Activation of GABA receptors attenuates neuronal apoptosis through inhibiting the tyrosine phosphorylation of NR2A by Src after cerebral ischemia and reperfusion. Neuroscience 150:938–949.

Zhang J, Diamond JS (2009) Subunit- and Pathway-Specific Localization of NMDA Receptors and Scaffolding Proteins at Ganglion Cell Synapses in Rat Retina. J Neurosci 29: 4274-4286.

Zhang S, Edelmann L, Liu J, Crandall JE, Morabito MA (2008) Cdk5 Regulates the Phosphorylation of Tyrosine 1472 NR2B and the Surface Expression of NMDA Receptors. J Neurosci 28:415–424.

Zhao C, Du C-P, Peng Y, Xu Z, Sun C-C, Liu Y, Hou X-Y (2015) The upregulation of NR2A-containing N-methyl-D-aspartate receptor function by tyrosine phosphorylation of postsynaptic density 95 via facilitating Src/proline-rich tyrosine kinase 2 activation. Mol Neurobiol 51:500–511.

Zhong H (2015) Applying superresolution localization-based microscopy to neurons. Synapse 69:283–294.

Zhou Y, Takahashi E, Li W, Halt A, Wiltgen B, Ehninger D, Li G-D, Hell JW, Kennedy MB, Silva AJ (2007) Interactions between the NR2B Receptor and CaMKII Modulate Synaptic Plasticity and Spatial Learning. J Neurosci 27:13843–13853.

Zhu J, Shang Y, Zhang M (2016) Mechanistic basis of MAGUK-organized complexes in synaptic development and signalling. Nat Rev Neurosci 17: 209-223.

Titre: Organisation et régulation différentielles des sous-types de Récepteurs NMDA révélées par imagerie de super résolution

Résumé: Les récepteurs du glutamate de type NMDA (NMDAR) sont des canaux ioniques impliqués dans les phénomènes de plasticité de la transmission synaptique dans le système nerveux central, des mécanismes supposés être à la base du développement neuronal, de l'apprentissage et de la formation de la mémoire. Les NMDAR forment des tétramères à la membrane plasmique, constitués de deux sous-unités obligatoires GluN1 et deux sous-unités variables GluN2 (GluN2A-D) ou GluN3. Dans le prosencéphale, les récepteurs comportant les sous-unités GluN2A (GluN2A-NMDAR) et GluN2B (GluN2B-NMDAR) sont les plus abondants et présentent des profils d'expression différents au cours du développement, les GluN2B-NMDAR étant fortement exprimés aux stades précoces tandis que l'expression des GluN2A-NMDAR augmente progressivement au cours du développement postnatal. Des contributions relatives de ces deux sous-types majoritaires de NMDAR aux propriétés de signalisation distinctes dépendent directement les phénomènes de plasticité neuronale, tels que l'adaptation des synapses glutamatergiques et des circuits neuronaux excitateurs. Bien que la régulation moléculaire des NMDAR ait fait l'objet d'intenses recherches ces dernières décennies, la localisation précise de ces deux sous-types de récepteurs dans la membrane postsynaptique demeurait méconnue. Pour répondre à cette question, nous avons étudié la distribution des NMDAR à la surface de neurones d'hippocampe de rats en combinant deux techniques de microscopie de super-résolution - la microscopie de reconstruction optique stochastique directe (dSTORM) et la déplétion d'émission stimulée (STED) - permettant de dépasser la limite de résolution inhérente à la diffraction de la lumière. Ces techniques nous ont permis de mettre en évidence que les sous-types de récepteurs GluN2A- et GluN2B-NMDAR présentent une nano-organisation différente à la surface neuronale. En effet, ils sont organisés en structures nanoscopiques (nanodomaines) qui diffèrent en nombre, en surface et en morphologie, notamment au niveau des synapses. Au cours du développement, l'organisation membranaire des deux sous-types de NMDAR évolue, avec en particulier de profonds changements de distribution des GluN2A-NMDAR. De plus, cette organisation nanoscopique est impactée différemment par des modulations de l'interaction avec les protéines d'échafaudage à domaine PDZ ou de l'activité de la kinase CaMKII suivant le sous-type de NMDAR considéré. En effet, la réorganisation des GluN2A-NMDAR implique principalement des changements de nombre de récepteurs dans les nanodomaines sans modification de leur localisation, tandis que la réorganisation des GluN2B-NMDAR passe essentiellement par des modifications de localisation des nanodomaines sans changements du nombre de récepteurs qu'ils contiennent. Ainsi, les GluN2A- et GluN2B-NMDAR présentent des nano-organisations différentes dans la membrane postsynaptique, reposant vraisemblablement sur des voies de régulation et des complexes de signalisation distincts.

Mots clés: récepteurs NMDA, sous-unités GluN2, dSTORM

Title: Super-resolution imaging reveals differential organization and regulation of NMDA receptor subtypes

Abstract: NMDA-type glutamate receptors (NMDARs) are a type of ion permeable channels playing critical roles in excitatory neurotransmission in the central nervous system by mediating different forms of synaptic plasticity, a mechanism thought to be the molecular basis of neuronal development, learning and memory formation. NMDARs form tetramers in the postsynaptic membrane, most generally associating two obligatory GluN1 subunits and two modulatory GluN2 (GluN2A-D) or GluN3 (GluN3A-B) subunits. In the hippocampus, the dominant GluN2 subunits are GluN2A and GluN2B, displaying different expression patterns, with GluN2B being highly expressed in early development while GluN2A levels increase gradually during postnatal development. In the forebrain, the plastic processes mediated by NMDARs, such as the adaptation of glutamate synapses and excitatory neuronal networks, mostly rely on the relative implication of GluN2A- and GluN2B-containing NMDARs that have different signaling properties. Although the molecular regulation of synaptic NMDARs has been under intense investigation over the last decades, the exact topology of these two subtypes within the postsynaptic membrane has remained elusive. Here we used a combination of super-resolution microscopy techniques such as direct stochastic optical reconstruction microscopy (dSTORM) and stimulated emission depletion (STED) microscopy to characterize the surface distribution of GluN2A- or GluN2B-containing NMDARs. Both dSTORM and STED microscopy, based on different principles, enable to overcome the resolution barrier due to the diffraction limit of light. Using these techniques, we here unveil a differential nanoscale organization of native GluN2A- and GluN2B-NMDARs in rat hippocampal neurons. Both NMDAR subtypes are organized in nanoscale structures (termed nanodomains) that differ in their number, area, and shape. These observed differences are also maintained in synaptic structures. During development of hippocampal cultures, the membrane organization of both NMDAR subtypes evolves, with marked changes for the topology of GluN2A-NMDARs. Furthermore, GluN2A- and GluN2B-NMDAR nanoscale organizations are differentially affected by alterations of either interactions with PDZ scaffold proteins or CaMKII activity. The regulation of GluN2A-NMDARs mostly implicates changes in the number of receptors in fixed nanodomains, whereas the regulation of GluN2B-NMDARs mostly implicates changes in the nanodomain topography with fixed numbers of receptors. Thus, GluN2A- and GluN2B-NMDARs have distinct organizations in the postsynaptic membrane, likely implicating different regulatory pathways and signaling complexes.

Keywords: NMDA receptors, GluN2 subunits, dSTORM

Institut Interdisciplinaire de Neurosciences, CNRS UMR5297 Université de Bordeaux, Centre Broca Nouvelle-Aquitaine, 146 rue Léo-Saignat, CS 61292 CASE 130, 33076 Bordeaux Cedex (France)